TECHNISCHE UNIVERSITÄT DRESDEN

Technical University Dresden

Faculty of Environmental Sciences

Dissertation title:

Agricultural Drought Risk Assessment of Rainfed Agriculture in the Sudan Using Remote Sensing and GIS: The Case of El Gedaref State

Dissertation to obtain the academic degree

Doctor rerum naturalium (Dr.rer.nat.)

Submitted by:

MSc, Elmoiz Yousif Elnayer Taha

Place of birth Gezira State, Sudan

Prof. Dr. habil. Elmar Csaplovics, Technical University of Dresden, Germany

Prof. Dr. Lars Ribbe, ITT, Cologne University of Applied Science, Germany

Dr. Nadir Ahmed Elagib, University of Cologne, Germany

Defense date: 20.09.2022

Explanation of the doctoral candidate

This is to certify that this copy is entirely congruent with the original copy of the thesis with the topic:

"Agricultural Drought Risk Assessment of Rainfed Agriculture in the Sudan Using Remote Sensing and GIS: The Case of El Gedaref State"

Dresden, May 2023

Elmoiz Yousif Elnayer Taha

Table of Contents

List of Tables

List of Figures

List of Abbreviations

AET	Actual Evapotranspiration
AMSR-E	Advanced Microwave Scanning Radiometer for EOS
APCO	African Plantation Company (Sudan)
ASCAT	Advanced Scatterometer
AWC	Available Water Content
CATDS	Centre Aval de Traitement des Données
CCP	Central Clay Plain (Sudan)
CHC	Climate Hazard Center
CHIRPS	Climate Hazards Group Infrared Precipitation with Station data
CMI	Crop Moisture Index
CNES	Centre national d'études spatiales
CWR	Crop Water Requirement
EASE	Equal Area Scalable Earth
EOS	End of Season
ESA	European Space Agency
ET_o	Evapotranspiration
FAO	Organization of the United Nations
FAOSTAT	FAO Statistics
FC	Field Capacity
FEWS NET	Famine Early Warning System Networks
GIS	Geographic Information System
GLDAS	Global Data Assimilation Systems
IAC	International Action Center
IGBP-DIS	International Geosphere Biosphere Programme - Data and Information Systems
Kc	Crop coefficient
LGP	Length of Growing Period
LST	Land Surface Temperature
LU/LC	Land use/Land cover

MABE	Mean Absolute Bias Error
MBE	Mean Bias Error
METRIC	Mapping Evapotranspiration With Internalized Calibration
MFC	Mechanized Farming Corporation of Sudan
MODIS	Moderate Resolution Imaging Spectro-radiometer
NASA	National Aeronautics and Space Administration
NDVI	Normalized Difference Vegetation Index
NOAA	National Oceanic and Atmospheric Administration
PAW	Plant Available Water
PET	Potential Evapotranspiration
PWP	Permanent Wilting Point
PDSI	Palmer Drought Severity Index
RS	Remote Sensing
RMSE	Root Mean Squire Error
SDGs	Sustainable Development Goals of the United Nations
SEBAL	Surface Energy Balance Algorithm for Land
SGB	Sudan Gezira Board
SOS	Start of Season
SDGs	Sustainable Development Goals of the United Nations
SMAP	Soil Moisture Active Passive
SMOS	Soil Moisture and Ocean Salinity
SPI	Standardized Precipitation Index
SSEB	Simplified Surface Energy Balance
SSEBop	Operational Simplified Surface Energy Balance
SUMA	Sudan Meteorological Station
SWDI	Soil Water Deficit Index
ubRMSE	Un Biased Root Mean Squire Error
UNDP	United Nations Development Program
UNESCO	United Nations Educational, Scientific and Cultural Organization
USAID	United States Agency for International Development

USGS	United States Geological Survey
WMO	World Meteorological Organization
WP	Welting Point
WRSI	Water Requirement Satisfaction Index

Acknowledgments

Pursuing a Ph.D. study is both a painful and enjoyable experience that enabled me to deepen my knowledge and discover my potential. This Ph.D. would not have taken this shape without the contribution and guidance I received from my respected supervisors and many other people throughout the preparation of this dissertation.

First, I would like to express my sincere gratitude to my supervisor Prof. Dr. habil. Elmar Csaplovics for his great unlimited deal of support and patiently advice and provided me continuous inspiration and constructive criticism. His insight has always enlightened me. From him, I learned how to think critically, how to select problems, how to solve them, and how to present their solutions.

I want to thank my supervisor Prof. Lars Ribbe, for his guidance throughout this project. I want to thank him very much for his support and understanding over these past five years. I'm grateful beyond measure for his help. I cannot begin to express my thanks to Dr. Nadir Elagib for always giving necessary suggestions through this venture, steering me in the right direction whenever he thought I needed it, and for his dedicated support and guidance. I am incredibly grateful for his contributions to improving my research skills and lifting me to this level.

The completion of my study would not have been possible without the financial support of the Centers for Natural Resources and Development (CNRD). I am especially indebted to Dr. Rui Pedroso, coordinator of the CNRD doctoral program (DNRD), for his continuous support during my Ph.D. studies. I want to express my gratitude to all staff at the Institute for Technology and Resources Management in the Tropics and Subtropics (ITT), TH Köln, especially Ms. Karola Schmclzer, Mr. Alexander Klein, Ms. Nora Ellen Lucidi, Mr. Joschka Thuner, and Ms. Ricarda Pedroso for their continuous and unlimited support. My gratitude to my colleagues, Muhammad Khalifa, Firoz, Uyen, Teresa, Samah, Amrita, Van, Nazmul, Zryab, Oscar, Asraful Latif, Mohammed Ab-delmuniem, and Pedro for being such good friends and for the knowledge that we shared during our personal and scholarly interactions. I am also thankful to my colleague Maren Krätzschmar for her help in translating the thesis abstract into German.

I am thankful to the African Plantation Company (APCO), Sudan, who were involved in the success of the field survey for this research project, allowing me into their buildings for follow-up surveys. Without whom, I would have no content for my thesis.

From the core of my heart, I would like to say a big thank you to my colleagues at the Agricultural Research Corporation, Sudan, the staff members of El Gedaref Research, Station, and the staff members of the Mechanized Rainfed Agriculture Authority of El Gedaref State, for their support during the field mission.

Nobody has been more important to me in pursuing this study than my family. I want to acknowledge my parents, whose love and prayer are with me in whatever I seek, and for all the unconditional support in this intense research period. Before anything else, I wish to thank my loving and caring wife, Aisha, and my wonderful children, who provide unending inspiration.

.

Abstract

Hitherto, most research conducted to monitor agricultural drought on the African continent has focused only on meteorological aspects, with less attention paid to soil moisture, which describes agricultural drought. Satellite missions dedicated to soil moisture monitoring must be used with caution across various scales. The rainfed sector of Sudan takes great importance due to it is high potential to support national food security. El Gedaref state is significant in Sudan given its potentiality of the agricultural sector under a mechanized system, where crop cultivation supports livelihood sources for about 80% of its population and households, directly through agricultural production and indirectly through labor workforce. The state is an essential rainfed region for sorghum production, located within Sudan's Central Clay Plain (CCP). Enhancing soil moisture estimation is key to boosting the understanding of agricultural drought in the farming lands of Sudan. Soil moisture measuring stations/sensors networks do not exist in the El Gedaref agricultural rainfed sector.

The literature shows a significant gap in whether soil moisture is sufficient to meet the estimated water demands of cultivation or the start of the growing season.

The purpose of this study is to focus principally on agricultural drought. The soil moisture data retrieved from the Soil Moisture Active Passive (SMAP) mission launched by NASA in 2015 were compared against in situ data measurements over the agricultural lands. In situ points (at 5 cm, 10 cm, and 20 cm depths) corresponding to 9×9 km SMAP pixel footprint are rescaled to conduct a point-to-pixel evaluation of SMAP product over two locations, namely Samsam and Kilo-6, during the rainy season 2018. Four errors were measured; Root Mean Squared Error (RMSE), Mean Bias Error (MBE), unbiased RMSE (ubRMSE), Mean Absolute Bias Error (MABE), and the coefficient of determination R^2. SMAP improve (significantly at the 5% level for SM). The results indicated that the SMAP product meets its soil moisture accuracy requirement at the top 5 cm and in the root zone (10 and 20 cm) depths at Samsam and Kilo-6. SMAP demonstrates higher performance indicated by the high R^2 (0.96, 0.88, and 0.97) and (0.85, 0.94, and 0.94) over Samsam and Kilo-6, respectively, and met its accuracy targeted by SMAP retrieval domain at ubRMSE 0.04 m^3m^{-3} or better in all locations, and most minor errors (MBE, MABE, and RMSE). The possibility of using SMAP

products was discussed to measure agricultural drought and its impacts on crop growth during various growth stages in both locations and over the CCP entirely.

The croplands of El Gedaref are located within the tropical savanna (AW, categorization following the Köppen climate classification), warm semi-arid climate (BSh), and warm desert climate (BWh). The areas of interest are predominantly rainfed agricultural lands, vulnerable to climate change and variability. The Climate Hazards Group Infrared Precipitation with Station data (CHIRPS), SMAP at the top surface of the soil and the root zone, and Soil Water Deficit Index (SWDI) derived from SMAP were analyzed against the Normalized Difference Vegetation Index (NDVI). The results indicate that the NDVI values disagree with rainfall patterns at the dekadal scale.

At all isohyets, SWDI in the root zone shows a reliable and expected response of capturing seasonal dynamics concerning the vegetation index (NDVI) over warm desert climates during 2015, 2016, 2017, 2018, and 2019, respectively. It is concluded that SWDI can be used to monitor agricultural drought better than rainfall data and SMAP data because it deals directly with the available water content of the crops. SWDI monitoring agricultural drought is a promising method for early drought warning, which can be used for agricultural drought risk management in semi-arid climates.

The comparison between sorghum yield and the spatially distributed water balance model was assessed according to the length of the growing period. Late maturing (120 days), medium maturing (90-95 days), and early maturing variety (80-85 days). As a straightforward crop water deficit model. An adapted WRSI index was developed to characterize the effect of using different climatic and soil moisture remote sensing input datasets, such as CHIRPS rainfall, SMAP soil moisture at the top 5 cm and the root zone, MODIS actual evapotranspiration on key WRSI index parameters and outputs. Results from the analyses indicated that SMAP best captures season onset and length of the growing period, which are critical for the WRSI index.

In addition, short-, medium-, and long-term sorghum cultivar planting scenarios were considered and simulated. It was found that over half of the variability in yield is explained by water stress when the SMAP at root zone dataset is used in the WRSI model (R^2=0.59–0.72

for sorghum varieties of 90–120 days growing length). Overall, CHIRPS and SMAP root zone show the highest skill (R^2=0.53–0.64 and 0.54–0.56, respectively) in capturing state-level crop yield losses related to seasonal soil moisture deficit, which is critical for drought early warning and agrometeorological risk applications.

The results of this study are important and valuable in supporting the continued development and improvement of satellite-based soil moisture sensing to produce higher accuracy soil moisture products in semi-arid regions. The results also highlight the growing awareness among various stakeholders of the impact of drought on crop production and the need to scale up adaptation measures to mitigate the adverse effects of drought.

Zusammenfassung

Forschungsarbeiten zur Überwachung der Dürre in der Landwirtschaft auf dem afrikanischen Kontinent konzentrieren sich bislang vor allem auf meteorologische Aspekte und schenken der Bodenfeuchte als Dürreindikator zumeist nur wenig Aufmerksamkeit. Die Bodenfeuchte ist jedoch ein grundlegender Faktor für das landwirtschaftliche Dürre Monitoring. Kenntnisse der verfügbaren Bodenfeuchte an der Oberfläche und in der Wurzelzone ermöglichen eine genaue Bewertung der Trockenheit in landwirtschaftlichen Gebieten. Satellitenmissionen zu ihrer Überwachung können auf Grundlage einschlägiger Expertise entlang verschiedener Skalen interpretiert werden.

Der Regenfeldbau im Sudan ist von großer Bedeutung, da er ein großes Potenzial für die nationale Ernährungssicherheit bietet. Dabei ist der Bundesstaat El Gedaref für das Land von zentraler Bedeutung, da er über ein großes Potenzial eines mechanisierten Landwirtschaftssektors verfügt, der durch den Anbau von Feldfrüchten den Lebensunterhalt von etwa 80 % der Bevölkerung und der Haushalte sichert. Direkt erfolgt dies durch die landwirtschaftliche Produktion, und indirekt durch die Beschäftigung von Arbeitskräften. Der Bundesstaat ist die wichtigste Regenfeldbau-Region für die Sorghum-Produktion und liegt in der Central Clay Plain (CCP) des Sudan. Wissen über die Bodenfeuchte ist ein Schlüssel zum besseren Verständnis Dürre in den landwirtschaftlichen Gebieten des Sudan. Im landwirtschaftlichen Regenfeldbau in El Gedaref existieren keine Messstationen/Sensornetzwerke für die Bodenfeuchte und es klafft eine große Lücke bei der Auswertung vielversprechender Bilddaten der Fernerkundung zur Schätzung der Bodenfeuchte. Es mangelt also an experimenteller Forschung, um Methoden der Fernerkundung für das Monitoring der Bodenfeuchte, die mit hoher zeitlicher Auflösung arbeiten, in nahezu Echtzeit einzusetzen. In ariden und semiariden Regionen wie dem Sudan kann es aufgrund hoher Verdunstungsraten zu dynamischen Veränderungen der Bodenfeuchte kommen. Infolge des schnellen Austrocknens der Böden reicht die Genauigkeit vieler Mess-Daten nicht aus, um die Bodenfeuchtigkeit in hoher zeitlicher Auflösung zu erfassen. Hinsichtlich der vorhandenen Literatur zeigt sich eine Lücke bei der Klärung der Frage, ob ein gewisses Maß an Bodenfeuchte ausreicht, um den geschätzten Wasserbedarf für den Anbau oder den Beginn einer Vegetationsperiode zu decken.

Diese Studie fokussiert auf das Phänomen Trockenheit in der Landwirtschaft. Dafür wurden Bodenfeuchtedaten der 2015 von der NASA gestarteten Mission Soil Moisture Active Passive (SMAP) mit In-situ Messungen über landwirtschaftlichen Flächen verglichen. In-situ-Messpunkte (in 5 cm, 10 cm und 20 cm Tiefe), die dem 9×9 km großen SMAP-Pixel-Footprint entsprechen, wurden neu skaliert, um eine Punkt-zu-Pixel-Bewertung des SMAP-Produkts über zwei Standorten, Samsam und Kilo-6, während der Regenzeit 2018 durchzuführen. Vier Arten von Fehlermessungen wurden verwendet: Root Mean Squared Error (RMSE), Mean Bias Error (MBE), unbiased RMSE (ubRMSE) und Mean Absolute Bias Error (MABE) sowie das Bestimmtheitsmaß R^2. SMAP verbessern (signifikant auf dem 5%-Niveau für SM). Die Ergebnisse zeigen, dass das SMAP-Produkt die Anforderungen an die Genauigkeit der Bestimmung der Bodenfeuchte in den oberen 5 cm und in der Wurzelzone (10 und 20 cm) in den beiden Standorten Samsam und Kilo-6 erfüllt. SMAP führt zu einem sehr guten Ergebnis, das sich in sehr hohen R^2-Werten (0,96, 0,88 und 0,97) und (0,85, 0,94 und 0,94) für Samsam und Kilo-6 widerspiegelt, und erfüllt die von der SMAP-Abrufdomäne angestrebte Genauigkeit mit einem ubRMSE von 0,04 m^3m^{-3} oder besser an allen Standorten und kleinstmöglichen Fehlern (MBE, MABE und RMSE). Es wird die Möglichkeit erörtert, das SMAP-Produkt zur Messung der landwirtschaftlichen Trockenheit und ihrer Auswirkungen auf das Pflanzenwachstum während verschiedener Wachstumsstadien an beiden Standorten und im gesamten CCP zu verwenden.

Die Anbauflächen befinden sich in der tropischen Savanne (AW Kategorisierung nach der Köppen-Klimaklassifikation), im warmen semiariden Klima (BSh) und im warmen Wüstenklima (BWh). Bei den betreffenden Gebieten handelt es sich überwiegend um landwirtschaftlich genutzte Regenfelder, die vulnerabel gegenüber dem Klimawandel und Klimaschwankungen sind. Die Daten der Climate Hazards Group Infrared Precipitation with Station (CHIRPS), (SMAP) an der oberen Bodenoberfläche und in der Wurzelzone sowie der aus (SMAP) abgeleitete Soil Water Deficit Index (SWDI) wurden mit dem Normalized Difference Vegetation Index (NDVI) verglichen. Die Ergebnisse zeigen, dass die NDVI-Werte nicht mit den Niederschlagsmustern auf der Dekadens-kala übereinstimmten. Bei allen Isohyeten zeigte der SWDI in der Wurzelzone eine zuverlässige und erwartete Reaktion bei der Erfassung der

jahreszeitlichen Dynamik in Bezug auf den Vegetationsindex (NDVI), über warmem Wüstenklima(BWh) in den Jahren 2015 - 2019. Es wurde festgestellt, dass der SWDI zur Überwachung der landwirtschaftlichen Trockenheit besser geeignet ist als die Niederschlagsdaten und die SMAP-Daten selbst, da sich dieser Index direkt auf den verfügbaren Wassergehalt der Pflanzen bezieht. Die Verwendung des SWDI zur Überwachung von Dürre in der Landwirtschaft ist eine vielversprechende Methode zur frühzeitigen Dürrewarnung, die für das Risikomanagement von Dürre in semiariden Klimazonen genutzt werden kann.

Der Vergleich zwischen Sorghum-Ertrag und räumlich verteiltem Wasserhaushaltsmodell wurde nach der Länge der Wachstumsperiode bewertet: spät reifende (120 Tage), mittel reifende (90-95 Tage) und früh reifende Sorten (80-85 Tage). Der Wasserbedarfsindex (Water Requirements Satisfaction Index, WRSI) ist ein einfaches Modell für die Evaluierung des Wasserdefizits von Kulturpflanzen und wird häufig in Frühwarnsystemen für Dürre und Hungersnöte verwendet. Er ist ein Indikator für die Leistung der Pflanzen, der auf der Verfügbarkeit von Wasser während einer Wachstumsperiode basiert. Es wurde ein angepasster WRSI-Index entwickelt, um die Auswirkungen der Verwendung verschiedener klimatischer und bodenfeuchtebezogener Fernerkundungsdaten wie CHIRPS-Regen, und SMAP-Bodenfeuchte in den oberen 5 cm und in der Wurzelzone sowie MODIS-Evapotranspiration auf die wichtigsten Parameter und Ergebnisse des WRSI-Index zu untersuchen. Die Ergebnisse der Analysen zeigen, dass SMAP den Beginn der Saison und die Länge der Wachstumsperiode, die für den WRSI-Index entscheidend sind, am besten erfasst. Darüber hinaus wurden Anbauszenarien für Sorghums orten mit kurzer, mittlerer und langer Wachstumsdauer betrachtet und die simulierten WRSI- und Modell-Ergebnisse mit den gemeldeten Erträgen im Staat El Gedaref verglichen. Es wurde festgestellt, dass mehr als die Hälfte der Ertragsschwankungen durch Wasserstress erklärt werden kann, wenn der SMAP-Datensatz in der Wurzelzone im WRSI-Modell verwendet wird (R^2=0,59-0,72 für Sorghum-Sorten mit einer Wachstumsdauer von 90-120 Tagen). Insgesamt zeigen CHIRPS und SMAP für die Wurzelzone die höchste Genauigkeit (R^2=0,53-0,64 bzw. 0,54-0,56) bei der Erfassung von Ernteertragsver-

lusten auf Ebene des Bundesstaates im Zusammenhang mit saisonalen Bodenfeuchtigkeitsdefiziten, wodurch die Effizienz von Dürrefrühwarnungen und agrarmeteorologische Risikoabschätzungen entscheidend verbessert wird.

Die Ergebnisse dieser Forschungsarbeit sind wichtig und nützlich für die kontinuierliche Entwicklung und Verbesserung der satellitengestützten Bodenfeuchtigkeitsmessung, um Bodenfeuchtigkeitsprodukte mit höherer Genauigkeit in semiariden Regionen bereitzustellen. Die Ergebnisse tragen auch dazu bei, das Bewusstsein der verschiedenen Interessengruppen für die Auswirkungen von Dürre auf die landwirtschaftliche Produktion zu schärfen und die Notwendigkeit von Anpassungsmaßnahmen zur Abschwächung der negativen Auswirkungen von Dürre zu verdeutlichen.

CHAPTER 1. Introduction

1.1. General Background

More recently, raising public awareness and appreciation of the issues linked to global climate change has grown in all sectors. Although massive efforts about climate change's potential influences and consequences have been made, there are inconclusive findings to move people to action on climate change impacts. With the availability of regional water resources, many researchers have suggested that climate change intensifies the magnitude and severity of extreme climate events such as droughts (Mirza, 2003).

In addition to the undoubted jeopardy to future water supplies induced by climate change (Brown et al., 2019), Extreme population growth (Gude, 2017), rapid urban expansion (Elliott et al., 2014), and demands for nature conservation have put additional stress on local water supplies in many regions (Liu, Jensen, 2018). Climate change exacerbates competition for already threatened water resources. As a water shortage-induced, Agricultural drought events have been demonstrated to adversely affect global agricultural production (Meza et al., 2020). Since soil moisture is strictly associated with agricultural droughts, the broad definition of agricultural drought revolves around insufficient soil moisture in the root zone to support average crop production (Hazaymeh, K. Hassan, 2016, Meliho et al., 2019, Wu et al., 2016).

Agricultural drought occurs at a critical time during the different growing stages of a crop and adversely affects crop production (Gebrehiwot et al., 2016). No direct link between climate change and drought. Climate change affects factors that accelerate the hydrological processes to be more intense (Mukherjee et al., 2018) and, thus, likely drive the meteorological drought. The latter originates from a shortage of precipitation and can bring many more types of droughts (Wu et al., 2016).

In the literature, the term drought has been used from an interdisciplinary perspective, especially in geography (Kabanda, 2017), agro climatology (Elagib et al., 2019b), sociology (Ternes, 2019), Anthropogenic (van Loon et al., 2016), pathology (Showalter et al., 2018,

Sinha et al., 2019), Epidemiology - COVID-19 (Arora, Mishra, 2020), with more focusing on climate affect studies. Because of the interaction between drought and different human factors, drought event means other things to diverse groups. Drought issues are tackled from various interpretations, differing mainly in their contents and implications. Several studies rank drought first among all disastrous and costliest natural hazards by the significance of its impacts, such as the loss of crops and livelihoods (Erfurt et al., 2019), Drought adversely affects the economy and harms the environment.

1.2. The potential of Rainfed Agriculture

Roughly 80% of the World's agricultural area relies on rainfed cropping systems (Valipour, 2013), this system generates about 60% of the food and nourishment demand of the World's population (Biradar et al., 2009). Rainfed cropping systems will continue dominating the bulk of the World's food production. The importance of rainfed agriculture differs regionally but produces most food for poor communities in developing countries. In sub-Saharan Africa (SSA), more than 95% of the farmed land is rainfed. In comparison, the corresponding figure for Latin America is almost 90%, South Asia about 60%, East Asia 65%, and the Near East and North Africa 75% (FAOSTAT, 2005).

Among 37 countries in the World that depend on food aid, there are 28 African countries. In 2017, the population in SSA increased by approximately 2.7 % compared to 2016 data (Statista, 2020), with food production at less than 2%. The World Bank estimates that if the current trends in population growth and food production continue, By 2030, most African countries are projected to bear the major burden to feed their population. Poverty and the number of underfed children will grow accordingly (Per Pinstrup-Anders, 2001). Currently, Africa is the second-largest populous continent after Asia, approximately 1.2 billion people live in Africa, and almost 226.7 million people suffer from chronic hunger. More than 60% of malnourished Africans live in eastern Africa. On the other hand, according to Inter Academy Council (IAC), West Africa has countered the trend in the rest of the continent, with malnutrition falling dramatically in recent years Food Policy (IAC, 2004). Compared to Asia, agriculture in Sub-Saharan Africa is predominantly rainfed and accounts for 95% of the total farmed land. The farming systems are diverse, and livestock is an essential part of the farming

systems. It is envisaged that it enhances the productivity of maize and rice. The rainfed agriculture lands in SSA are facing a projected increase in water stress and food insecurity (Hadebe et al., 2017), its impacts will be short-term, resulting from more frequent and more intense extreme weather events, and long-term, caused by changing temperatures and precipitation patterns. Cereal crops have the lion's share in the total cultivated crops (Hadebe et al., 2017), and rainfed agriculture is pretended to be more susceptible to drought events (Alemaw, Simalenga, 2015, Vanschoenwinkel, van Passel, 2018). In these fragile ecosystems, drought is emphasized as one of the significant sources of the challenge for food security (Ahmed, 2020), livelihoods (Anderson et al., 2021), and yield gap of important rainfed crops in Sub-Saharan Africa (Rattalino Edreira et al., 2021).

1.3. The Agricultural Sector of Sudan

Agriculture in Sudan is practiced mainly through three different systems: irrigated farming system, rainfed mechanized, and farming with traditional rainfed subsectors. Irrigated agriculture accounted for an average of about 21% of the value of total agricultural production between 1991 and 1999. Rainfed agriculture accounts for 90% of the total area under cultivation in Sudan; mechanized rainfed agriculture accounts for 6.3%, and traditional rainfed agriculture 12.5% (Table 1-3). Pastoralism (predominantly livestock production in traditional rainfed areas) has always been classified as a separate farming system, even though livestock is integrated with other farming systems, particularly conventional rainfed farming. From 1991 to 1999, the average value of livestock production accounted for about 47% of the total value of agricultural production.

1.3.1. The Irrigated farming system

Irrigated farming plays a pivotal role in the country’s agricultural production, of which the gravity-fed Gezira scheme of 840.000 Hectares is the most important (Khalifa et al., 2020). This system has been one of the pillars of agricultural development strategy. At independence on 1 January 1956, Sudan had approximately 840.000 Hectares. The irrigation system has been a primary source of export revenues. This sector produces 95% of the long-stable finest cotton, produces 100% of sugarcane, 15% sorghum grains, and 32% Sudanese groundnuts.

Other main irrigated crops are fodder, wheat, and vegetables, with other crops comprising maize, sunflower, potatoes, roots and tubers, and rice. There are 1.68 to 2.1 million hectars of land under irrigation . This sector is dominated by large national schemes like Gezira, New Halfa, Rahad, and Sugar schemes; tenancy sizes in the irrigated schemes range from 4.2 to 16.8 hectars. The main crops grown under irrigation include cotton, sugarcane, sorghum, groundnuts, wheat, legumes, fruits, vegetables, and irrigated fodder. The sub-sector contributes 100% wheat and sugar, about 99% cotton, 52% groundnut, and 25% sorghum produced in Sudan. Recent years have witnessed a rapid increase in modern irrigation techniques.

1.3.2. Mechanized rainfed farming system

This farming system began in the central clay plain during Second World War and is concentrated in El Gedaref, Blue Nile, White Nile, Sennar, and Southern Kordofan states. The total annual area has increased rapidly from less than 840.000 hectars during British colonization to an average of about 6.5 million hectares, with an average farm area of 420 hectars. The main crops grown in this sector are sorghum (representing the major crop), with forecast production at about 4 million tons (FAO, 2019), sesame seeds, and cotton. Mechanized farming accounts for about 65% of sorghum, 53% of sesame, 5% of millet, and almost 100% of sunflower produced in Sudan. Historically, this sub-sector has been a source of sorghum exports and meeting internal needs, particularly in urban areas (MEPD, 2003). This farming system reveals very wide annual instabilities due to unpredictable amounts of rainfall, which can result in late planting, and prolonged dry spells.

1.3.3. The Traditional Rainfed Sub-Sector

According to (Abdalla and Abdel Nour, 2001), 75% of the total population of Sudan lives in this sector. This sector includes nomadism, transhumance (traveling with animals and cultivating short-maturity survival crops), and sedentary farming, including many livestock. Although there is some traditional rainfed farming in each state, the system is dominant in the States of Kordofan, Darfur, El Gedaref, Sennar, Blue Nile, and White Nile. The total cropped area in this system varies from 5.040.000 to 8.820.000 million hectars which varies annually with variations in rainfall. Crops grown are sorghum, sesame, and cotton in clay soils, millets,

and groundnuts in sandy soils; the sector is also a significant producer of Gum Arabic and animal wealth. Out of the country's total production, this sector contributes 92% millet, 50% groundnuts, 28% sesame, 5% sorghum, and almost all gum Arabic.

1.4. History of drought in Sudan

With an area of 1.886.068 million km^2, following Algeria and the Democratic Republic of Congo, Sudan ranks number three in the African continent in terms of size. The majority of Sudan is a gently sloping vast plain covered by croplands, rangelands, open shrublands, and mixed forests. The country's north and northwest are primarily part of the Sahara desert (Ritchie, Haynes, 1987), shifting gradually to semi-desert, low-rainfall savannah, and high-rainfall savannah towards the south (Mahmoud, Obeid, 1971). Rainfall varies greatly from north to south, from 25-700 mm, and falls in 2-5 months between June and October, with temperatures ranging from 30-40ºC in summer and 10-25ºC in winter. The Nile water basin contributes most of Sudan's available surface water. They are discharging about 84 billion (109) cubic meters of water annually, as estimated at the High Aswan Dam (Mallakh, 1959). However, only 18.5 billion cubic meters of this may be used in Sudan following the 1959 water use agreement with the Arab United Republic "Eygpt and Syria" (Whittington et al., 2014)

Table 1-1 Climate of the mechanized rainfed sector (World Development Report 2006, 2005)

Parameter	Semi-arid zone	Semi-humid zone
Annual rainfall (mm)	500-600	600-800
Length of the season (days)	100-120	120-150
Beginning of the growing season	3rd week June	1st week June
End of the growing season	1st week October	1st week June
No. of rainy days	45-50	60-70
Max. temp (ºC)	31-34	30-33
Min. temp (ºC)	21-22	20-22
Diurnal range of temp (ºC)	10-12	10-11
Relative Humidity at 06 a.m. (%)	70-80	80-90
Relative Humidity at noon (%)	45-55	55-65
Solar radiation (cal/cm^2/day)	500	450
Sunshine duration %	50-60	45-55
Potential evapotranspiration (mm/day)	5	4-5

Throughout Sudan's history, years of drought have left catastrophic famine events. Table (1-2) outlines drought and famine caused by locust invasion, mouse attacks, cholera pandemics, and other causes. The earliest famine to be documented by historians occurred in the Kingdom of Sennar in 1684 (Mercer, 1971). The 1835-38 period is known as the "years of famine" (Spaulding, 1982), especially the year 1836, which witnessed a high propagation of the cholera epidemic that killed a population already weakened by hunger (Mengel et al., 2014). The 1888-89 famine, also called "Sanat Sittah," has been said to be an extreme famine caused by two successive years of rains failure (Slatin, 1896) and by political instability and unrest. Hundreds of thousands people perished from hunger and disease. Rain rates were high in the following season; however, crops were destroyed by locusts, swarms, and other pests.

In the 20th century, Sudan suffered severe droughts that affected several parts of the country. 1913 witnessed a devastating drought caused by rain shortages (G. T. Renner, 1926), but major famine was avoided by importing cereal and distributing it free (Baily, 1935). The directory of the 1984-1985 famine emphasizes that drought is the leading causing factor in famine in Sudan (Ibrahim, 1988). It's not an overstatement to say that the worst famine in the history of Sudan occurred during 1984-1985 (Ibrahim, 1988). It generally affected the people of western Sudan in Darfur and Kordofan as a response to the drought (Locke, Ahmadi-Esfahani, 1993).

The displacement and localized famine prompted United States Aid (USAID) to spearhead the emergency supply of food (Keen, 1991). Farmers identified 36 years of drought and famine between 1912 and 1974, 26 years in eastern Kordofan, and 18 years east of Darfur. Eight of these years were common to both areas. Seventeen of these years were given local names to describe sources of survival, scarcity of necessities, and magnitude of toleration. Fifty percent of these perceived periods of drought were meteorologically confirmed, with rainfall well below average. Records of rainfall failed to recognize the other years, perhaps, according to Ibrahim, (1988), because of the nature of rainfall in semi-arid areas where rain is highly localized or because the recall of events by local inhabitants may need to be corrected. According to the latest estimates of the Food and Agriculture Organization of the United Nations

(FAO), more than 700 million people will have been exposed to severe undernourishment and food insecurity by 2018.

Soil moisture fundamentally influences water and energy exchange at the land surface-atmosphere interface and, thus, is one of the critical variables in various disciplines, such as hydrology and agricultural sciences. It is the primary source of water for crops and natural vegetation. Therefore, good quality soil moisture datasets at various scales are prerequisites to sustainable land, crop, water management, and land surface algorithms. A drought phenomenon is a gradual, not avoidable, process predominantly followed by long-lasting catastrophic consequences. Given the diverse types of droughts, the methods used to describe agricultural drought mainly revolve around monitoring available soil water content and crops' later unmet water demand (Zargar et al., 2014). Drought conditions have been demonstrated to be adversely affecting agricultural yield (Elagib, 2014).

Table 1-2 Sudan's history of documented famine due to drought and other causes

Years of Drought or Famine	Name and Damage	Areal Extent	Source
1684	"Um Lahm" The great famine	Sinnar Kingdom (1504-1821)	(Fisher, 1976)
1835-38	Years of famine	Central Sudan	(Brokensha, Hill, 1971)
1836	Cholera spread over the country	Central Sudan	(Brokensha, Hill, 1971)
1885	Slight famine	Central and eastern Sudan	al-Gudal (1983)
1888-89	Due to a year without rain, hundreds of thousands perished. Crops failed, food became increasingly scarce, cereal prices increased, and people sold their children as slaves to save their lives before later buying them back at higher prices.	Central, northern, eastern, and western Sudan,	(Slatin, Carl, 1896) Duncan (1952) (Farwell, 1967) (Churchill, 1889)
1888-89	Thousands died of hunger and disease	Central, northern, eastern, and western Sudan	(Baily, 1935)
1890	Locusts and mice consumed the products	The Nile area	Farwell (1967) Duncan (1952)
1913	A lack of rain, free distribution of cereal in places of hardship and cheap prices elsewhere, and cereal imported from India	Mainly northern Sudan	MacMichael (1934)
1914	"The year of the flour" (flour brought from India because of insufficient rains)	Central Sudan	Henderson (1965)
1927	Minor famine	Central and eastern Sudan	al-Gudal (1983)
1984-85	Animal herd mortality rises, and human migration. The Sudanese government requested immediate assistance from international organizations.	Western Sudan, Kordofan and Darfur	(Helen Young, Musa Adam Ismail, 2019)

Estimating the soil moisture content is very important for water-budgeting such as agricultural applications. Soil moisture information can be used as an indicator for the prediction of agricultural drought. The importance of soil moisture is partitioning water and energy balance between soil and atmosphere (Brocca et al., 2015). The United States Department of Agriculture (USDA) has used soil moisture as a fundamental data source to monitor crops' growth stages and agricultural yield (Bolten et al., 2010). Most studies conducted to investi-

gate the agricultural drought in the African Continent were concentrated only on meteorological aspects, with less attention paid to soil moisture parameter which describes the agricultural drought.

1.5. Aim and Scope of the Study

1.5.1. Research questions and concepts

For underpinning human survival on our planet, it is a must to connect people with nature to achieve sustainable management of land resources. Negligence of these resources jeopardizes pivotal nature's contributions to people, endangering the supply of universal food security. To reverse this picture, it is crucial to transfer people's actions to sustain agriculture to secure food production. This transformation had already begun in 2015 when the world launched commitments to end all forms of hunger, starvation, and malnutrition (Cohen, 2019, Renzaho et al., 2017), through the Sustainable Development Goals (SDGs) by 2030. Luckily, the (SDGs) included significant agriculture and food production.

The (SDGs) recognize explicitly that sustainable agriculture has been embedded deeply with other (SDGs) targets (Streimikis, Baležentis, 2020). The interlinkages among sustainable agriculture, empowering small farmers, promoting gender equality, ending rural poverty, ensuring healthy lifestyles, tackling climate change, and other issues addressed within the set of 17 (SDGs) in the Post-2015 Development Agenda. There are many threats to progress. The Post-2015 publishing used to conduct this study still shows that climate variability and change undermine efforts to eliminate hunger.

The world must be on the right track to ending hunger by 2030. If recent trends continue, the number of hungry, starving, and undernourished people will surpass %10 of the world population by 2030 (Mason-D'Croz et al., 2019). Unpredicted the impacts of the COVID-19 pandemic on agricultural workers (Luckstead et al., 2021), the invasion of desert locusts in horn and eastern Africa may be obscuring those estimates by devastating the livelihood and food security (Kinyuru, 2021).

Sudan is predominantly an agriculturally dependent country; given that the country is endowed with vast arable lands, 80% of the total land cover is suitable for crop production. The land between 400 and 800 mm of rainfall is considered the belt of rainfed agriculture, with a total area of 67 million hectares, nearly 70% of which is considered suitable for crop cultivation (El Karouri, 2010). Cereal crops play an essential role in the life of the country's indigenous people, who massively depend on them for their food demands. Agricultural drought is the primary constraint affecting crop yield.

There are no-exist studies on monitoring agricultural drought using remote sensing soil moisture products. Furthermore, a big challenge for drought monitoring is that there needs to be more consistency in the globally accepted drought indices. The applicability of particular drought indices depends on a specific region, season, and application (Hao et al., 2017a).

Poorly distributed and sporadic agro-meteorological stations and uncertainties about the data acquired from existing unsophisticated meteorological stations.

From the viewpoint mentioned above, relevant research questions to be undertaken by this study are:

1. What kind of data on agricultural drought studies is needed?
2. How does agricultural drought impact crop productivity?
3. Which drought indices are better for evaluating the agricultural drought post-launching of remote sensing soil moisture products?
4. Can advanced technology (i.e., RS and GIS) improve the seasonal forecasting of agricultural drought?

1.5.2. Research objectives

The main goal of this study is:

To understand the amount of available SM in the surface and the root zone and their impacts on the agricultural drought of El Gedaref State.

The specific goals are fivefold:

- Validate the SMAP L4 3-hourly soil moisture product provided by NASA against ground soil moisture measurements;
- Evaluate the relationship between soil moisture obtained by Soil Moisture Active Passive SMAP, rainfall, and Normalized Difference Vegetation Index (NDVI) dynamics;
- Obtain crops' available water content from a new SMAP-derived Soil Water Deficit Index (SWDI).
- Asses the agro-meteorological risk on sorghum production and;
- Characterize the Spatio-temporal variation in the timing of the onset of the growing season using the length of the growing season and end of the growing season available soil moisture content.

Different ways were used in this study to obtain data. We used open sources remotely sensed (RS). These datasets provide a solution for regions where there is no existing data. Near real-time Soil Moisture Active Passive (SMAP) in the surface and the root zone, Normalized Difference Vegetation Index (NDVI), rainfall, land use, and land cover (LU/LC), soil Field Capacity (FC), and soil Permanent Wilting Point (WP).

For validation, in-situ measurements were conducted from July to October, the growing season, during the rainy season of 2018, to measure SM correctly and create a harmonized and comparable dataset of soil moisture to be validated with SMAP level-4 SM product.

1.6. Structure of the Thesis

This thesis consisted of five chapters; aside from the introduction and conclusion chapters, three deal with the four research questions listed in (section 1.2.1).

Chapter 1-Introduction:

This chapter provides an overview of the focus problem of the current research. Besides, it gives information about the objectives and the research questions.

Chapter 2- Validation of SMAP soil moisture product over agricultural land of Sudan:

This chapter provides a general overview of the current status of the remote sensing soil moisture products. It delivers information on the various validation methods and the adequate ones for the countries with sporadic agro-meteoroidal stations, such as the case of Sudan.

Chapter 3- Available soil moisture and drought threshold of different climatic zones of El Gedaref State:

This chapter compares moisture availability depending on different physical soil properties, such as soil field capacity and permanent wilting point. These parameters are essential and vary with soil texture. Such comparison will enable us to know the plant's available water and the rate at which crops are depleting this water. Then, we can determine the crop water requirements.

Chapter 4- Does soil moisture compensate for the evapotranspiration demand of sorghum in El Gedaref State?

This chapter depicts crop performance based on water availability to different sorghum varieties during their growing season.

Chapter 5- conclusion

The study was concluded in chapter five. A summary of the findings of the study was provided, its theoretical contributions, and some recommendations for future studies and policy for sound, sustainable and scientific management of our shared natural resources.

1.7. Overview of the study site

As a case study, El Gedaref state of Sudan is predominantly agricultural, and rainfed mechanized agriculture was initiated during the 1940s. The rainfed sector of El Gedaref state has advantages due to its high potential to support the national food supply. Its central clay soil is appropriate for sorghum cultivation, considered the primary staple food for most Sudanese people. Its production can also support in-come gain with exportation. According to the Food and Agriculture Organization of the United Nations (FAO), 9.6 million people in Sudan are facing worse levels of acute food insecurity in 2021.

1.7.1. The geographical location

El Gedaref state (Figure 1-1), one of the seventeen states of Sudan, is located between longitudes 33° 34- and 37°E and between latitudes 12° 40- and 15° 45 N. El Gedaref state borders four other Sudanese states, namely Kassala state to the north, Khartoum state to the northwest, Gezira state to the west, and Sennar state to the south. The total area of El Gedaref state is approximately 72,000 km^2. It has been divided administratively into eight localities: El Fashaga, El Faw, El Gallabbat East, Basonda (added recently), El Gal-labbat West, El Gedaref, Rahad, and El Butana (Elhadary, 2010). Available literature has shown that the introduction of Mechanized rain-fed farming in El Gedaref State and Sudan dates back to the early 1940s (Sulieman, Buchroithner, 2009). It started with 8820 hectars and now reached 3.360.000 million hectars.

The Mechanized Farming Corporation of Sudan (MFC) used to play a role in facilitating credit securing and determining the lease period of (25 years) as a maximum period, and lately, ensuring that (10%) of land leased should be allotted for tree planting around the scheme (Elhadary, 2010) This 10 percent shelter belt aims to enhance soil fertility and mitigate the impacts of torrents flush floods (UNDP, 2007). Technically, the distribution of mechanized schemes to investors is based on the idea of determining a rectangular area divided into plots of 420 hectares (later increased in some places to 630 hectares) each, half of these plots were rented to farmers. The rest is left as fallow. After four years, private farmers had to exchange the formerly rented land together with fallow plots to allow the soil to recover its fertility and rejuvenate.

1.7.2. Physical environment

Crop production depends on several associated environmental factors, such as rainfall and temperature (Bali, Singla, 2021), and agronomic factors, such as nutrients and land preparation (Rempelos et al., 2020). Unlike the agronomic factors, which are controllable and manageable, the environmental factors, particularly climate, and soil, are uncontrollable under normal conditions. Although it is difficult to modify the environmental factors, it is possible to mitigate their adverse impacts on crop production by applying suitable crop management

practices. Henceforward, an adequate understanding of the environment and its various aspects and limitations are essential for enhancing crop production in the mechanized rainfed sector. The following is an appraisal of the two most crucial components of the region's physical environment (climate and soil) and their effect on crop production.

1.7.3. Climate

The current and projected expansion in mechanized rainfed agriculture lies within the southern part of the semi-arid climate zone with 500-600 mm annual rainfall and the semi-humid climatic area of 600-800 mm annual rainfall (Hussein M. Sulieman, 2010). North El Gedaref and El Demazin are representative sites of the semi-arid and semi-humid climatic zones, respectively.

Table 1-1 summarizes the two climatic zones' climatic conditions during the rainy season (World Bank, 2005). However, projections more considerably indicate increased variability and unpredictability in seasonal rainfall and increased occurrences and intensity of drought. Differences in the rain and other climatic factors should be taken into consideration in discussing the potential productivity in each of the different sites within the considerable land area covered by mechanized rainfed agriculture and not treating all sites as identical units.

Climate significantly affects all phases of agricultural activities, from initial seedbed preparations to harvesting. Knowledge of the climate is essential for selecting appropriate crops and cultivars and optimal inputs which meet crop requirements for commercial and sustainable productivity.

1.7.4. Rainfall

Rainfall is the main driving element for successful farming under dry land farming, such as in semi-arid regions; it determines the most suitable crop cultivars and their productivity (Chaves et al., 2016). Adequate moisture is the most important climatic factor of productivity and becomes the ultimate objective for farmers in the rainfed sector (A. T. Ayoub, 1999), sufficient soil moisture is considered one of the main requirements for an optimum crop sowing date (Bussmann et al., 2016b). However, with the possible introduction of conversation tillage into the region, more moisture could be available to the crops. According to (Wesely

and Hicks, 2000), if modern soil moisture technology is applied, the rainfall could be adequate and conducive to high productivity and profitable farming.

Mechanized rainfed agriculture in Sudan is practiced mainly in areas between 400 mm and 800 mm isohyets. The rainy season in these areas occurs in a well-defined season that extends from June to the first week of October. It starts with light to medium showers in May and June, followed by heavy rains in July and August. In September, it starts to slacken down to less intense storms before it ends up towards the middle of October. The amount of rainfall in the mechanized rainfed sector differs according to the location, as shown in Table (1-3), which gives the average monthly and annual rainfall of three major centers of mechanized rainfed agriculture (Adam, 2000).

Rainwater is the primary source of safe drinking water and sanitation for El Gedaref and the rest of the state's localities (Ibrahim, 2009). Different water harvesting techniques have been used to utilize the rainwater (Figure 1-1), such as "Hafir" [local name for an artificial impoundment with its embankment that collects, stores, and supplies water for humans, farm machinery, and livestock during the dry periods]. Rooftop rainwater harvesting can be used for household consumption. It offers self-sufficiency to the water supply. The ground-based rain gauge networks in the rainfed sector of Sudan are sporadic. Farmers are using predominantly not sophisticated rain gauges made by local ironsmiths. The main problem of such meters lies in providing less accurate estimates. The commonly purple/pinky witchweed root parasitic plant (Striga hermonthica) is spreading in the rainfed sector of Sudan. It causes tremendous damage to its favorite host, "sorghum" the infected plants are accompanied by stunted biomass. Striga exudates cause a significant reduction in sorghum yield in sub-Saharan Africa (Kountche et al., 2019).

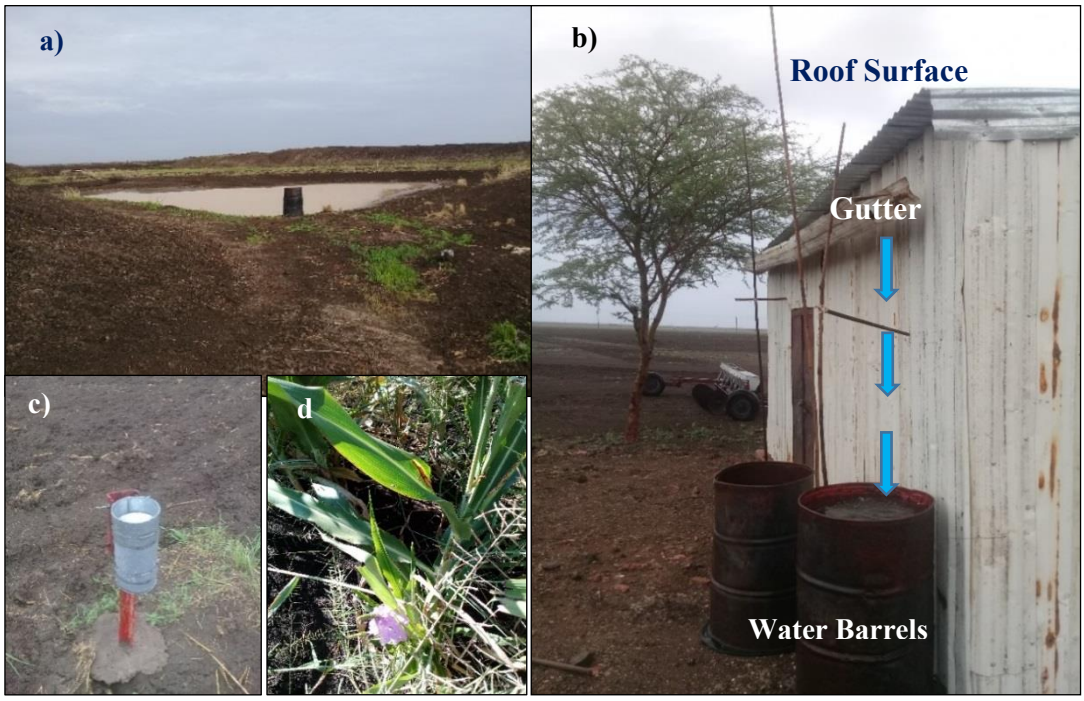

Figure 1-1 Overview of the study sites: Hafir system a), rooftop water harvesting b), traditional rain gauge c), and striga plant d), photos taken by Elmoiz Taha, rainy season

1.7.5. Soil

Undoubtedly, crop production's success or failure is determined by the soil's general makeup. The soil provides the crops with nutrients, water requirements, physical support, and other physiological needs. Depending on the soil's weakness or strength in delivering the conditions for healthy growth and development, certain soils are considered more suitable for crop production than others.

The soils of the CCP are extensively dark-colored and belong to the order of Vertisols (Figure 1-3). They are synonymous with black cotton soils, dark cracking clays, regulars, and grumusols of earlier classification. According to FAO-UNESCO estimates (Batjes, 1997), the Vertisols of Sudan cover an area of about 63 million hectars. One 42 million hectars of which receive considerable rainfall. Most of these soils have developed from the weathering of the local rocks of the Ethiopian highlands and dropped to the Sudan plains (Deckers et al., 2001) The sediment load was carried and laid down by the Blue Nile, Rahad, and Dinder rivers. The Blue Nile average sediment load was quantified between 130 and 170 million tons/year

(ALI et al., 2014). In some locations, the Vertisols had a different mode of formation, like the soils of southern El Gedaref, which has developed in situ from the local weathering products of the colluvial material of El Gedaref/Galabat ridge.

Due to their vertisolic nature, the soils of the CCP are characterized by some unique morphological, physical, and chemical properties which distinguish them from other soil types in Sudan. In the dry season, the upper layer of the profile breaks into dry, hard, vertical prismatic blocks separated by cracks with rough cleavage. The general account of this soil is given by (A. H. Bunting and J. D. Lea, 1962, Magboul Musa Sulieman, Ibrahim Saeed Ibrahim, 2013, VOS t. N. C., VIRGO, 1969, Worrall, 1961), and soil survey administration reports.

1.7.6. The roads network and transportation

Significant parts of El Gedaref state suffer from decay and deterioration of physical infrastructure, particularly in road systems and transportation (Figure 1-4). Every year, the accumulated rainwater cuts off almost the cracked localized potholes and asphalted and graveled roads, isolating several villages in the state (Mueller et al., 2007). Vehicle trucks cannot carry commodities, and passengers unable to leave and enter most parts of the state.

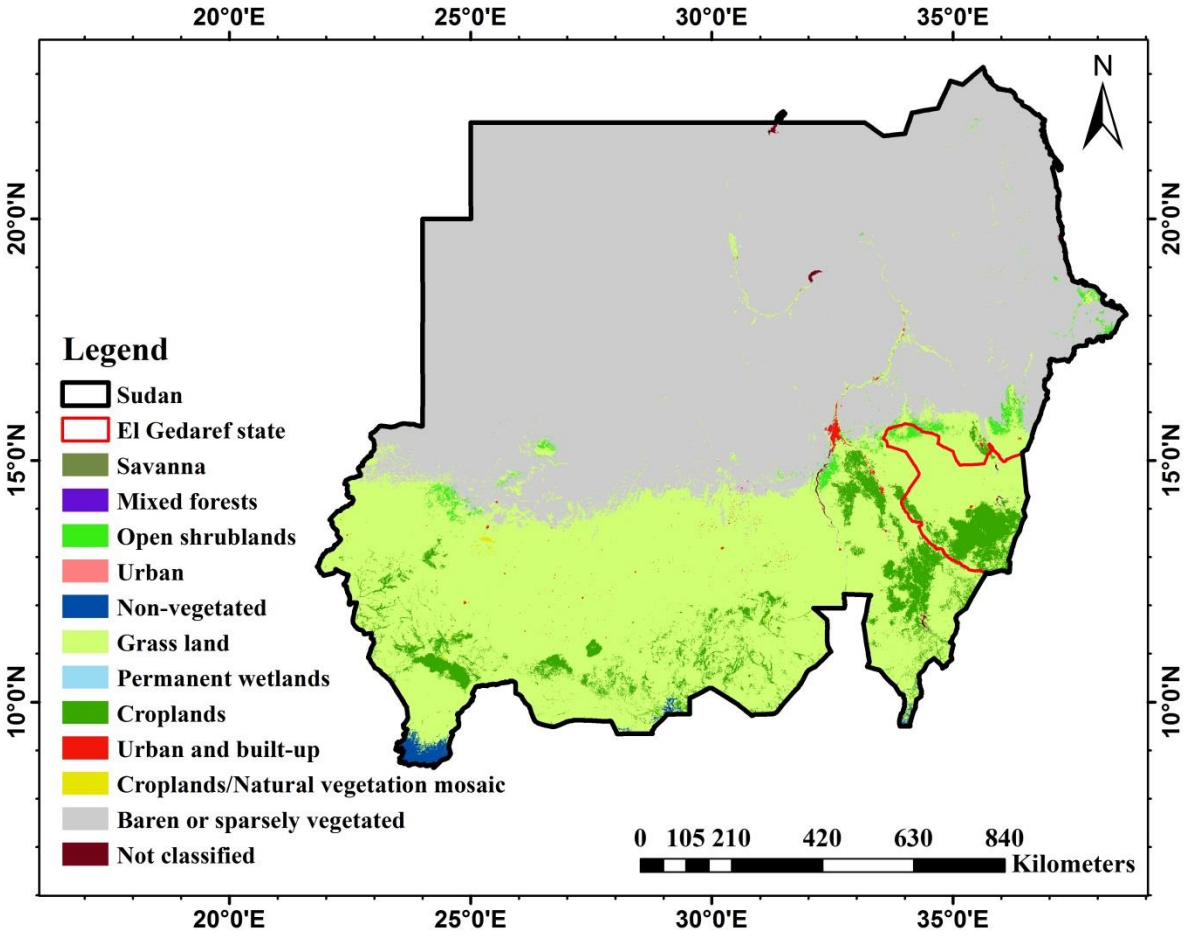

Figure 1-2 Sudan Land use/Land cover classification 2019, source: landsat time series composite, https://earthexplorer.usgs.gov

Figure 1-3 Soil of the central clay plain (CCP) of Sudan, classified by FAO-UNESCO as dark cracking black cotton soils, image taken by Elmoiz Taha during the rainy season of 2018 at Samsam, Rahad river basin, El Gedaref State, Sudan

Figure 1-4 Accumulated rainwater makes towns, villages, and agricultural lands inaccessible in El Gedaref state, images taken by Elmoiz Taha during the rainy season of 2018

Table 1-3 Sudan - Cereal production by sector ('000 tonnes)

Sector	Sorghum					Millet					Wheat				
	5-yr average 2014/15-2018/19	2018/19	2019/20	2019/20 as % 2018/19	2019/20 as % 5-yr average	5-yr average 2014/15-2018/19	2018/19	2019/20	2019/20 as % 2018/19	2019/20 as % 5-yr average	5-yr average 2014/15-2018/19	2018/19	2019/20	2019/20 as % 2018/19	2019/20 as % 5-yr average
Irrigated															
Total	692	627	646	103	93	7	4	4	105	62	544	696	723	104	13
Semi-mechanized															
Total	2667	2498	1394	56	52	93	48	65	135	70	-	-	-	-	-
Traditional rainfed															
Total	1580	2310	1968	85	125	1243	2595	1064	41	86	5	4	4	100	80
Gra.total	**4939**	**5435**	**4008**	**245**	**270**	**1343**	**2647**	**1133**	**281**	**218**	**549**	**700**	**727**	**204**	**93**

CHAPTER 2. Validation of SMAP product over agricultural lands of Sudan

2.1. Introduction

There are different techniques used to estimate soil moisture. These techniques are divided into three categories, in situ soil moisture measurements, hydrological land surface modeling, and remote sensing. However, the in situ soil moisture measurement is the most accurate. This technique damages natural ecosystems (Robinson et al., 2008). Consuming a lot of time to measure soil moisture at the exact location (Bernard et al., 1984), and it is costly to measure soil moisture at a large scale (Evan J. Coopersmith et al., 2015). The major limitation is that it provides point measurements and does not account for sm spatial variability (Myeni et al., 2019a).

The precision of remote sensing soil moisture algorithms requires weather and meteorological information. This information is very scarce in many regions of the planet due to sporadic operational meteorological stations (Hazra et al., 2019) Therefore, soil moisture data are only available in some parts of the world; owing to that reason, it becomes hard to implement techniques and algorithms related to remotely sensed soil moisture estimation. In the earlier times, when the new technologies did not become sophisticated, the farmers were using conventional methods to know how much soil moisture existed in the soil profile from the texture of the soil. They tried to guess the soil moisture content.

2.1.1. Drought definition

Drought is a slowly not avoidable process occasionally followed by long-lasting devastating consequences across large regions. Drought is characterized by below-normal precipitation for months to years. It is a temporary dry period, in contrast to the permanent aridity in arid areas. It occurs in most parts of the world, even in wet and humid regions (Dai et al., 2015). Drought is defined as a dry period relative to its local normal condition.

The precision of remote sensing soil moisture algorithms requires weather and meteorological information. This information is very scarce in many regions of the planet due to sporadic

operational meteorological stations (Hazra et al., 2019) Therefore, soil moisture data are only available in some parts of the world; owing to that reason, it becomes hard to implement techniques and algorithms related to remotely sensed soil moisture estimation. In the earlier times, when the new technologies did not become sophisticated, the farmers were using conventional methods to know how much soil moisture existed in the soil profile from the texture of the soil. They tried to guess the soil moisture content.

On the other hand, arid regions are prone to drought (Surendran et al., 2019), because their rainfall amount critically depends on intermittent rainfall events (Malin Falkenmark, Johan Rockström, 2008). It is challenging to describe drought accurately, and this is considered a principal obstacle, therefore is no agreed method to define drought. The definition of drought differs from region to region, and it has many facets in any region. There are two dominant forms of drought definitions conceptual and operational. Conceptual definitions are formulated in general terms and are used to help understand what a drought is. Working definitions are precise and used to identify the begging of drought, end, and degree of severity of a drought.

2.1.2. Characterization of droughts

Due to their overwhelmingly devastating consequences, it is crucial to characterize droughts. Drought characterization will allow operations such as preparedness, early warning, and mitigation strategies (Felix N. Kogan, 2000) The literature categorizes droughts into four types: meteorological, agricultural, hydrological, and socioeconomic (Figure 2-1). Meteorological drought emerges owing to the water insufficiency induced by the imbalance between rainfall and evapotranspiration. Liu et al., (2016) define agricultural drought as inadequate moisture to meet a particular crop's requirement during its growing seasons. Hydrological drought is attributed to the lack of streamflow and groundwater recharge water supply (Liu et al., 2016). Socioeconomic drought is associated with a lack of water to meet the demand for some economic goods in combination with all or one of the other drought types (Carrão et al., 2016, Gaikwad et al., 2015, Park et al., 2016, Sujay Rakshit et al., 2014). Park et al. (2016) demonstrated that all types of drought are highly linked and rain insufficiency induced.

2.1.1. Agricultural Drought

Agricultural drought still needs to be better understood and challenging to predict, and land soil moisture is difficult and costly to measure on the ground on a large scale. Accordingly, many efforts have been made to provide long-term near-surface soil moisture globally. In rainfed agriculture, soil moisture has been the main factor affecting crop production (Baig et al., 2013). Agricultural drought, identified as soil moisture drought, is characterized by crop yield uncertainty and limited agricultural productivity (Martínez-Fernández et al., 2016). Sandeeb et.al (2021) define agricultural drought as agro-meteorological drought. Meteorological drought triggers other types of drought, including agricultural.

2.1.2. Drought indices

The description of drought is a complicated task as there needs to be more agreement on the globally accepted drought indices. Furthermore, the applicability of particular drought indices depends on a specific region, season, and application (Hao et al., 2017b). Various types of drought indices are used in drought monitoring, of which the most widely used drought in-dictators include vegetation indices such as the Normalized Difference Vegetation Index (NDVI) (Al-Hedny, Muhaimeed, 2020, Javed et al., 2020, Javed et al., 2021, Lu et al., 2019, Nanzad et al., 2019, Xie, Fan, 2021). Meteorological indices such as the Palmer Drought Severity Index (PDSI) and Standardized Precipitation Index (SPI) (Livada, v. d. Assimakopoulos, 2007, Shah et al., 2015, Tufaner, Özbeyaz, 2020), and agricultural drought indices such as the Crop Moisture (CMI) (Cong et al., 2017, Erik S. Krueger et al., 2019, Prajapati et al., 2021, Wu et al., 2020, Yagci et al., 2014).

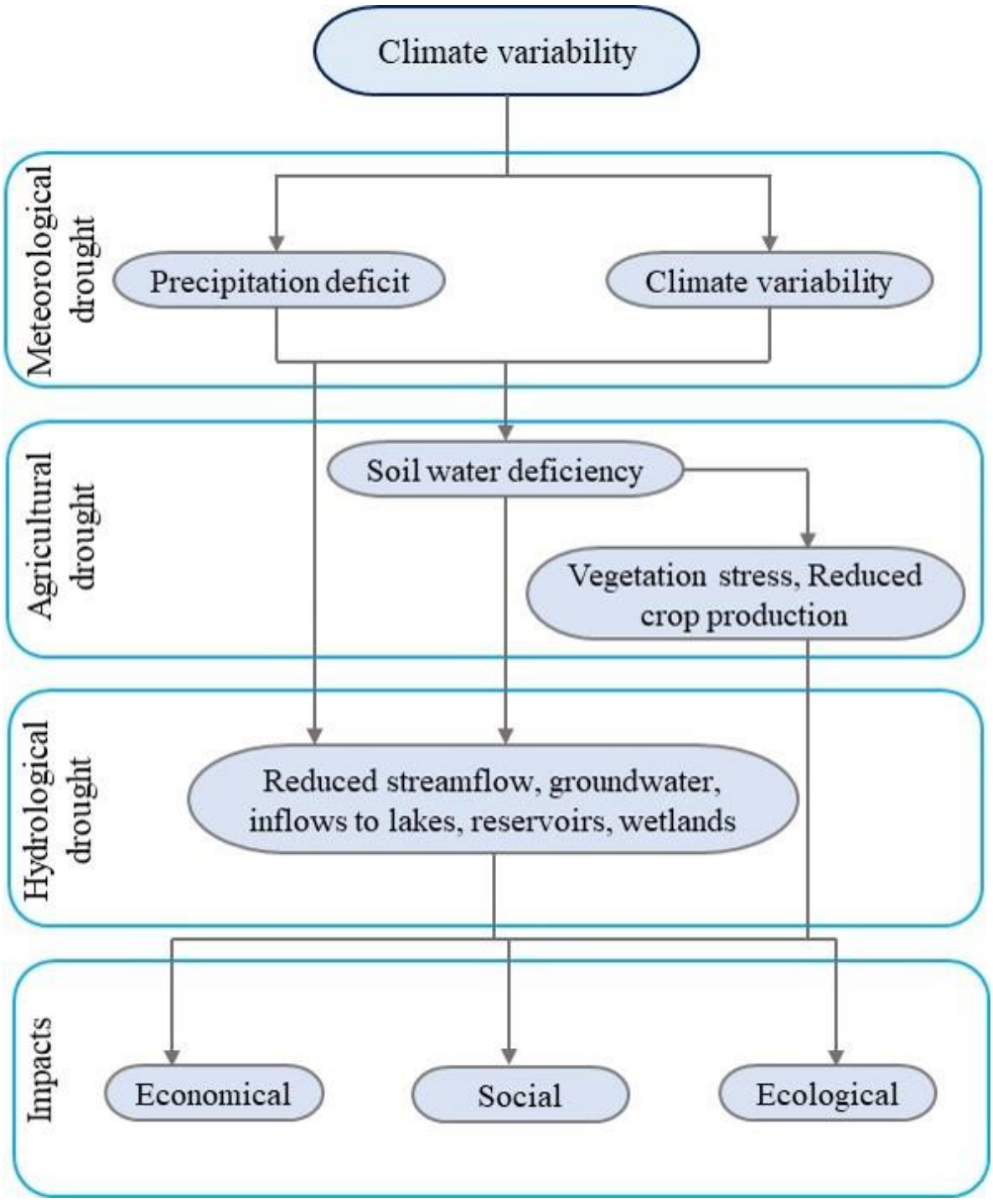

Figure 2-1 Types of drought, their connections, and consequences adopted from (Maity et al., 2016)

Soil moisture data from satellite products exhibit very different mean values than actual ground values (Mukherjee et al., 2018).To solve this obstacle, validation against the ground soil moisture dataset (Martínez-Fernández et al., 2015), is a must to improve the performance of the product's algorithms (Louvet et al., 2015). Different methods used to improve the algorithms include land models (Caldwell et al., 2019), ground measurements from sparse sensor testbeds (Mälicke et al., 2020), core validation site measurements (Reichle et al., 2017), and field campaigns (Gruber et al., 2020).

The latter method can be adequately compared to models. It can use the long-term standardized dataset to overcome the limited data obtained from almost newly launched satellite products Furthermore, the precision of the remote sensing soil moisture algorithm requires meteorological information, which is very scarce and sporadic in many regions of the planet due to the decreasing number of timely and reliable operational meteorological stations. Soil moisture data are scarce or absent in different parts of the world; owing to that reason, it becomes hard to implement techniques and algorithms related to remotely-sensed soil moisture assessment.

Studying agricultural drought in Sudan will be very important and helpful in supporting the continuous Sustainable Development Goals (SDGs) of the United Nations to be attained by 2030. It connected directly to as many as five goals. These goals include eliminating poverty (Crespo Cuaresma et al., 2018) providing sustainable jobs and promoting equality (Goal 1), and ending all forms of hunger (Banik, 2019). Poverty eradication (Goal 2), creating conditions that enable people to have quality jobs (Goal 8), ensuring consumption and production pattern (Goal 12), and taking urgent actions to mitigate the impact of climate change (Goal 13). Unlike indirect links to other goals.

The soil moisture content (θ) is the water in the soil mass. It is commonly expressed as the amount of water (in mm of water depth). θ measurements have been used to detect field saturation, soil field capacity, instigation of plant water stress, and plant extraction limits that are fundamental to determining irrigation triggers and the onset of deficit water conditions present in a depth of one meter of soil. For example: when an amount of water (in mm of water depth) of 100 mm is present in a depth of one meter of soil, the soil moisture content

is 100 mm/m see (Figure 2-2). The soil moisture content can also be expressed in the percent of volume. In the example above, 1 m^3 of soil (e.g., with a depth of 1 m, and a surface area of 1 m^2) contains 0.100 m^3 of water (e.g., with a depth of 100 mm = 0.100 m and a surface area of 1 m^2). This results in soil moisture content in volume percent of:

$$\frac{0.100\text{m}^3}{1\ \text{m}^3} \times 100\% = 10\%$$

Thus, a moisture content of 100 mm/m corresponds to a moisture content of 10 volumes percent.

Note: The amount of water stored in the soil is not constant with time, but may vary.

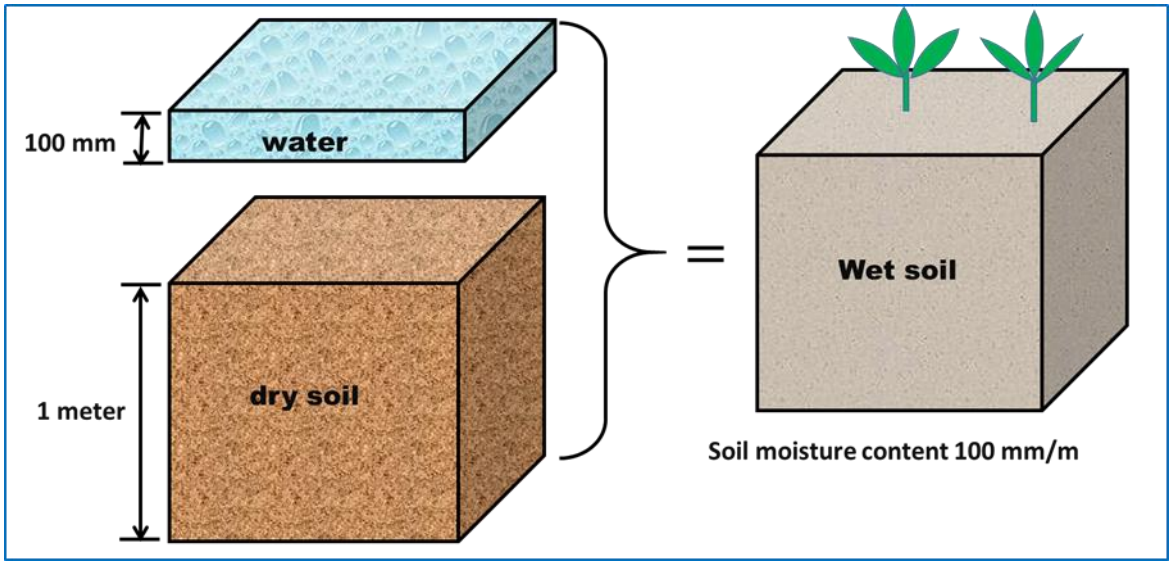

Figure 2-2 Soil moisture content of 100 mm/m : adopted from FAO paper no. 56

The soil pores will fill with water during a rain shower or irrigation application. The soil is said to be saturated if all soil pores are filled with water. There is no air left in the soil. It is easy to determine in the field if the soil is saturated. Some (muddy) water will run amongst the fingers if a handful of saturated soil is squeezed.

Plants need air and water in the soil. At saturation, no air is present, and the plant will suffer. Many crops cannot withstand saturated soil conditions for more than 2-5 days. Rice is one of the exceptions to this rule. The period of saturation of the topsoil usually lasts only a short

time. After the rain or the irrigation has stopped, part of the water in the larger pores will move downward. This process is called drainage or percolation. The water drained from the pores is replaced by air. In coarse-textured (sandy) soils, drainage is complete within a few hours. In fine-textured (clay) soils, drainage may take some (2-3) days. Field capacity (FC) is commonly used as a central concept and parameter in irrigation management and hydrological modeling studies. After the drainage stops, the large soil pores are filled with air and water, while the smaller pores are still full of water. At this stage, the plant roots start to draw water from what remains in the reservoir; the soil is said to be at FC. At FC, the soil's water and air contents are considered ideal for crop growth. Little by little, the water stored in the soil is taken up by the plant roots or evaporated from the topsoil into the atmosphere. If no additional water is supplied to the soil, it gradually dries out. The dryer the soil becomes, the more tightly the remaining water is retained and the more difficult it is for the plant roots to extract. At a particular stage, the water uptake is insufficient to meet the plant's needs. The plant loses freshness and wilts; the leaves change color from green to yellow. Finally, the plant dies.

The soil moisture content at the phase where the plant cannot extract water from the soil is called the permanent wilting point (Ghorbani et al., 2017). The soil still holds some water, but it is too difficult for the roots to suck it from the soil. The amount of water available to the plant is stored in the soil at field capacity minus the water remaining in the soil at the permanent wilting point. Three methods are mainly followed for the estimation of soil moisture variability. These are in situ or ground point measuring, soil-water models, and remote sensing techniques.

2.2. Ground point methods

For many years the direct ground measurements of soil moisture have been used as the primary information source for obtaining moisture situations. This approach uses different point techniques to determine soil moisture content, such as. Gamma-ray attenuation (Pires, Pereira, 2014), Nuclear techniques (Al-Ain et al., 2009), Electromagnetic techniques (Huth, Poulton, 2007),Tensiometry techniques (Jackisch et al., 2020), and hygrometric techniques.

However, ground point methods cannot overcome the low spatial coverage globally. Furthermore, measuring ground soil moisture is costly as it needs resampling to analyze the spatio-temporal change. On the other hand, resampling can destroy the sampling location (Baugh et al., 2020), be time-consuming, and make remote areas hard to access. Physical and chemical soil properties partially hamper ground point measurement. It needs plenty of physical effort Soil water models and time. From the health aspect, ground point methods such as nuclear techniques cause damage to public health and the environment due to radiation (Ramana, 2009).

Among diverse alternatives of soil moisture estimation, models are widely used (Narayanan, Hirsave, 2001, Nichols, 2011, Saradjian, Hosseini, 2011), especially in combination with data assimilation techniques. A precise description of plant ecology requires the assimilation of the interaction between precipitation, infiltration, and evapotranspiration. Models use physically-based neutralization to represent the hydrological operations controlling soil moisture dynamics. Thus, soil moisture in the model system can be determined by using the following relationship:

$$SMt = SMt - 1 + P - R - L - E - T + C - Q \quad (1)$$

Where: SMt = Soil moisture volume at time t, SMt-1 = Soil moisture volume at previous time, P = Precipitation, R = Surface runoff, L = Net lateral subsurface outflow, E = Evaporation, T = Transpiration, C = Capillary, Q = Percolation

Errors in the model physics are not avoidable, which causes biases in model outputs in some regions affecting the accuracy of such models. Therefore data assimilation techniques can be applied to improve model performance and the errors in the model.

2.3. Remote Sensing for soil moisture monitoring

Remote sensing platforms have become increasingly strategic for the global monitoring of earth resources. Remotely-sensed monitoring of soil moisture has witnessed progress in different parts of the world; therefore, soil moisture data have expanded dramatically during the last decades based on several satellite missions (Wang, Qu, 2009). The considerable advances

in remote sensing have enabled scientists and multiple groups of users to obtain frequent and precise soil moisture maps anywhere on earth.

Such as X, and C radars and radiometers (e.g., AMSR-E, ASCAT, RADARSAT, WindSAT), and lower frequency L bands radars and radiometers, including Soil Moisture and Oceanic Salinity SMOS launched on 2 November 2009 as one of the European Space Agency's Earth Explorer (ESA) missions and Soil Moisture Active Passive SMAP.

Surface and root-zone soil moisture data have become widely available with several missions at different spatial and temporal resolutions to detect bare or vegetated soil surface moisture content. There are different disciplines related to agriculture that will benefit from these missions. (e.g., monitor drought, assist crop productivity (Ainiwaer et al., 2020, Jalilvand et al., 2019, Tao et al., 2005), floods forecasting (Camici et al., 2019, Hu et al., 2020, Kim et al., 2019), linking water, energy, and carbon cycles (Brust et al., 2021, 2021, McDonald et al., 2010, Qiu et al., 2018, 2018).

2.4. Literature review

2.4.1. Global soil moisture instruments

Remote sensing technology allows the study of large areas while reducing time and logistics costs associated with fieldwork. Remotely sensed monitoring of soil moisture has witnessed progress in different parts of the world; therefore, the soil moisture data have risen steadily during the last decades from many satellite missions. Various studies have demonstrated that satellite missions can retrieve soil moisture globally (Table 2-1), such as the Soil Moisture and Ocean Salinity SMOS (Louvet et al., 2015). Advanced Microwave Scanning Radiometer for the Earth Observing System AMSR-E (Xie et al. 2014), Advanced Microwave Scanning Radiometer AMSR-2 (Zhang et al. 2017b), and the Soil Moisture Active Passive SMAP Ning (Zhang et al. 2019b), the Special Sensor Microwave/Imager (SSM/I) mission (Ridder, 2003).

2.4.2. Global validation of remote sensing soil moisture products

Soil moisture datasets retrieved from all of these missions are extensively used. However, as a result of the different algorithms, in situ soil moisture observations will be important in

validating remote sensing datasets dedicated to soil moisture algorithms such as open domain near-real-time of SMAP mission (Reichle et al., 2017). SMAP initiated several activities to lead to a more accurate and robust in situ measurement component of its soil moisture product validation. These activities comprise establishing an in situ sensor testbed to facilitate the combination of data provided by the sensor and in situ measurements, initiating an evaluation of scaling techniques, and developing a program for validating reliable information about the temporal changes and spatial distribution of surface and root zone soil moisture. This can support soil moisture estimation for hydrological purposes such as flood prediction through improved model states, crop yield prediction, and drought monitoring for agricultural lands (Pan et al. 2014).

Measuring crop production in relationship to moisture availability would lead to a better understanding of the environmental constraints on crop growth, such as agricultural drought. Ideally, the assessment would involve soil moisture, but measurements of this parameter on a large scale are scarce. Accurate soil moisture algorithms often require input data that are difficult to obtain for developing countries such as those in Africa (Malo, Nicholson, 1990). The challenges of the satellite validation, such as retrieval errors, sampling errors, and inadequate ground observations, constitute the main reason for data uncertainty. For satellite validation purposes, the soil moisture community differentiates between dense networks with many soil moisture stations placed within a single satellite footprint and sparse networks where footprint-scale areas usually contain only a single or very few stations. As far as we know, numerous studies have been conducted to validate remote sensing soil moisture globally, with less attention paid to African countries.

Apart from the study of (Louvet et al., 2015), who validated the Soil Moisture and Ocean Salinity (SMOS) from Level 3 (SMOS L3SM) product. The French CNES-CATDS provided this product for West Africa using soil moisture data collected from a sparse network of ground agro-climatological stations of the study area. Very few studies were conducted to validate remote sensing soil moisture products with in situ measurements in Africa (Table 2-2), generally because of non-existing ground measurements of essential variables such as the current study.

Although the above literature delivers helpful information about the validation of remote sensing soil moisture products in different parts of the world, on the other hand, it implies a lack of empirical studies for consideration of near-real-time remotely sensed soil moisture products operating at smaller temporal resolution. In arid and semi-arid regions such as the African continent, the dynamic of surface soil moisture can be very quick due to high evaporation rates. As a result of the quick drying-out of soils, many products can be insufficient to catch soil moisture in smaller temporal resolution.

To solve this problem, the SMAP level-4 operating at smaller temporal and global spatial resolutions can be an excellent alternative to other missions. It takes less time to put the information regarding soil moisture availability into practice in the field. Successfully agricultural schematization in arid and semi-arid regions is sensitive to soil moisture Spatio-temporal variation. The discovery of knowledge relevant to such near-real-time products over rainfed agriculture would provide insights into this essential agricultural sector's current and future status (Reichle et al., 2017). Such a study will help to implement adequate planning for the future.

Very few studies were conducted to validate SMAP against in situ measurements using different methodologies, such as core validation sites. SMAP level-4 product met its soil moisture accuracy requirements with ubRMSE of 0.038 m^3m^{-3} and 0.030 m^3m^{-3} for surface and root zone soil moisture at the 9-km scale. Root zone soil moisture performed well in a SMAP comparison versus in situ measurements in Spain (Pablos et al., 2018). Moreover, compared to in situ measurements across the globe, the SMAP and SMOS are to provide estimations for soil moisture in the top 5 cm of soil with (ubRMSE) no more prominent than 0.04 cm^3cm^{-3}.

2.4.3. Remote sensing soil moisture products validation in Sudan

Sudan is an example of a predominantly agricultural country with severe soil moisture data scarcity and high vulnerability to climate variation and food insecurity. There is a big gap in verifying the most promising remote sensing products to estimate soil moisture. Reuniting remote sensing estimates and in situ measurements relies on reference datasets consisting of

ground observations, radar or other satellite data, or a combination of observation types to measure and characterize the errors in satellite estimates. Rainfed agriculture in Sudan is spreading across its vast CCP arable lands. Sorghum (Sorghum bicolor (L) Moench) is the most important cereal crop serving as a significant source of food and the largest produce ranked by area (Elagib, 2014). The harvested area of sorghum in Sudan constitutes 17% and 24% of the total global and African harvested areas, respectively (FAO, 2019). El Gedaref State, where agricultural machinery is used, is the most crucial region for sorghum production (Lotfie et al. 2018). 76-79% of root biomass is concentrated in the 10-20 cm layer of soil (Chen et al. 2019).

Consequently, understanding the Spatio-temporal variability of soil moisture in this layer is essential to achieve better land management and improve food security. There is an urgent need for accurate and continuous near-real-time in situ soil moisture measurements to cover a wide range of agro-climatic zones of the rainfed agricultural lands of Sudan. Agricultural activities increased tremendously in CCP in the last decades. There is a necessity to use in situ measurements to implement the validation process. The objective of this chapter is two-fold: (1) to validate the SMAP level-4 3-hourly product provided by NASA against in situ soil moisture measurements across different agricultural rainfed lands of El Gedaref state, Sudan, and (2) to study the Spatio-temporal soil moisture pattern during the crops growing season.

Table 2-1. Remote sensing instruments and satellite platforms (past and current) for global soil moisture observation

Instrument	Satellite	Freq. (GHz)	Band	Spat. resolution	Temp. resolution (day)	Sensor type
AMSR-2	GCOM-W1	6.9-89	S, X	25-50 km	2	passive
AMSR-E	Aqua	6.9-89	C, X	25-50 km	2	passive
Aquarius	Aquarius	1.26	L (active)	76-156 km	7	active/passive
		1.41	L (passive)			
ASAR	ENVISAT	5.33	C	30-1000 m	5	active
ASCAT	MetOp	5.25	C	25-50 km	2	active
MIRAS	SMOS	1.4	L	35-60 km	3	passive
NISAR	NISAR		L and S	0.1-50 km	12-60	active
PALSAR	ALOS	1.27	L	10-100 m	46	active
RADARSAT-1&2		5.40	C	10 m	24	active
Tandem-L	Tandem-L	1.2	L	3.20 m	8	active
Sentinel-1 A& -1B			C	5-20 m	6-12	active
SMAP	SMAP	1,26	L (active)	3 km (active)	2-3	active/passive
		1.41	L (passive)	40 km (passive)	2-3	
	GEOS-5, SMAP			9 km	3 (hours)	
SSM/1	SSM/1	19.35	K	13-69 km	12 (hours)	passive
WindSAT	Coriolis 6.8-37		C, X, and K	8-71	8	passive

Table 2-2 A summary of several studies conducted to validate remote sensing-based soil moisture data

Author (s)	Scale	Time	Main objective (s)	Main findings
(Colliander et al., 2017)	Selective (core sites)	January-November2015	To process the data for metrics computations, and the results from using the core sites in the SMAP validation	SMAP soil moisture data product meets its expected performance of 0.04 m^3 m^{-3} volumetric soil moisture (un RMSE)
(Badou et al., 2019)	Benin Republic	(2005-2008).	To suggest a frame-work for validation of remotely sensed soil moisture without in situ soil moisture	soil moisture from different hydrological models pro-vides valuable proxy meas-urements for testing the re-liability of satellite soil moisture
(Rodríguez-Fernández et al., 2017)	USA	May 2015	To implement and val-idate the SMOSNRT soil moisture product.	SMOS product exhibits per-formances similar to those of the Level 2 soil moisture product
(Beck et al., 2020)	USA and Europe.	2015 - 2019	To undertake a com-prehensive evaluation of 18 state-of-the-art global near-surface 30 soil moisture products	Data assimilation yields sig-nificant benefits
(Karthikeyan et al., 2017)	USA	Last four decades	To develop passive and active microwave soil moisture retrieval algorithms over the Contiguous United States	Soil moisture products have significantly will continue to make key contributions to the progress of hydro-meteorological and climate sciences.
(Meng et al., 2019)	China		To address the lack of high-resolution histori-cal datasets in West China	XJLDAS, high-resolution forcing data-driven CLM3.5, can be used to generate accurate soil mois-ture (1km) in Xinjiang

2.5. Study design and methodology

2.5.1. Validation sites

This research focused on El Gedaref state (Figure 2-3), one of the seventeen states of Sudan, located between longitudes 33° 34- and 37°E and between latitudes 12° 40- and 15° 45 N. El Gedaref state borders four other Sudanese states, namely Kassala state to the north, Khartoum state to the northwest, Gezira state to the west, and Sennar state to the south. The total area of El Gedaref state is approximately 72,000 km2. It has been divided administratively into eight localities: El Fashaga, El Faw, El Gallabbat East, Basonda (added recently), El Gallabbat West, El Gedaref, El Rahad, and El Butana (Elhadary, 2010). According to the widely globally used climate classification of Köppen-Geiger (Beck et al., 2018), the average annual precipitation ranges between 250 mm in the warm desert climate, 250-500 mm in the warm semi-arid climate, and 750- 1200 in the tropical savanna.

The rainfed mechanized agricultural sector of El Gedaref state has advantages due to its high potential to support the national food supply. Its central clay soil is appropriate for sorghum cultivation, which is considered the leading staple food for most of the Sudanese people. Its production can also support income gain with exportation (Bussmann et al., 2016b).

There are two locations where the study was conducted in order to validate the SMAP level-4 soil moisture product. Both locations are predominantly agricultural lands in eastern Sudan, El Gedaref State. At fully mechanized African Plantation Company (APCO) and in mechanized agriculture at Kilo-6. The region is a part of the central clay plains of Sudan (CCP) that extends eastward from the Nuba Mountains to the Ethiopian boundary split only by the Ingessana Hills and from Khartoum state in the north to the far reaches of southern Sudan. APCO is located at Rahad locality in Samsam adjacent to the Rahad River south of El Gedaref State. The APCO area is characterized as sub-humid with an average annual rainfall of about 850 mm (Figure2-3) with largely missing ground climatic data records. APCO climatic substations will cover these data. The data includes maximum and minimum air temperature (^{0}C), relative humidity (RH %), rainfall (mm), wind speed (ms-1), and radiation (Wm-2). SM is not measured, which is considered the principal element of the soil with plant

growth. APCO covers an area of about 350 km^2 with an average elevation of 465 meters above sea level (Figure 2-3). The growing season starts in the first week of June and ends in the first week of November, with entire rainy days ranging between 60-70 days during rainy months of the year. APCO area suffers from extreme events, floods, and droughts. The major crops of the study locations are cereals, sesame, sunflower (in both places), cotton, and watermelon seeds (only at Samsam) which are usually cultivated during the rainy season.

Kilo-6 is located in the central part of the state, approximately 6 kilometers from the city center of El Gedaref, with an average annual rainfall of about 550 mm and an average elevation of 540 meters over the sea level. Kilo-6 has a subtropical steppe climate (Classification: BSh), the average annual temperature is 31.28 °C, 1.24% warmer than the country's national averages. Kilo-6 experiences 76.0 rainy days (20.82% of the total year days).

2.6. Data collection, methods, and sources

2.6.1. Experimental design

The measurements were designed to capture the top 5 cm and root zone Spatiotemporal soil moisture distribution during the rainy season of 2018. The SMAP level-4 three hourly soil moisture product provides a global surface (top 5 cm of the soil column) and root zone soil moisture (top 100 cm of the soil column) that is spatially and temporally complete. The SMAP level-4 soil moisture product described in this section was compared to the in situ soil moisture measurements derived by averaging all points mentioned in (Table 2-3) in the two locations at the time closest to the SMAP overpass. Both locations contributed 20 days with the top 5 cm of soil moisture and 20 days with the root zone. The 20 days also list the measurement depths used for computing top 5 cm and root zone measurements (at 10 and 20 cm). The in situ measurements of the top 5 cm SM and root zone at 10 cm and 20 cm were conducted at two nested scale extents (0.5 km, 3 km) to understand the soil moisture variability across these scales (Figure 2-3).

One 3×3 km focus area and one 9×9 km focus area were selected for intensive sampling based on different topography, soil properties, and vegetation characteristics. The 3×3 km square grids were sampled intensively at 9 locations at a spacing of 1 km. In addition, nine

areas were also selected at 3 km spacing around each intensive sampling grid to cover a 9×9 km square grid corresponding to the coarse resolution of the SMAP footprint. At present, the in-situ soil moisture measurements were taken only within three hours to be consistent with the satellite overpass, which occurs every three hours.

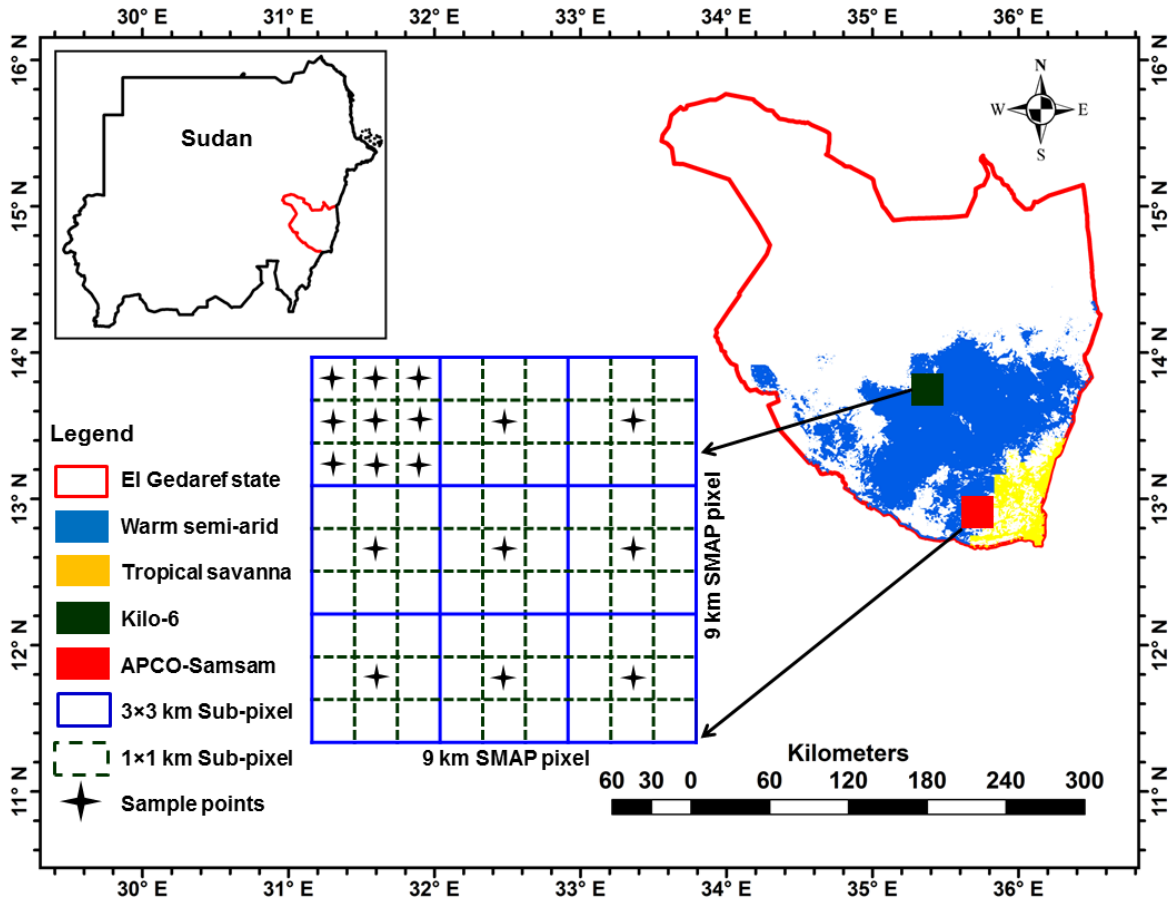

Figure 2-3 Study locations and in situ soil moisture measurements points

2.6.2. Field campaigns and volumetric soil moisture

The methodological procedure followed in this chapter to correlate the variability in the satellite soil moisture and in-situ soil moisture measurements over the croplands of El Gedaref State showed in (Figure 2-4). The in situ measurements were conducted from July to October, the growing season, during the rainy season of 2018, to measure soil moisture correctly and create a harmonized and comparable dataset of soil moisture to be validated with SMAP level-4 soil moisture product. A portable theta probe sensor was employed for measuring in

situ soil moisture in the study locations. The sensor is equipped with a dedicated moisture meter for instant readout. It measures the volumetric soil moisture content vertically. Based on that, holes were drilled using an auger to depths of 0-5, 10, and 20 cm. Seventeen holes were drilled in pixel size (9×9 km). The site selection, sampling strategies, sample preparation, analysis, and results are described extensively by Singh et al. (2016). The sampling was interrupted during days of heavy rains, which hindered logistics, as well as to avoid sample disturbance. It is crucial to allow the soil to reach the maximum water level. This action usually takes place 2–3 days after rain in the clay soils (Gülser, Candemir, 2014, Xu et al., 2015). In situ, soil moisture samplings were taken during the day from 9 am to 12 pm synchronous with the SMAP 3-hourly satellite descending orbit in the equator, which occurs at 6:00 am. The medians in situ soil moisture were aggregated separately in each grid for each day.

2.6.3. SMAP level-4 soil moisture algorithm

Only a few public-domain sources offer soil moisture data. SMAP mission currently provides near-real-time Level 2 to 4 soil moisture products derived from its L-band passive microwave radiometer. The SMAP level-4 soil moisture 3-hourly geophysical soil moisture dataset 9 km mission provides global estimates of the surface and root zone (Reichle et al., 2017) The level-4 soil moisture data are generated and distributed on the global, cylindrical, 9-km Equal-Area Scalable Earth and version 2 (EASEv2) grids.

The level-4 soil moisture outputs include soil moisture estimates for the surface (0–5 cm) and the root zone (0–100 cm). The mission aims to help scientists understand the relationship between the earth's water, energy, and carbon cycles, decrease uncertainties in earth system modeling, and improve the ability to monitor and predict natural hazards such as droughts.

The NASA SMAP mission provides many surprises, which have assisted in modeling the earth's climate, forecasting the weather (Forgotson et al., 2020), and monitoring crop growth (Patricia M. Lawston et al., 2017). The SMAP estimates the root zone SM in the top 100 cm of the soil profile based on SMAP observations (Zhang et al., 2019a). Obtaining root zone soil moisture is needed for various applications targeted by SMAP. The level-4 soil moisture

algorithm utilizes an ensemble Kalman filter (EnKF) to merge SMAP observations with soil moisture estimations from the NASA Catchment land surface model (Pezij et al., 2019). Using observation-based surface meteorological forcing data, the NASA catchment model characterizes the vertical transfer of soil moisture between the surface and root zone. The data are processed in the same way as the surface SMAP.

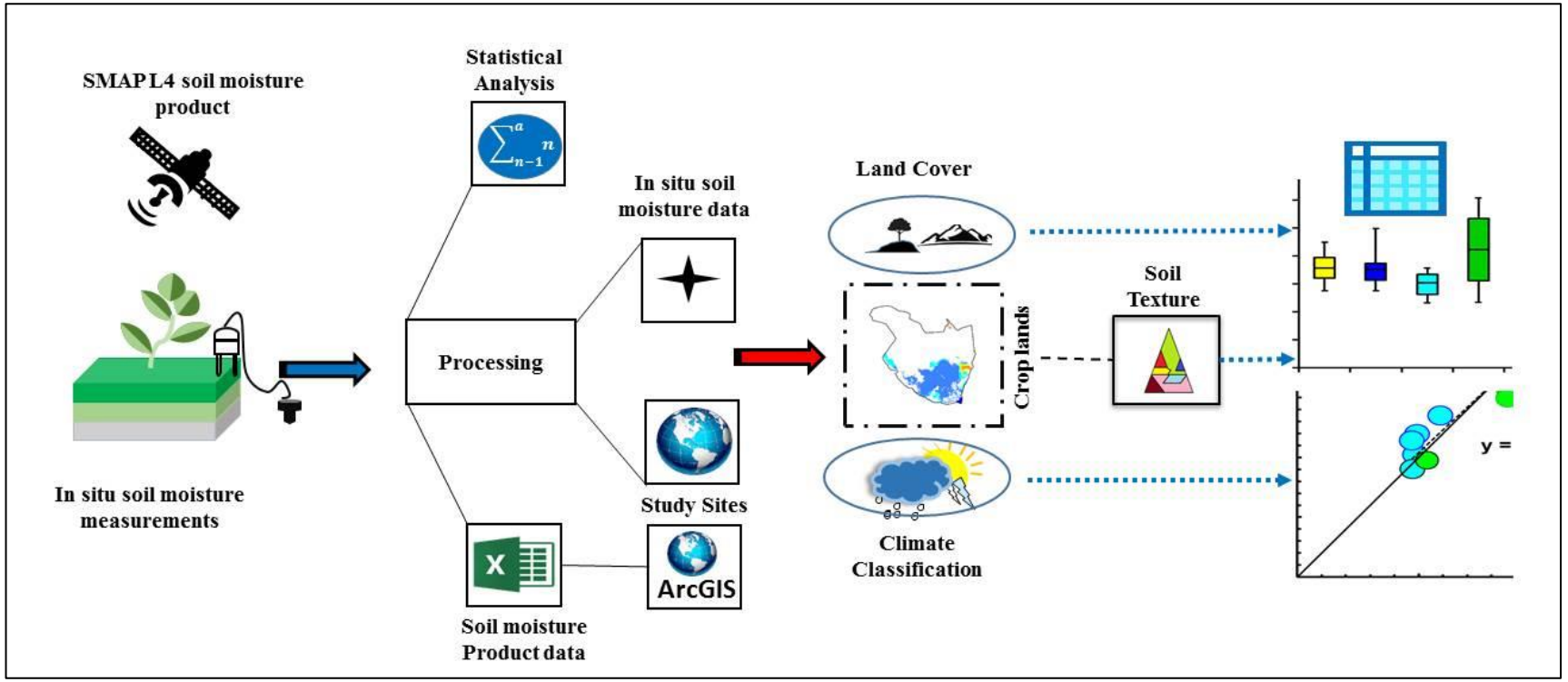

Figure 2-4 Flowchart of the methodological procedure followed in this chapter to correlate the variability in the satellite SM and In situ soil moisture measurements over the croplands of El Gedaref state

Table 2-3 In-situ monitoring points over the two locations and Land Cover/Land Use LC/LU

Samsam			Kilo-6		
Coordination	**Elevation (m)**	**LU/LC**	**Coordination**	**Elevation (m)**	**LU/LC**
N:12°59’ 22.1”: E: 35°08’ 47.2”	461	Sorghum	N:14°01’ 58.6”: E: 35°13’ 16.2”	539	fallow land / annual grass
N:12°59’ 42.9”: E: 35°09’ 08.2”	461	Wide Level-tilled	N:14°02’ 24.8" : E: 35°13’ 12.7”	538	fallow land / annual grass
N:12°59’ 59.5”: E:35°09’ 26.1”	462	Disc-plowed	N: 14°02’ 19.9”: E: 35°12’ 49.8”	536	fallow land / annual grass
N:13°00’ 15.5”: E:35°09’ 43.5”	462	Center Camp 4	N: 14°01’ 56.0”: E: 35°12’ 57.0”	543	fallow land / annual grass
N:13°00’ 23.4”: E:35°09’ 31.1”	458	Sorghum	N:14°01’ 49.7”: E: 35°12’ 33.2”	538	fallow land / annual grass
N:13°00’ 00.9”: E:35°09’ 17.1”	460	Sorghum	N: 14°02’ 13.5”: E: 35°12’ 25.9”	535	fallow land / annual grass
N:12°59’ 48.4”: E:35°08’ 54.4”	461	Sorghum	N: 14°02’ 06.9”: E: 35°12’ 00.4”	535	fallow land / annual grass
N:12°59’ 32.1”: E:35°08’ 36.3”	467	Sorghum	N: 14°01’ 37.5”: E: 35°12’ 00.7”	537	fallow land / annual grass
N:12°59’ 46.3”. E:35°08’ 17.6”	466	Sorghum	N:14°01’ 24.2”: E: 35°12’ 19.7”	537	fallow land / annual grass
N:13°00’ '04.1”: E:35°08’ 35.4”	460	Sorghum	N:14°01’ 24.2”: E: 35°12’ 41.9”	538	fallow land / annual grass
N:13°00’ 25.2”: E:35°08’ 57.0”	463	Sorghum	N: 14°01’ 11.9”: E: 35°12’ 53.8”	541	Sesame
N:13°00’ 38.8”: E:35°09’ 09.4”	459	Sorghum	N: 14°00’ 54.3”: E: 35°12’ 54.2”	548	Sesame
N:13°00’ 50.6”: E:35°08’ 54.5”	462	Sorghum	N:14°00’ 56.8”: E: 35°13’ 14.3”	545	fallow land / annual grass
N:13°00’ 34.6”: E:35°08’ 37.9”	458	Sorghum	N:14°01’ 46.0”: E: 35°13’ 14.8”	545	fallow land / annual grass
N:13°00’ 18.9”: E: 35°08’ 23.1”	459	Sorghum	N: 14°01’ 46.0”: E: 35°13’ 04.9”	543	fallow land / annual grass
N:12°59’ 58.2”: E: 35°07’ 59.0”	453	Sorghum	-	-	Stream Water body)
N:12°59’ 22.1”: E: 35°08’ 47.2”	461	Sorghum	N:14°01’ 58.6”: E: 35°13’ 16.2”	539	fallow land / annual grass

In this study, the shapefiles corresponding to the study locations were clipped from the global SMAP L4 soil moisture maps. The resulting maps of the top 5 cm and the root zone were averaged daily.

2.7. Evaluation of SMAP product

To measure the inconsistency between the measured and the observed soil moisture, three errors, and one linear metric was used, including the standard deviation of residuals /Root Mean Square Error (RMSE), the Mean Absolute Bias Error (MABE), the Mean Bias Error (MBE), the coefficient of determination (R^2)

$$\text{RMSE } (m^3m^{-3}) = \sqrt{\frac{1}{n}\sum_{i=1}^{n}(S_i - G_i)^2} \quad (2)$$

$$\text{MBE } (m^3m^{-3}) = \frac{1}{n}\sum_{i=1}^{n}(S_i - G_i) \quad (3)$$

The unbiased RMSE and the RMSE are related through:

$$\text{ubRMSE}^2 \ (m^3m^{-3}) = \text{RMSE}^2 - \text{MBE}^2 \quad (4)$$

$$\text{MABE } (m^3m^{-3}) = \frac{1}{n}\sum_{i=1}^{n}|S_i - G_i| \quad (5)$$

$$R^2 = \frac{\left(n(\sum_{i=1}^{n} G_iS_i) - (\sum_{i=1}^{n} G_i)(\sum_{i=1}^{n} S_i)\right)^2}{\left(n(\sum_{i=1}^{n} Gi^2) - (\sum_{i=1}^{n} G_i)^2\right)\left(n(\sum_{i=1}^{n} Si^2) - (\sum_{i=1}^{n} S_i)^2\right)} \quad (6)$$

where S_i and G_i are the SMAP soil moisture estimate (m^3m^{-3}) and ground soil moisture observation (m^3m^{-3}), respectively, n number of data. RMSE and MABE indicate how robust the data is around the line of best fit. RMSE and MABE range between zero (no error) and$+\infty$ (high error). MBE captures the average bias in the prediction and ranges between $-\infty$ and $+\infty$. Both indicate a high error, whereas no error is indicated by MBE of zero. Negative MBE

values signal the overall underestimation, whereas positive values indicate the overestimation of soil moisture by the product. R^2, also known as the coefficient of determination, is the ratio of the response variable variation that the predictor explains. R^2 is always between 0 (no correlation) and 100% (total correlation).

2.8. Result and discussion

2.8.1. In-situ soil moisture behavior during the rainy season

Figure (2-1) shows the Spatio-temporal box-whisker plot of in situ soil moisture measured at three depths during the rainy season of 2018. Along a number line using the minimum, maximum, and quartiles of the data collected during the field campaign across the two locations. The position of the box in its whiskers and the position of the line in the box also tell us whether the data is symmetric or skewed (non-normal). Generally, in both locations, for the top 5 cm of the samples taken for 17 points, the median centered on 250-300 (m^3m^{-3}) and 220-260 (m^3m^{-3}) during the second and third dekads of July at the Samsam and Kilo-6 respectively. At the Samsam site in the top 5 cm, the top whiskers had varying values ranging between 380-270 (m^3m^{-3}), much longer than the bottom whiskers, which vary between 300-200 (m^3m^{-3}), and the line is gravitating towards the bottom of the box. Therefore, the median of the groups of in situ soil moisture boxes was variable. The box plots are comparatively tall and uneven; this suggests that overall soil moisture data between the two sites during this season in the two locations.

With the shrinking and swelling characterizing clay soils in the study locations, water tends to leak away from the soil surface before saturation through large cracks, leaving some heterogeneous (moist and dry) spots on the soil surface. Field observations showed that the soil hydraulic properties varied considerably in space, even within a given soil type. Such spatial variability affects the hydrological response conditioned by an ensemble of moisture retention curves (Ivanov et al., 2010). In the root zone (10 and 20 cm), where vegetation depends on water in this zone, water from precipitation percolating through soil and filtered kept being consumed per plant. During (August and September) in both locations, the medians were relatively in the middle of the boxes (August and September), and the whiskers were about

the same on both sides of the boxes; the statistical data set was generally symmetric. However, very few days during this period showed skewness (positive and negative). In general, soil moisture content increased clearly in the two locations during August and September.

Our results are reinforced by the Standardized Multi-Criteria Drought Index (SMDI) to determine the spatial distribution of drought zones in Sudan. Elagib et al. (2019a) used SMDI and found a progressive increase in wet conditions from southeast to northwest and a decreased in the same way from northwest to southeast of El Gedaref State. The high soil moisture distinguished by the Rahad locality could be attributed mainly to the land cover type. Yao et al. (2012) stated that soil moisture in arid and semi-arid regions is higher under the cultivated land than the other land cover surfaces. In the northern location, most of the lands were fallow and dominated by annual pasture grass.

The average RMSE between SMAP and in situ soil moisture is 0.015 m^3m^{-3} within SMAP mission target accuracy. This is similar to the RMSE 0.02 cm^3cm^{-3} reported by (Shellito et al., 2016) when comparing soil moisture observations from NASA SMAP with those from in situ probes upscaled to SMAP footprint. Our results were consistent with the findings of (Colliander et al. 2017), who validated SMAP level-4 soil moisture against in situ measurements obtained from core validation stations and spares networks. They found RMSE of 0.059 and 0.048 m^3m^{-3} over woody savannas and of 0.057 m^3m^{-3} of 0.046 m^3m^{-3} over croplands for the surface and the root zone soil moisture, respectively.

The soil started to dry out very quickly in the two locations during October. Figure 2-1 showed a rapid decrease in soil moisture during the second dekad of October, and drier conditions prevailed in Samsam 200-250 (m^3m^{-3}) than that of Kilo-6 250-300 (m^3m^{-3}) in the top 5 cm. Soil moisture at depths of (10 and 20 cm) was kept within the range of 300-320 (m^3m^{-3}) in both sites.

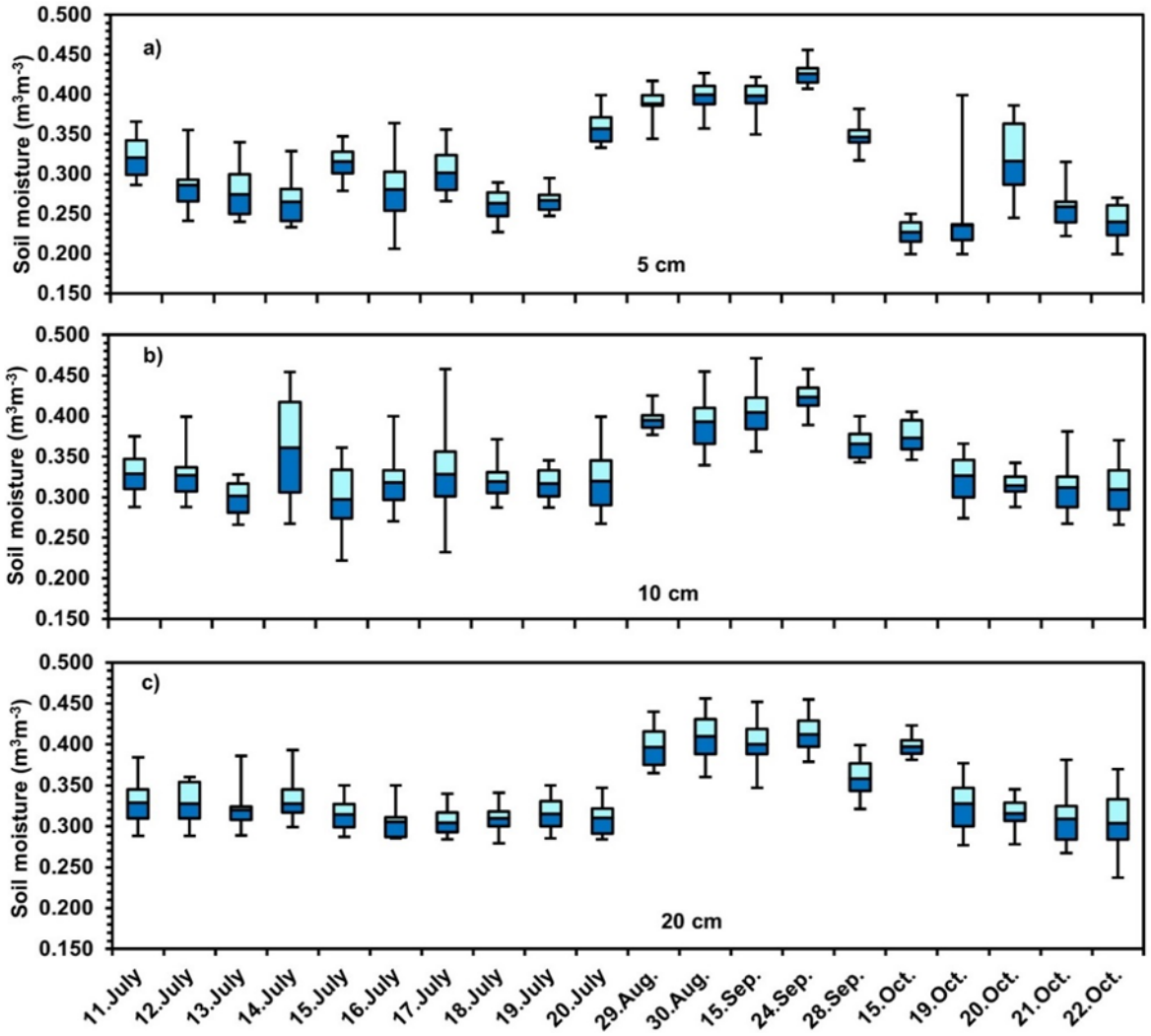

Figure 2-5 Box-Whisker plot of in situ soil moisturemeasured at three depths during a field visit in 2018: a) to c) Samsam study area and d) to f) Kilo-6 study area

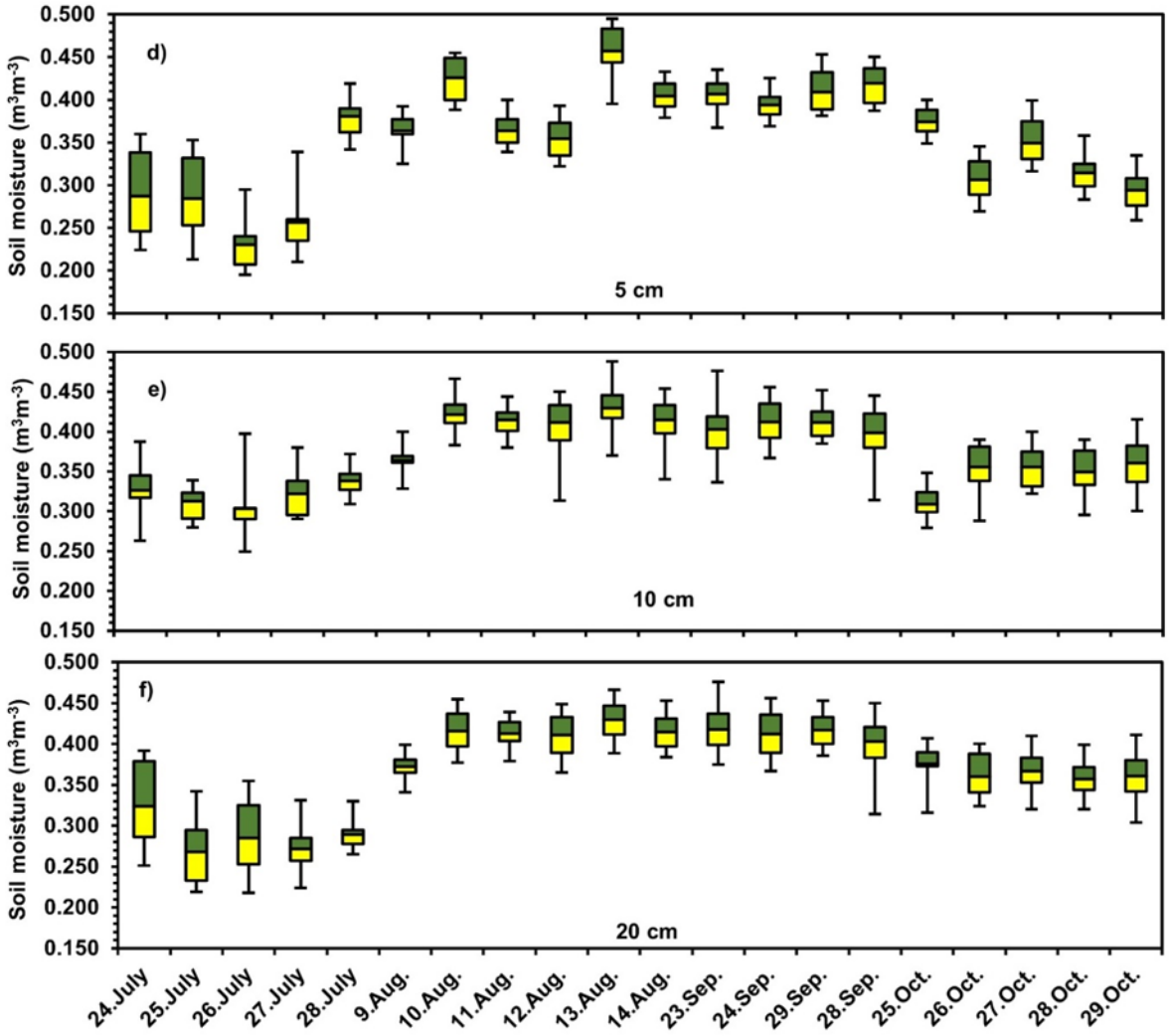

Figure 2-5 (Continued)

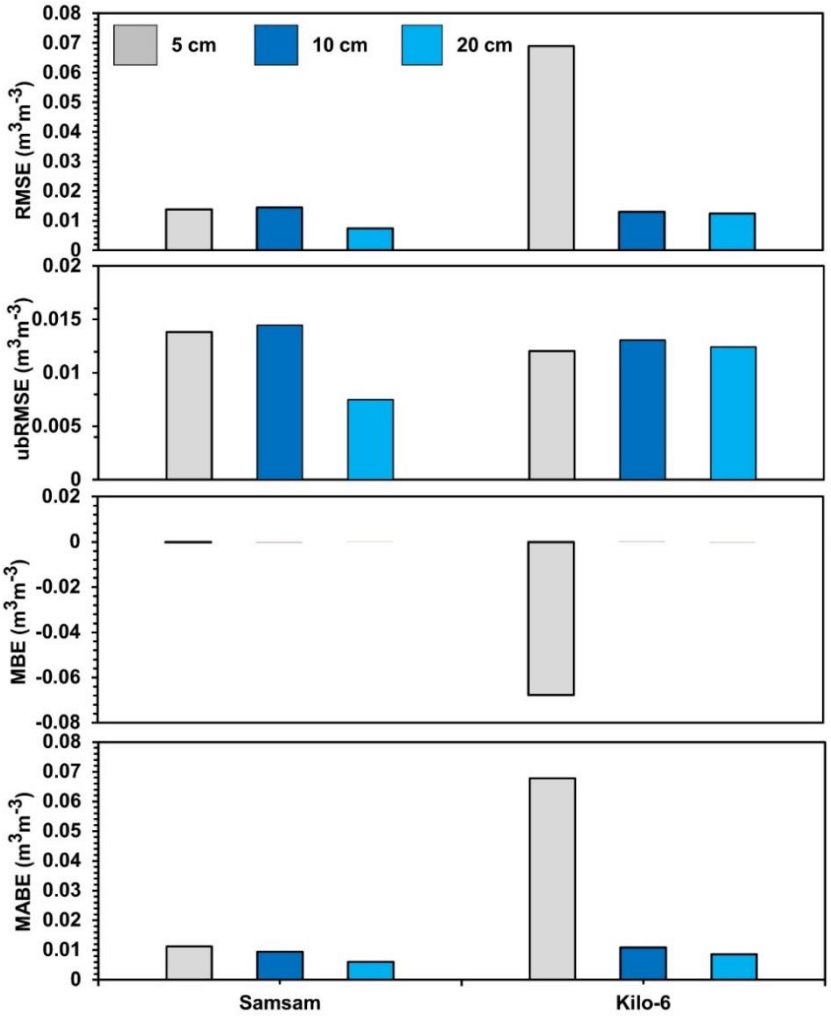

Figure 2-6 Performance errors of SMAP product for average 3-hourly soil moisture as evaluated on the two study sites

Figure 2-7 presents the scatter plots of the relationships between the 3-hourly average estimation of SMAP L4 SM and the in situ soil moisture measurements during the rainy season of 2018. The linear regression shows a strong positive correlation between the two datasets. The two datasets showed an uphill pattern as the in situ soil moisture content increases, the soil moisture taken by SMAP increases. The soil moisture drops sharply in October.

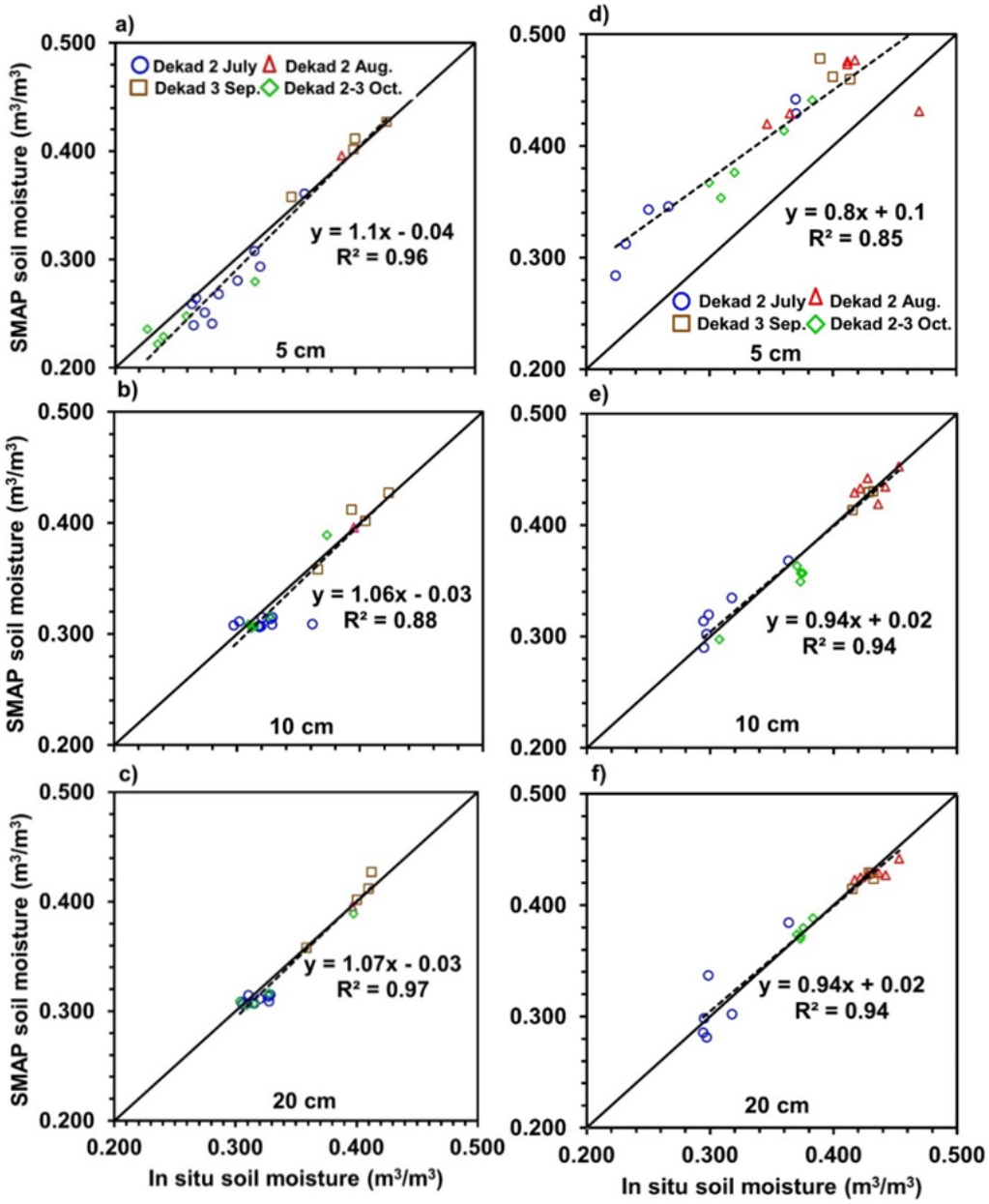

Figure 2-7 Scatter plots of 3-hourly average SMAP soil moisture estimates (m^3/m^3) versus in situ soil moisture measurements at the root zone and top 5 cm during the rainy season (July to October) of 2018 (a), (b), and (c) Samsam and (d), (e), and (f) at Kilo-6. The continuous and dotted lines represent the 1:1 and regression lines, respectively

2.8.3. SMAP soil moisture distribution over CCP

The same Spatio-temporal pattern of SMAP SM is remarkable in the entire CCP, and soil moisture exhibited a huge Spatio-temporal variability. A few example maps for sampled locations and the surrounding clay plains of Sudan are shown in (Figure 2-9). During the last dekad of each month of autumn 2018, the soil moisture starts very low during the last dekad of July, increases steadily during the last dekads of August and September, and then drops sharply during October. October is similar to July, with a slight increase in soil moisture over southern parts of CCP, which receives more rainfall annually.

The distribution pattern of soil moisture over the entire CCP changes steadily in conjunction with the amounts of rain. The most significant annual rainfall occurs during August. The southern parts of CCP have had greater soil moisture content and longer wet days. One of the main advantages of our measurements is that SMAP soil moisture data was validated during the entire growing season of the same year in different agricultural locations. Timely, frequent, and complete agricultural land soil moisture information obtained throughout the rainy season in this study is vital for agricultural planning, production, and food security.

In this study, the first period represents the crop growing dates, often during July. The following periods represent the different crop growth stages and occur during August, September, and October. However, the crop yield responds significantly to growing dates, and the selection of optimum growing dates is scheduled according to crop type. Elramlawi et al. (2018) stated that the sorghum yield increases when early growing dates are considered in contrast to the delayed growing dates, which showed a decrease in yield over CCP. The start of this study matches the optimum growing dates of sorghum, the primary crop cultivated in the CCP. The recommended growing dates by the Agricultural Research Corporation of Sudan are between 15 July the 1st August (El Karouri, 2010). A 10-15% potential reduction in sorghum yield from moisture stress occurs in this stage.

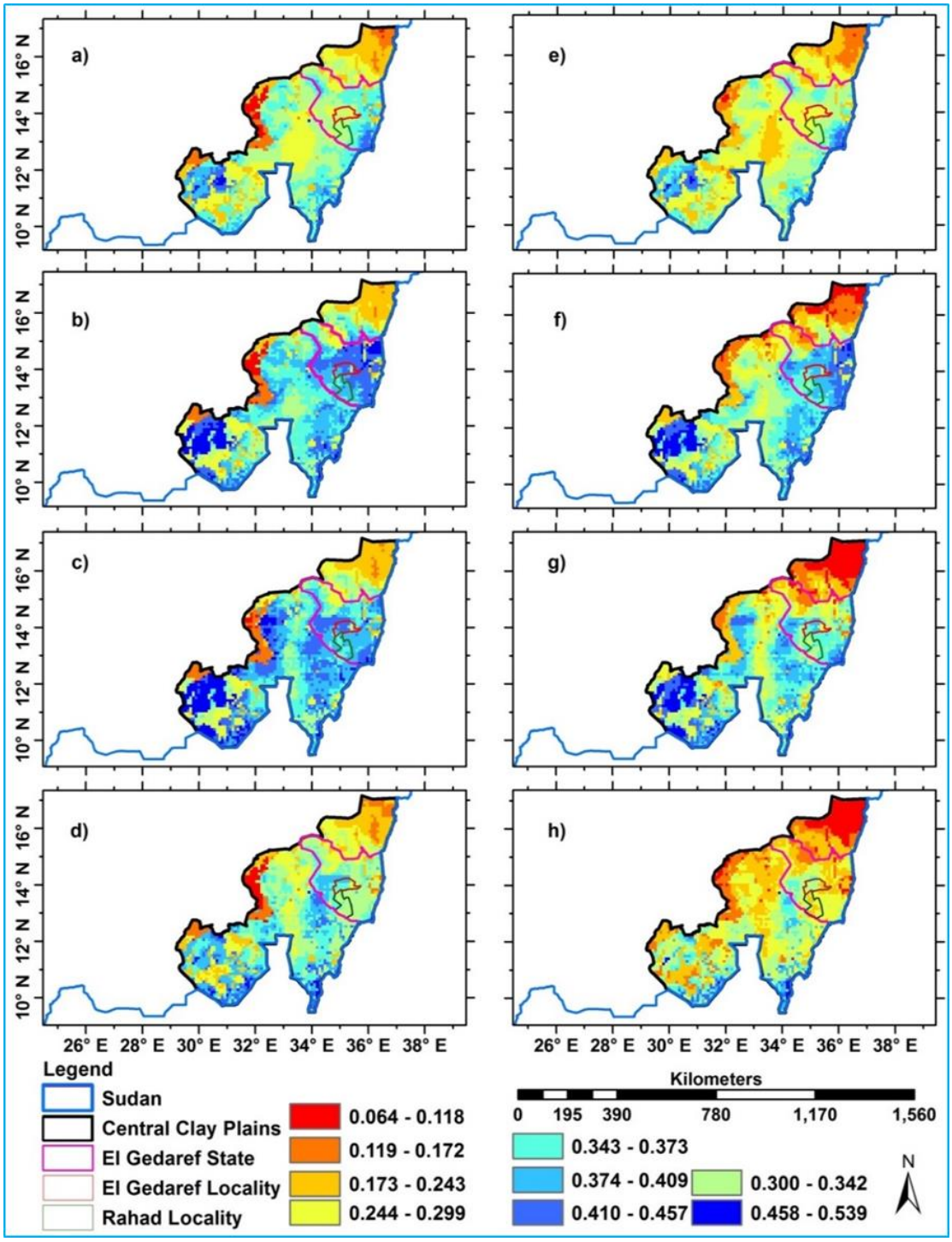

Figure 2-8 Spatio-temporal distribution of 3-hourly SMAP L4 mean soil moisture (m^3/m^3) during the last dekad of four months at the root zone (a, b, c, and d) and the top 5 cm (e, f, g, and h) on the study sites, Samsam and Kilo-6, compared to the surrounding Central Clay Plain (CCP) of Sudan during the 2018 rainy season

CHAPTER 3. Available soil moisture and drought threshold of different climatic zones of El Gedaref State

3.1. Introduction

Soil moisture datasets of good quality at various scales are prerequisites to sustainable land, crop, and water management and land surface algorithm. A drought phenomenon is a gradual, not avoidable, process predominantly followed by long-lasting catastrophic consequences. Given the diverse types of droughts, the methods used to describe agricultural drought mainly revolve around monitoring available soil water content and crops' later unmet water demand (Zargar et al., 2014). Giessen et al. (2014) stated that the decreasing numbers of sub-Saharan African meteorological and hydrological stations are considered a significant concern for science and society. Accordingly, it is crucial to use remote sensing technologies as an alternative to ground-based methods.

Furthermore, a considerable challenge is understanding the data's limitations to be used (Champagne et al., 2016). Lately, quick and substantial advances in remote sensing have enabled scientists to obtain, frequently and precisely, soil moisture maps of anywhere on the planet (Martínez-Fernández et al., 2015). Soon, this can be extended to various groups of users. Furthermore, surface and root-zone SM data have become widely available in the last few decades, with several missions dedicated to retrieving soil moisture, including the Soil Moisture Active Passive (SMAP) data.

Drought conditions can be demonstrated to be adversely affecting agricultural yield (Elagib, 2014). The description of drought is a complicated task as there is a lack of agreement on the globally accepted drought indices. Furthermore, the applicability of particular drought indices depends on a specific region, season, and application (Hao et al., 2017b). Various types of drought indices are used in drought monitoring, of which the most widely used drought indicators involve vegetation indices such as the Normalized Difference Vegetation Index (NDVI). Meteorological indices such as the Palmer Drought Severity Index (PDSI) and Standardized Precipitation Index (SPI), and agricultural indices such as the Crop Moisture Index (CMI).

3.1.1. Importance of RS products in Sudan

Numerous studies have been conducted to monitor agricultural drought using SM products on a global scale. For example, Myeni et al. (2019b) targeted the provision of an inclusive overview of the current status of the soil moisture estimate for the African continent and the recognition of the commonalities and gaps in the literature. The study's findings determined the capability of Soil Moisture Ocean Salinity (SMOS) data for monitoring soil moisture. Haubrock et al. (2008) assessed German land surface soil moisture based on a pixel-wise comparison with synchronous in-situ measured data. They found that it could be applicable to obtain appropriate modeling of surface soil moisture from high spectral resolution remote sensing data. An attempt to understand the spatial aspects of the agricultural vulnerability of Indian agrarian land using remote sensing was conducted by Nithya and Rose (2014). They produced an agricultural vulnerability map that helped prepare mitigation measures in the area under investigation, reducing the impacts of climate variation on agriculture.

Less attention has been paid to the African continent monitoring agricultural drought using remote sensing soil moisture products. A thorough search of the related literature yielded only one article from Anderson et al. (2012), which examined the 2010–2011 Horn of Africa drought using AMSR-E passive microwave sensor estimates of SM, precipitation, evapotranspiration, and terrestrial water storage. No other study has been conducted to estimate the response of remotely sensed soil moisture and rain on the soil moisture drought (agricultural drought) in sub-Saharan Africa based upon generally available datasets. Such studies would enable researchers to perceive whether soil moisture is sufficient to meet the estimated water demands of cultivation and the start of the growing season. Therefore, the main goal of this chapter was to understand the amount of available soil moisture on the surface and the root zone in the agricultural lands of Sudan. Also, measuring soil moisture content is key to the strategic management of water resources. The specific goal focuses on spatially evaluating the relationship between soil moisture, rainfall, and NDVI dynamics and obtaining the available water content for crops from a new SMAP-derived Soil Water Deficit Index (SWDI).

3.2. Research methods

3.2.1. Study zones

According to the widely globally used climate classification of Köppen-Geiger (Beck et al., 2018), the average annual precipitation ranges between 250 mm in the warm desert climate, 250-500 mm in the warm semi-arid climate, and 750- 900 in the tropical savanna. The cropland of El Gedaref state is distributed in three isohyets (Figure 3-1).

3.2.2. Data

Different datasets were obtained from open sources for use in the current study. These datasets provide a solution for regions where there is little existing data. Real-time Soil Moisture Active Passive (SMAP) in the surface and the root zone, NDVI, rainfall, land cover, field capacity (FC), and wilting point (WP) used in this analysis are shown in (Table 3-3). All of these datasets were obtained from open sources for a period extending from 1 June to 31 October 2015, 2016, 2017, 2018, and 2019. The soil moisture datasets used in this study were retrieved from the SMAP, newly launched by the National Aeronautics and Space Administration (NASA). Data are only available for the years following 2015; therefore, 2015, 2016, 2017, 2018, and 2019 were selected.

Furthermore, various other studies have dealt with the same subject over the same period. This period was chosen to be consistent with these studies to simplify the comparison of the findings. Moreover, the year 2015 was dry in Sudan. The rainfall level at El Gedaref weather station was 390 mm less than the annual average of 550 mm (MAA, 2017). Hence, it was interesting to investigate the SM patterns and, in turn, the agricultural drought in this year.

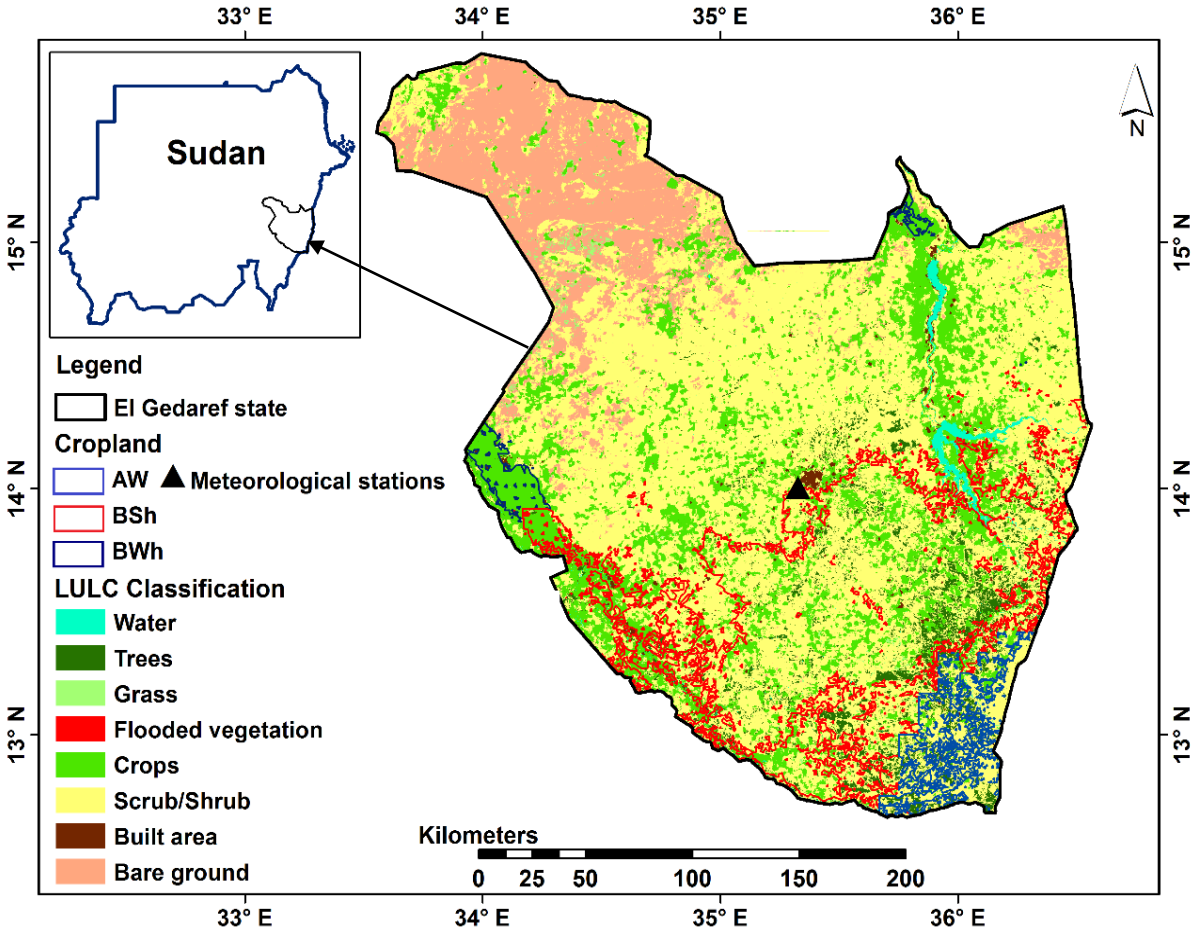

Figure 3-1 Location map of the study area shows cropland, meteorological stations, and climatic zones. The climatic zones across the study area, such as tropical savanna (AW), warm semi-arid climate (BSh), and warm desert climate (BWh), were determined using Köppen–Geiger climate types at 1 km resolution, according to rainfall variation.

3.2.2.1. Soil Moisture Active Passive (SMAP)

Soil Moisture Active Passive (SMAP) is a new soil moisture mission launched by NASA on 31 January 2015, initially for a short three-year mission but extended up to date, for mapping global soil moisture and detecting whether soils are frozen or melted. The mission intends to help scholars understand the relationship between the earth's water, energy, and carbon cycles, decrease uncertainties in earth system modeling, and enhance the ability to observe and forecast natural hazards like droughts. The NASA SMAP mission provides many surprises, which have assisted in modeling the earth's climate, forecasting the climate, and monitoring crop growth.

The SMAP estimates the root zone soil moisture in the top 100 cm of the soil profile based on SMAP observations. Obtaining root zone soil moisture is essential for various applications targeted by SMAP. The L4-SM algorithm utilizes an ensemble Kalman filter (EnKF) to merge SMAP observations with soil moisture estimations from the NASA catchment land surface model (Kolassa et al., 2017). Using observation-based surface meteorological forcing data, the NASA catchment model characterizes the vertical transfer of soil moisture between the surface and root zone. The data is processed in the same way as the surface SMAP.

3.2.2.2. The Climate Hazards Group Infrared Precipitation with Station data (CHIRPS)

The Climate Hazards Group Infrared Precipitation with Station data (CHIRPS) is a global precipitation dataset. It starts at 50°S-50°N and covers all longitudes. The data was launched in 1981 and has continued to date. The CHIRPS combines 0.05° resolution satellite imagery with ground station data to form a rainfall network time series for trend analyses and drought monitoring. Version 2.0 of CHIRPS was completed on 12 February 2015 and became accessible for public use. (For more and elaborated information on CHIRPS, please refer to Funk et al. (2015).

3.2.2.3. The Moderate Resolution Imaging Spectroradiometer (MODIS)

The Moderate Resolution Imaging Spectroradiometer (MODIS) vegetation indices produced every dekad interval with various spatial resolutions provide harmonious spatial and temporal comparisons of vegetation greenness, a composite property of leaf area, chlorophyll, and canopy structure. Two vegetation indices derived from atmospherically corrected reflectance in the red, near-infrared, and blue wavebands, are used in drought monitoring – the Vegetation Condition Index (VCI) and the Normalized Difference Vegetation Index (NDVI). The latter quantifies vegetation by measuring the difference between near-infra-red (which vegetation strongly reflects) and red light (which vegetation absorbs), healthy vegetation (chlorophyll) reflects more near-infrared (NIR), and green light compared to other wavelengths. Still, it absorbs more red and blue light.

NDVI has good records for historical and climate applications such as drought detection. The NDVI is calculated as follows:

$$\mathrm{NDVI} = \frac{\mathrm{NIR} - \mathrm{Red}}{\mathrm{NIR} + \mathrm{Red}} \quad (7)$$

where NIR is the reflectance in the near-infrared wavelengths, and Red is the reflectance in the visible wavelengths.

3.2.2.4. Field capacity and permanent wilting point of the study sites

Before using the SWDI index, it was necessary to use the parameters FC and PWP in the area under investigation. Examining suitable methods for determining these parameters is the key to popularizing soil moisture data as a drought indicator.

The Global Gridded Surfaces of Selected Soil Characteristics (IGBP-DIS), is a worldwide cooperative project with the goal of providing accurate and useful data about soil parameters. Derived surfaces having certain soil properties are appropriate for modeling and inventory needs. It is useful to the community of researchers studying global change. This project contains 7 data surfaces: soil-carbon density, total nitrogen density, field capacity, wilting point, profile available water capacity, thermal capacity, and bulk density.

Table 3-1 Field capacity (FC) and Permanent wilting point (PWP) for the climatic zones

Climatic Zone	FC	PWP
Tropical savanna (AW)	0.44	0.21
Warm semi-arid climate (BSh)	0.42	0.19
Warm desert climate (BWh)	0-42	0.17

3.2.2.5. The Soil Water Deficit Index (SWDI)

The Soil Water Deficit Index (SWDI) has demonstrated promising results in quantifying agricultural drought based on soil moisture deficit. This index can identify the characteristics that define agricultural drought events. We use SWDI to quantify agricultural drought based on the surface soil moisture for the top 5 cm depth and the root zone at 10 and 20 cm. This

is important for agricultural drought monitoring (Mishra et al., 2017). The SWDI is calculated in Eq. (7):

$$\mathrm{SWDI} = \left(\frac{\theta - \theta_{\mathrm{FC}}}{\theta_{\mathrm{AWC}}}\right) \tag{8}$$

Where θ is the soil water content, θ_{FC} denotes field capacity; θ_{AWC} is the available moisture content and calculated by subtracting θ_{FC} with volumetric soil moisture content at wilting point θ_{wp} as in Eq. (8):

$$\theta_{\mathrm{AWC}} = \theta_{\mathrm{FC}} - \theta_{\mathrm{WP}} \tag{9}$$

The FC and PWP data at 0.08° spatial for the different climatic zones were generated from the (IGBP-DIS) and shown in (Table 3-2). The SWDI has three ranges > 0, = 0, < 0 (Martínez-Fernández et al. 2016). The zero value represents the critical threshold in the SWDI index separating drought and non-drought situations. In contrast, positive values denote no drought because surplus water than the outstanding amount of water that can be held by soil pores (θFC) is available for crop uptake. Negative values signify agricultural drought due to the unavailability of moisture content for plant germination or development. However, the impact of agricultural drought depends on crop type and growing stage.

The SWDI was computed in a dekadal time scale (Martínez-Fernández et al. 2016), and the drought classification based on SWDI is provided in (Table 3-2). The theory of runs is applied (Mishra and Singh 2010) to calculate drought characteristics, such as the percentage of drought events and total drought severity (TDS), using weekly SWDI. The run theory can be applied to a time series of drought variables (i.e., SWDI and NDVI) to classify drought and wet events based on either below or above the selected threshold level (Mishra and Singh 2010). The percentages of drought events show the severe to extreme drought occurrence (%) during the study period for different locations.

Table 3-2 Classification of SWDI for different drought categories

SWDI Value	Drought Category
≥ 0	No drought
0 to -2	Mild
-2 to -5	Moderate
-5 to -10	Severe
≤ -10	Extreme

3.2.2.6. Moderate Resolution Imaging Spectroradiometer (MODIS) Land Cover

The Moderate Resolution Imaging Spectroradiometer (MODIS) Land Cover Type Product (MCD12Q1) provides a unique combination of science datasets (SDSs) that map global land cover at 500 meters spatial resolution at yearly time steps (2001-2019) for six different land cover legends. The maps were created from classifications of spectro-temporal features derived from MODIS data. The supervised classifications then undergo additional post-processing that incorporates prior knowledge and ancillary information to refine specific classes further. The primary land cover scheme identifies 17, including 11 natural vegetation classes, three human-altered classes, and three non-vegetated classes. Layers for land cover type 1-5, land cover property 1-3, land cover property assessment 1-3, land cover quality control (QC), and a land-water mask are provided in each MCD12Q1 version 6 hierarchical data format 4 (HDF4) file. The land cover dynamics product includes layers on the timing of vegetation growth, maturity, and senescence that mark the seasonal cycles.

3.2.3. Data processing in GIS

The gridded datasets used in this study were processed in Geographic Information System (GIS), ArcGIS 10.1 software. The SMAP geophysical soil moisture data of the surface and the root zone used in this study were 3-hourly data with a spatial resolution of 9 km. The raw SMAP image processing involved (i) removal of the invalid values in ArcGIS using the formula SMAP = Setnull (SMAP ≤ 0, SMAP) in the raster calculator tool. Then, (ii) the study areas were extracted using an extract by mask tool aggregating the 3-hourly composite data into dekad corresponding to the NDVI time series. The CHIRPS daily rainfall dataset summated every dekad using ArcMap to correspond to the NDVI time series. The NDVI data

used in this study were dekad composite data with a spatial resolution of 500 m. For this study, we used the SWDI developed by Martinez et al. (2015), which showed robust results in detecting agricultural drought based on soil moisture. It deals directly with the Available Water Content (AWC), which, in the area of agricultural drought considered, is more applicable than soil moisture itself (Martínez-Fernández et al., 2016b).

According to the MODIS land cover classifications, we considered only areas with 60% cultivated cropland to avoid the mosaics of small-scale cultivation at 40–60% that were mixed with the natural tree, shrub, or herbaceous vegetation. Figure (3-2) shows the flowchart of the methodological procedure followed in this chapter to correlate the variability in rainfall, soil moisture, and SWDI and their influence on NDVI as an indicator for agricultural drought.

Table 3-3 Specifications of the data used in this study from 1st June to 31st October 2015, 2016, 2017, 2018 and 2019

Datasets	**Source/Satellite/Sensor**	**Period**	**Resolution**	**Download site**
SMAP level 4 (Surface SM)	SMAP Radiometer	Global 3-hourly (aggregated every dekad)	9 km	https://search.earthdata.nasa.gov/search
SMAP level 4 (Root Zone SM)	SMAP Radiometer	Global 3-hourly (aggregated every dekad)	9 km	https://search.earthdata.nasa.gov/search
NDVI	MODIS/MCD43A4_NDVI	Every dekad	250 m	https://search.earthdata.nasa.gov/search
CHIRPS Rain-fall	CHIRPS	Daily (aggregated every dekad	5000 m	https://chg.geog.ucsb.edu/data/chirps/
FC and WP			37 m	https://webmap.ornl.gov
SWDI	(Index)		> 0, = 0, < 0	https://www.sciencedirect.com/science/ar-ticl
Land Cover	The MODIS Terra + Aqua	Yearly	500 m	http://earthexplorer.usgs.gov

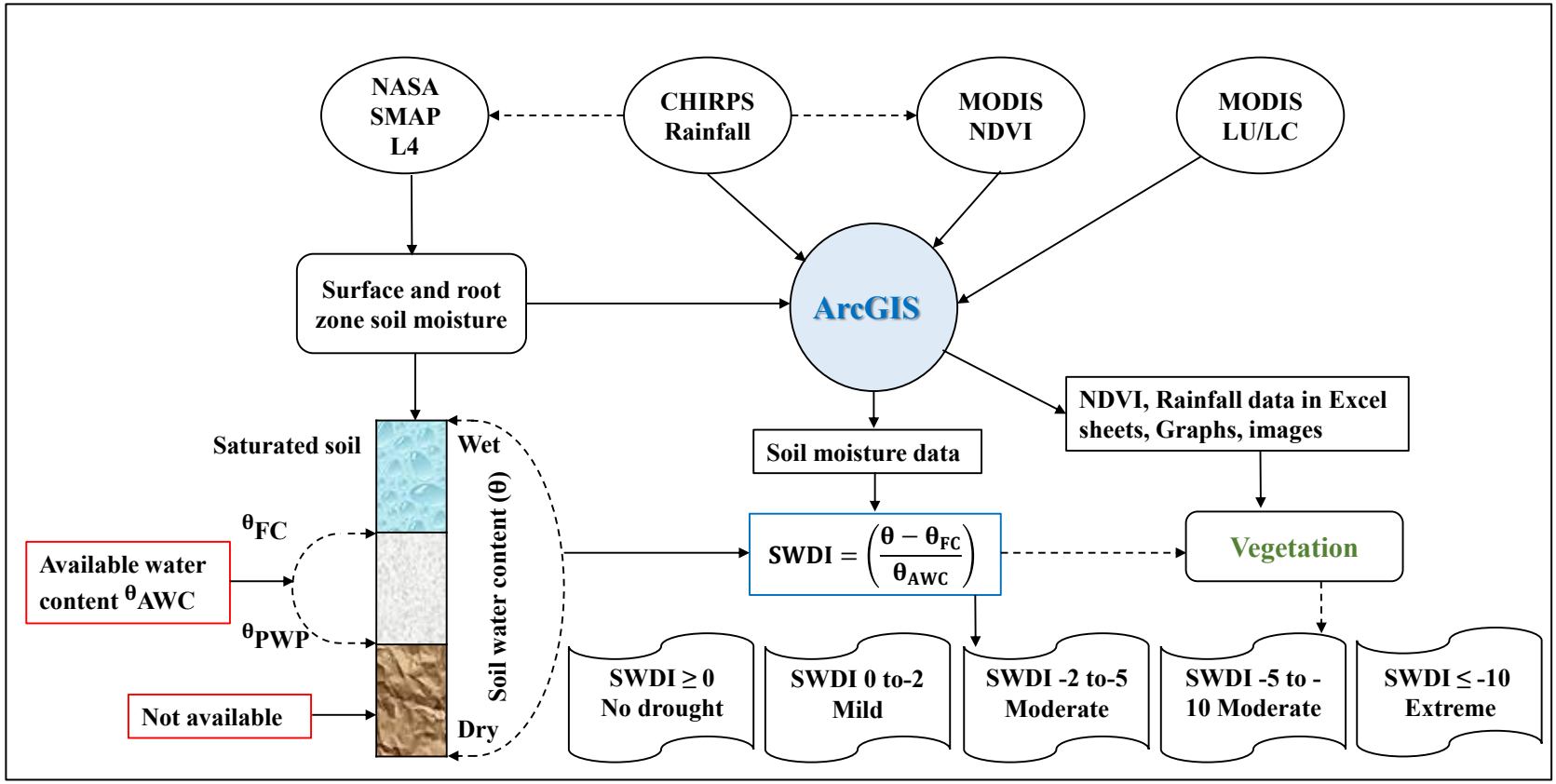

Figure 3-2 Flowchart of the methodological procedure followed in this chapter to correlate the variability in Rainfall, SM, and SWDI and their influence on NDVI over the croplands of El Gedaref State

3.3. Results and discussion

3.3.1. Rain impact on vegetation

As expected, the total rainfall during all years was higher in the tropical savanna, followed by a warm semi-arid climate, while the semi-desert climate received the least rain (Figure 3-3). The relationship between rainfall and vegetation patterns varied significantly in various places (Ding et al., 2007). Jammes et al, (2006) studied the relationship between NDVI and rainfall patterns in the African Savanna. They found a time lag of one and two months between seasonal NDVI production and the seasonal pattern of rainfall. In the current study, the dynamics of the NDVI in the three locations disagreed with rainfall patterns from May to October in all the years. This was attributed mainly to the time-lag period of adequate rain affecting vegetation.

During dry spells, daily rainfall of less than 5 mm was not considered efficient, as this rain would probably evaporate from the soil surface before it penetrates the soil profile. Adequate rain penetrates the soil profile and becomes available to the plants, as clearly shown in the current study and different works of literature (Rousvel et al., 2013). In the present study, the maximum effective period of precipitation in the NDVI was more than one month. The adequate rainfall in August affected the greater values of NDVI at the end of September and during the first part of October. The influence of rain on the variations of NDVI in the growing season was low. It was likely that other ecological factors strongly influenced the NDVI dynamics. The temporal and spatial vegetation dynamics depend on various environmental and biophysical factors, such as soil characteristics.

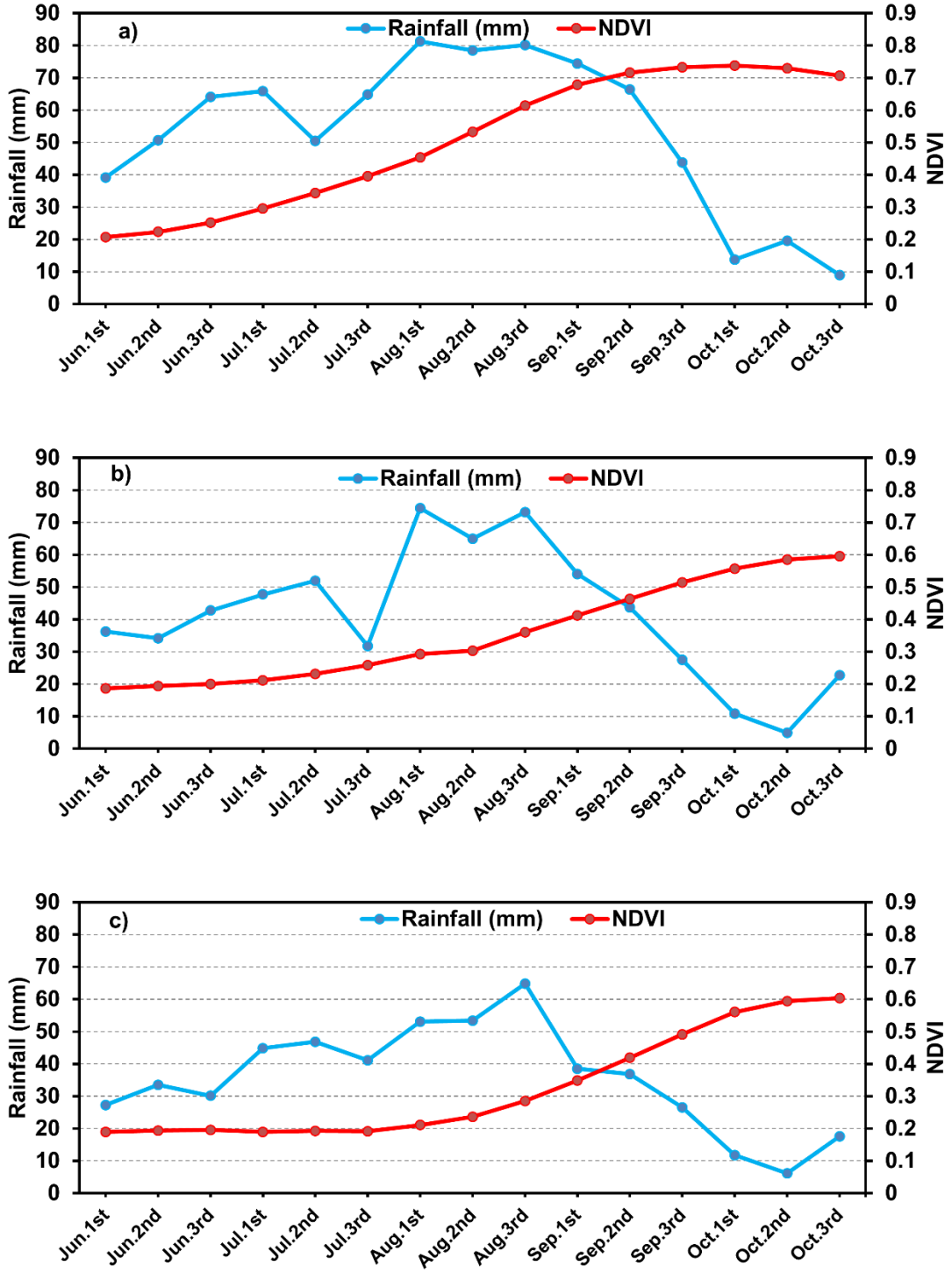

Figure 3-3 Dekadal NDVI means dynamic vs. rainfall (mm) from 2015 to 2019 over different climatic zones across the study area such as: a) tropical savanna (AW), b) warm semi-arid climate (BSh), and c) warm desert climate (BWh). All R values are not significant at (a) p = 0.046, (b) p = 0.055 and (c) p = 0.043

3.3.2. The response of soil moisture on vegetation index

The soil moisture measured as m^3m^{-3} in the root zone over the cropland locations is shown in (Figure 3-4). It was found that NDVI and soil moisture have a stronger correlation from June through to October in all locations. The response of NDVI dynamics in the three sites to the soil moisture is higher during the investigation period. The higher values of NDVI at the beginning of the autumn season could be attributed mainly to the erratic and variable distribution of rains. Early rainfall provoked the germination of seasonal pastoral grasses, which in turn maximized the values of the NDVI. The spatial heterogeneity of the ecosystem considerably affects the vegetation's response to soil moisture.

Although the SMAP radiometer was better able to measure soil moisture up to 5 cm depth, understanding the amount of available soil moisture in the root zone provides an accurate assessment of drought in agricultural lands (Velpuri et al., 2016) validated SMAP soil moisture versus in-situ soil moisture measurements for drought monitoring in the rangelands of the US high plains. The results showed the highest correlation with surface soil moisture (top 5 cm) and a strong correlation to a depth of up to 20 cm. Also, a high correlation of up to 25 cm was found by Zamora et al. (2016), between SMOS soil moisture and in-situ soil moisture measurements over a semi-arid Mediterranean agricultural area. The NDVI values were closely tied to SM; therefore, NDVI will change in line with soil moisture change. Niu et al. (2018) illustrated that the time-lag effects on vegetation responses to SM vary significantly across a large scale.

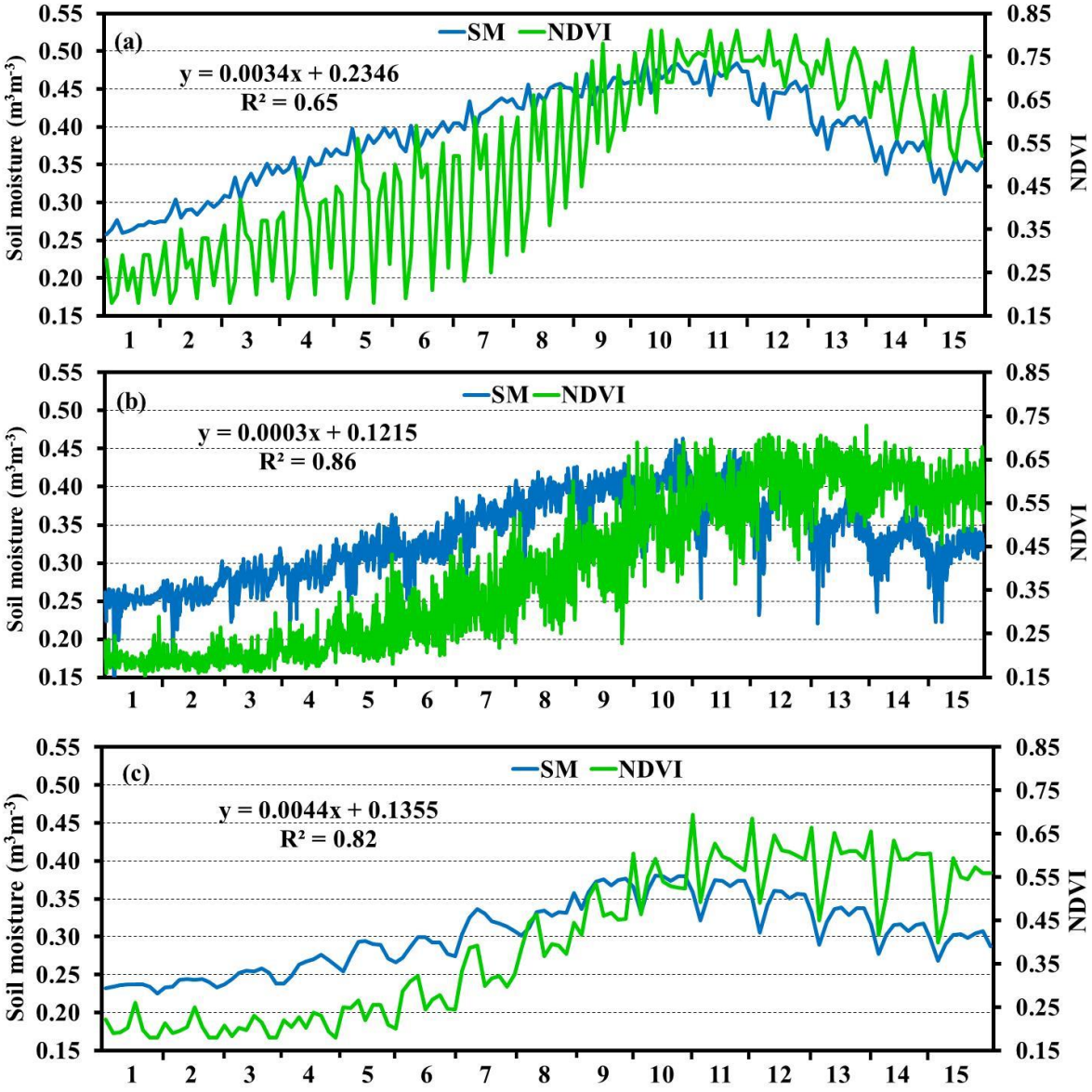

Figure 3-4 Time series of root zone soil moisture (m^3m^{-3}) at NDVI), from 2015 to 2019 over different climatic zones across the study area such as: a) tropical savanna (AW), b) warm semi-arid climate (BSh), and c) warm desert climate (BWh). 1 represents the 1st dekad of June. 15 represents the 3rd dekad of October. All R values are significant at (a) $p < 0.001$, (b) $p = 0.001$ and (c) $p = 0.001$

3.3.3. Available soil moisture and drought threshold

Measuring the available water content is more vital than rain, even soil moisture, for monitoring agricultural drought (Martínez-Fernández et al., 2016). The SWDI index in the current study was calculated using SMAP SM based on equation 2. The FC represents the outstanding amount of water available after rain, irrigation, and drainage (Lopez and Barclay, 2017; Kirkham, 2014), while the PWP is where the plant can no longer extract water from the soil. The plant begins to wilt even if water is added and agricultural drought occurs. The difference between FC and WP is considered to be the available water for the crop.

The quantity of soil moisture defines the SWDI drought classes. In different isohyets, soil characteristics such as (FC) and (WP) denote the drought threshold (drought and no drought conditions) and drought classes as well (Table 3-3). (FC) and (WP) vary with different soil types.

As expected, in all years, soil moisture in the surface of the soil and root zone (Figure 3-3) increased progressively from southeast to northwest. It decreased the same way from northwest to southeast, giving tropical savanna the most prolonged moist period compared to warm semi-arid and desert climates. The available soil moisture in tropical savanna for 2016, 2017, and 2018 started from the first dekad of July. It ended in the last dekad of October (110–120 days), except for the dry year of 2015, which had a shorter moist period starting from the first dekad of August and ending in the second dekad of October (85 days). These observations could be considered to be an indication of drought in vulnerable areas for rainfed agriculture of El Gedaref State.

Table 3-2 Drought classes and corresponding soil moisture quantities (m^3m^{-3}) over the study locations

		Soil moisture (m^3m^{-3})		
SWDI values	Drought classes	BWh	BSh	AW
≥ 0	No Drought	≥ 0.428	≥ 0.398	≥ 0.398
0 to -2	Mild	0.428- 0.383	0.398- 0.346	0.398- 0.346
-2 to -5	Moderate	0.383- 0.327	0.346- 0.300	0.346- 0.300
-5 to -10	Severe	0.327- 0.250	0.300- 0.221	0.300- 0.221
≤ -10	Extreme	0.250- 0.000	0.221- 0.000	0.221- 0.000

NDVI values in every dekad were highly correlated with the SWDI in the root zone in all locations (Fig.4, 5, and 6). The results were highly significant over the three climatic zones. The NDVI is closely tied to SWDI, and, therefore, NDVI values will change very closely with the SWDI change during the period from June to October 2015, 2016, 2017, 2018, and 2019. The results illustrated that the risk of crop failure increases with later sowing dates because these should precisely coincide with the optimum soil moisture content. Field crops are sensitive to growing dates, and optimum growing dates are highly correlated with the high productivity of crops (Anwar, Bhanger, 2003, Wood et al., 1983).The delay in the sowing date was attributed to the soil profile's lack of available water content.

In Sudan, late sowing dates influence depressing crop productivity. For example, at the Tozi Research Farm on the central clay plain of Sudan, sorghum yield was extraordinarily reduced by the late growing dates. The late growing dates of 17 to 21 August compared with early sowing on 15 July reduced the grain yield from 3,230 to 1,111 kg per hectare (El Karoory, 2010). This corresponds to a reduction in yield of 62 kg per hectare for every day's delay in the growing date.

Other experiments at Tozi confirmed late growing's negative impact on sorghum and sesame yields (El Karouri, 2010). Similar results were reported at the Simsim farm, where delayed growing dates resulted in a yield reduction of one sag of sorghum Dura (202–214 kg) per hectare when the ever-increasing date was postponed for a week beyond the optimum growing date. The same trend was reported at Simsim for sunflowers, where the 15 to 20 July sowing date yielded 1,214 kg/hectare compared with 433 kg/hectare for the 15 to 20 August sowing date. The late sowing date resulted in the reduction of the disc size and poor seed filling. Similarly, the 15 July cultivation out-yielded the 10 August cultivation of sunflowers by 35% (El Karouri, 2010).

Although the SMAP radiometer optimally measures soil moisture up to 5 cm depth, understanding the amount of available soil moisture in the root zone provided an accurate assessment of drought in agricultural land.

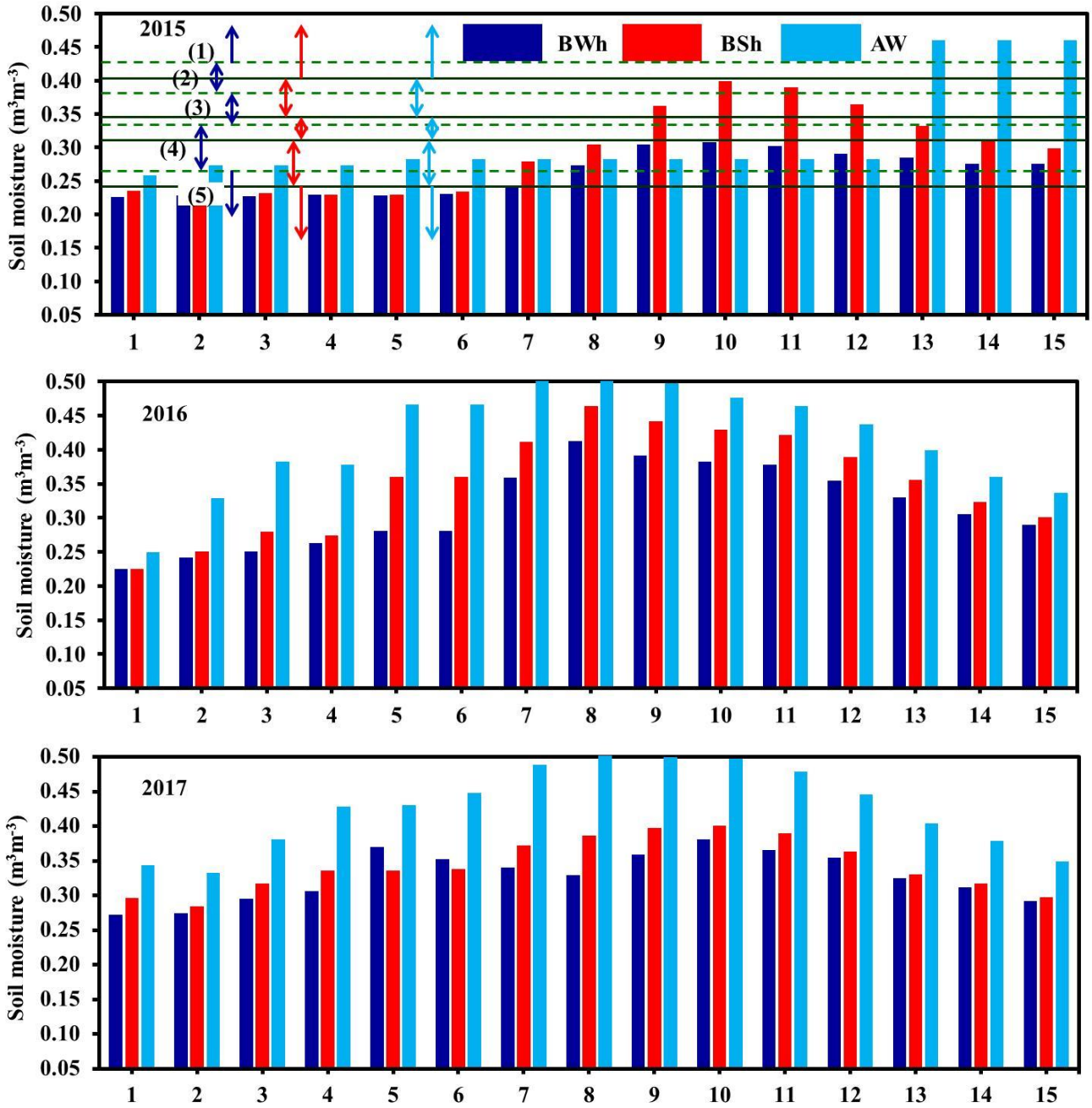

Figure 3-5 Cropland dekadal drought as assessed by Soil Water Deficit Index (SWDI), (1), (2), (3), (4), and (5) represents drought classes: no drought, mild, moderate, severe, and extreme, respectively, dotted lines represent the range of drought class over tropical savanna (AW), solid lines represent the range of drought class over warm desert climate (BWh), and warm semi-arid climate (BSh), 1 represents the 1st dekad of June. 15 represents the 3rd dekad of October

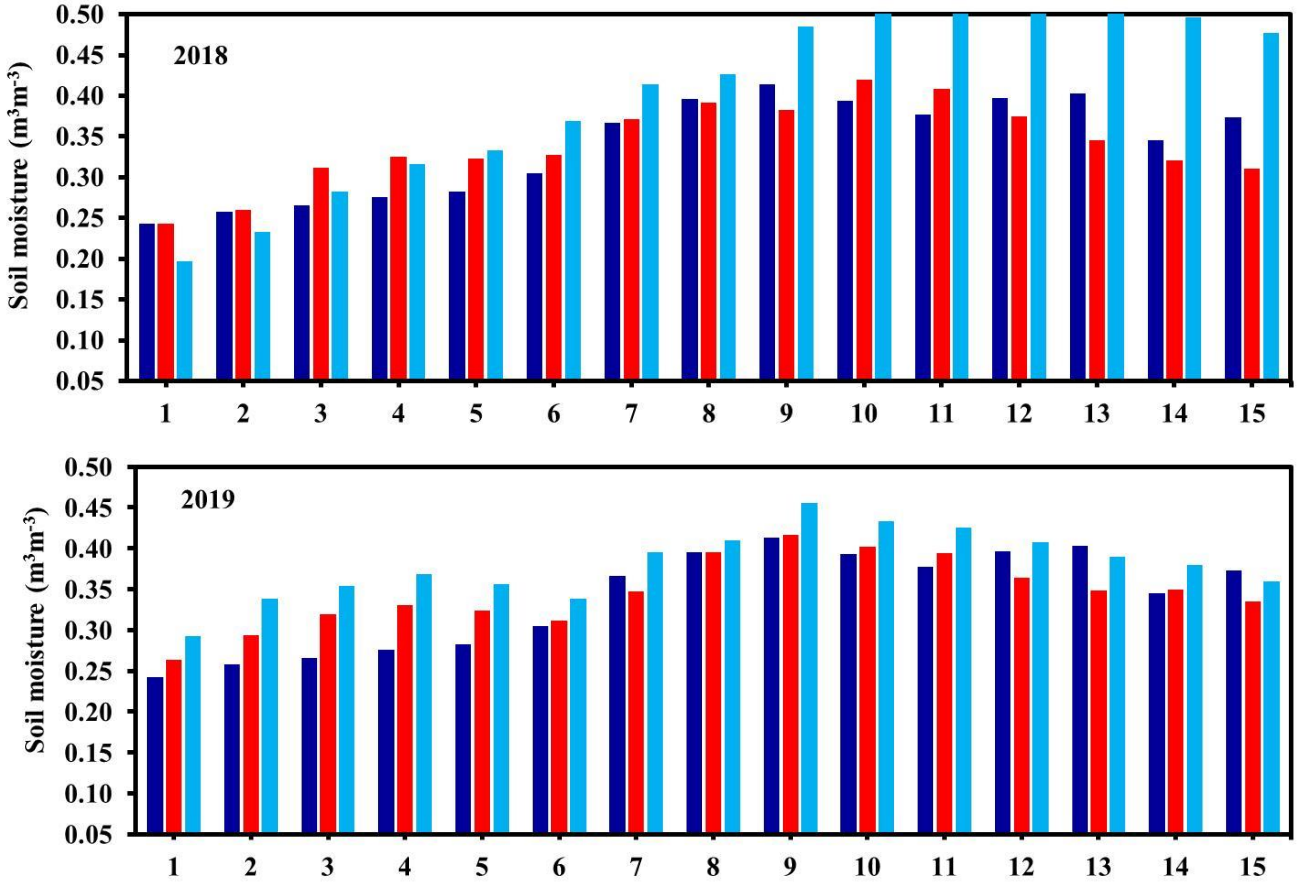

Figure 3-5 (Continued)

3.4. Spatial variation in SWDI

Drought classes range from extreme drought to no drought. The SWDI time series, the SWDI-based spatial distribution in the root zone, and the top 5 cm of drought zones across El Gedaref State (Figure 3-6 to Figure 3-15) generally, a northwest-to-southeast gradient of the drought-to-wet conditions in all five years were observed. Nevertheless, there is still a remarkable spatial variation in the drought threshold from one year to another. Based on the average areal SWDI, 2015 was the driest within the data period, followed by 2018. During the growing season of 2015, the area of El Gedaref State under severe to extreme drought at the root zone, as assessed by SWDI, ranged from 48% -58% during the period from June to the first dekad of August.

As expected, most drought zones are located within (BWh) and (BSh) lands. 2015 represents the year notoriously known for the poor rainfall performance in Sudan (Behnke et al., 2020). The seasonal rainfall has been below average across most rainfed agricultural lands. Below-average rainfall delayed the primary season growing across most of Sudan.

Based on SWDI obtained values, each drought class has corresponding soil moisture content (Table 3-3).

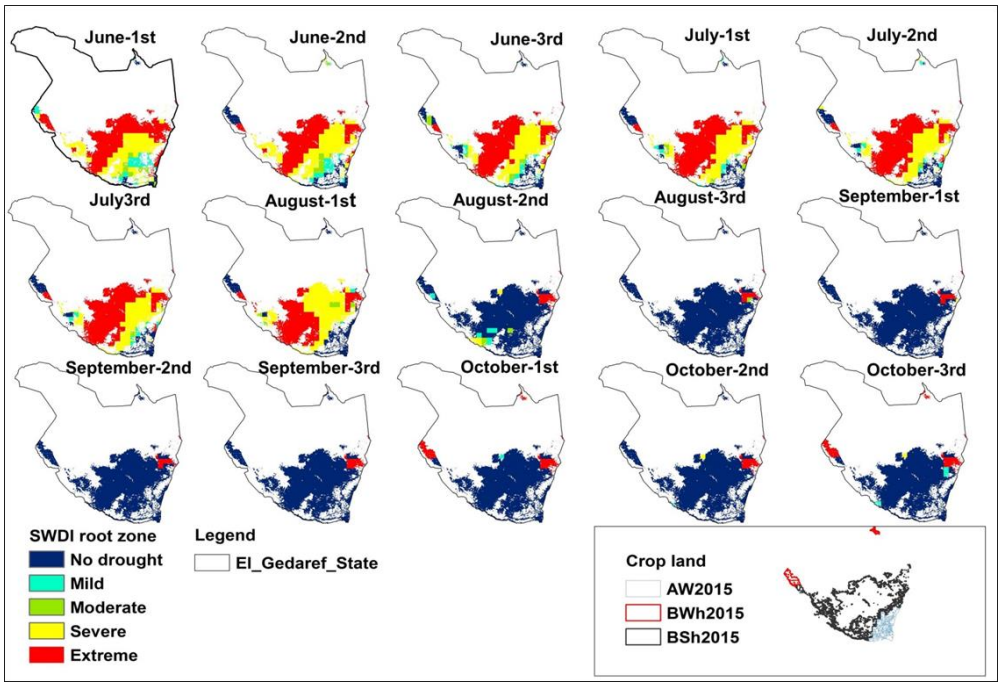

Figure 3-6 Spatial variations in the root zone SWDI over climatic zones across the study area such as tropical savanna (AW), warm semi-arid climate (BSh), and warm desert climate (BWh) during the growing season of 2015

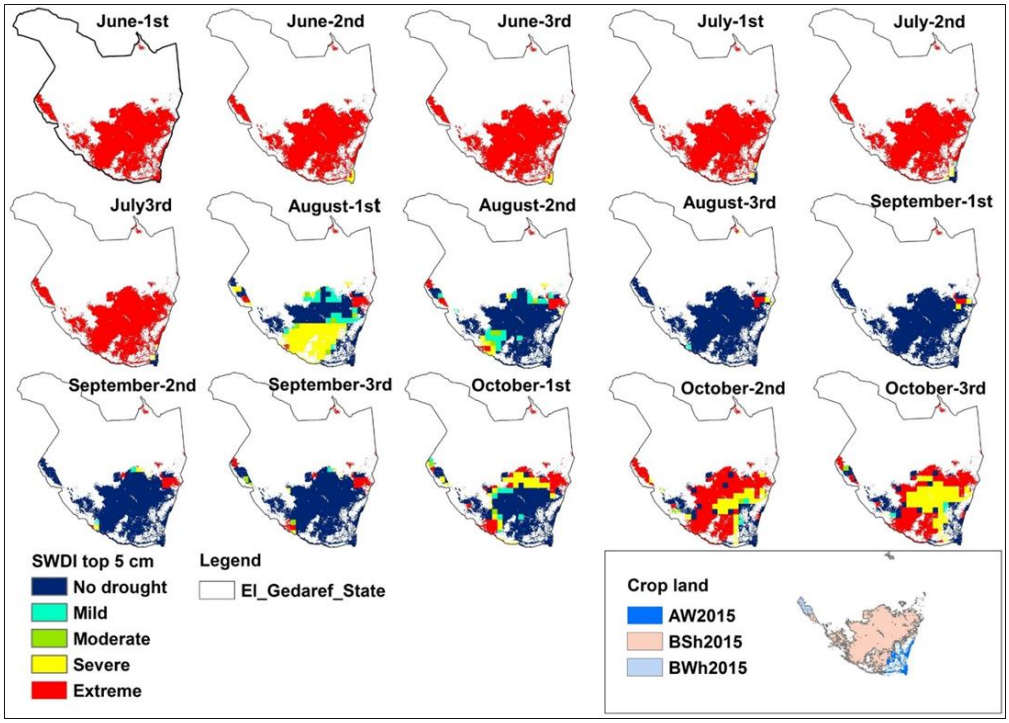

Figure 3-7 Spatial variations in the top 5cm SWDI over climatic zones across the study area such as tropical savanna (AW), warm semi-arid climate (BSh), and warm desert climate (BWh) during the growing season of 2015

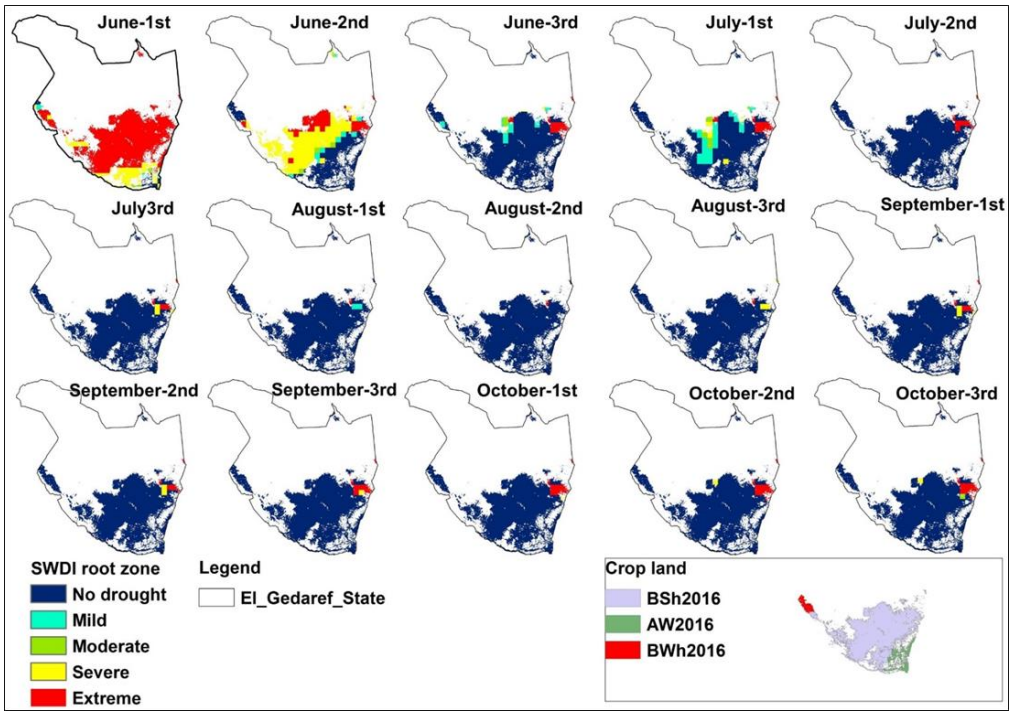

Figure 3-8 Spatial variations in the root zone SWDI over climatic zones across the study area such as tropical savanna (AW), warm semi-arid climate (BSh), and warm desert climate (BWh) during the growing season of 2016

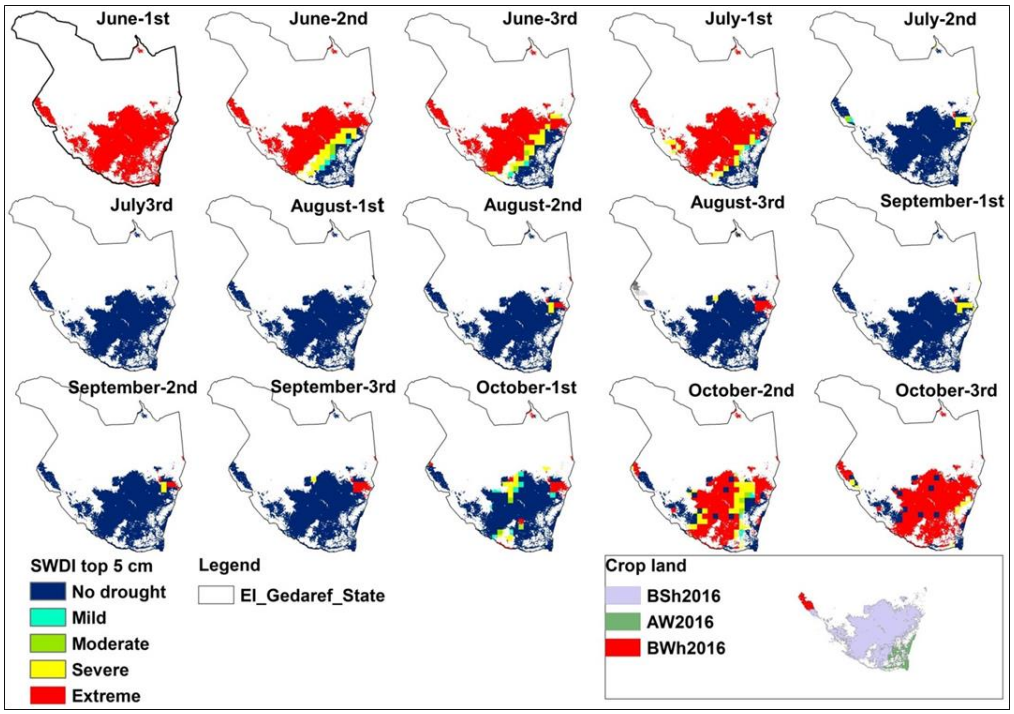

Figure 3-9 Spatial variations in the top 5cm SWDI over climatic zones across the study area such as tropical savanna (AW), warm semi-arid climate (BSh), and warm desert climate (BWh) during the growing season of 2016

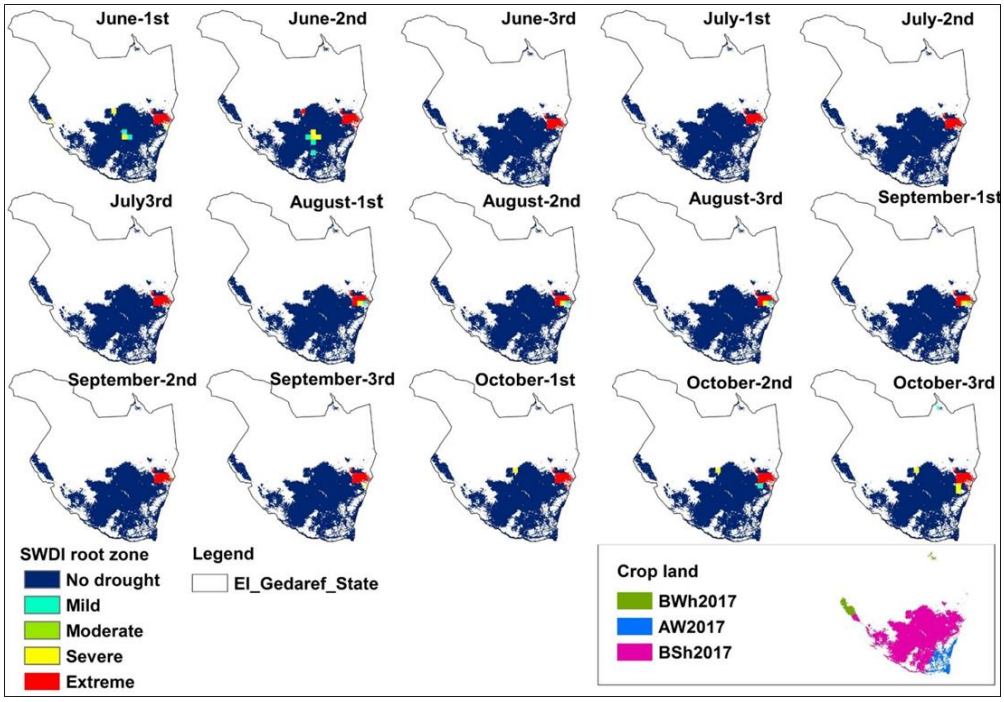

Figure 3-10 Spatial variations in the root zone SWDI over climatic zones across the study area such as tropical savanna (AW), warm semi-arid climate (BSh), and warm desert climate (BWh) during the growing season of 2017

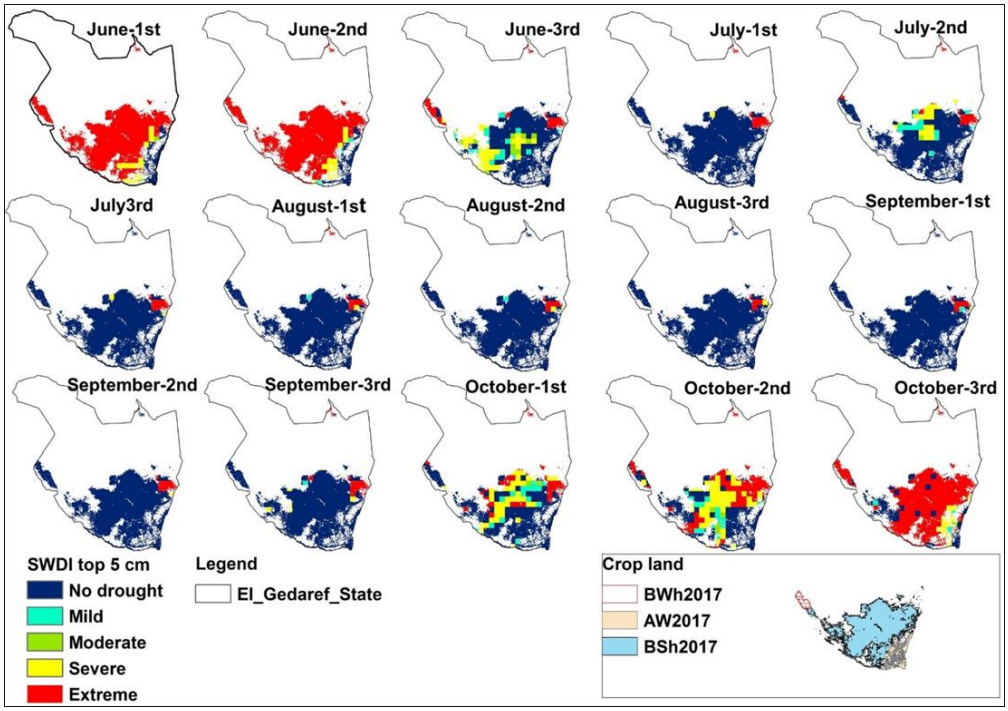

Figure 3-11 Spatial variations in the top 5cm SWDI over climatic zones across the study area such as tropical savanna (AW), warm semi-arid climate (BSh), and warm desert climate (BWh) during the growing season of 2017

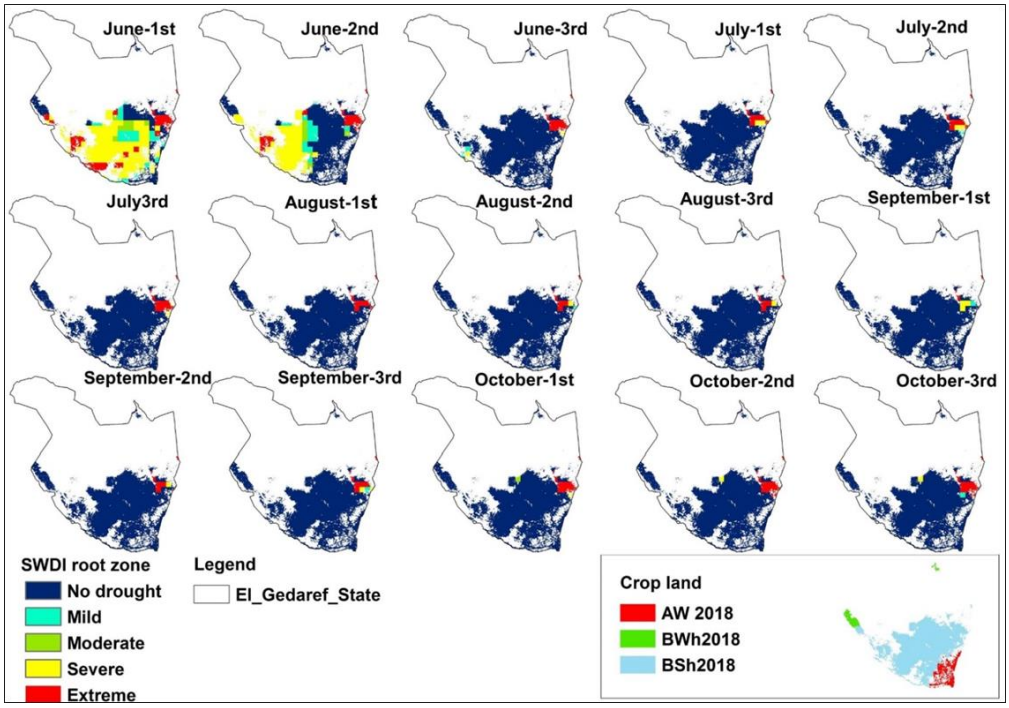

Figure 3-12 Spatial variations in the root zone SWDI over climatic zones across the study area such as tropical savanna (AW), warm semi-arid climate (BSh), and warm desert climate (BWh) during the growing season of 2018

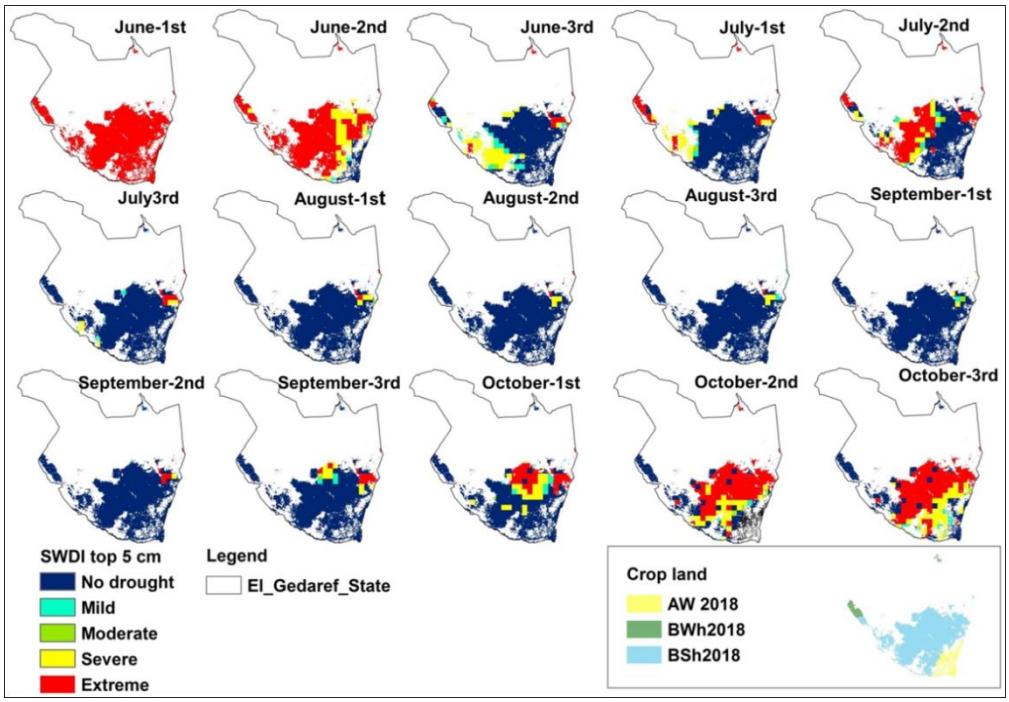

Figure 3-13 Spatial variations in the top 5cm SWDI over climatic zones across the study area such as tropical savanna (AW), warm semi-arid climate (BSh), and warm desert climate (BWh) during the growing season of 2018

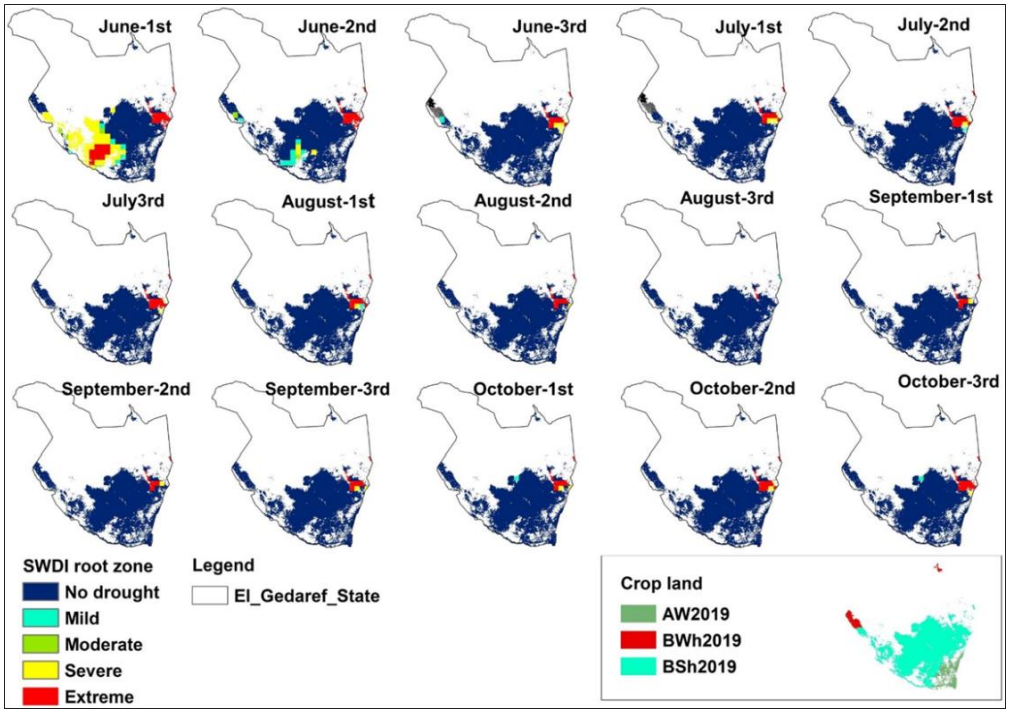

Figure 3-14 Spatial variations in the root zone SWDI over climatic zones across the study area such as tropical savanna (AW), warm semi-arid climate (BSh), and warm desert climate (BWh) during the growing season of 2019

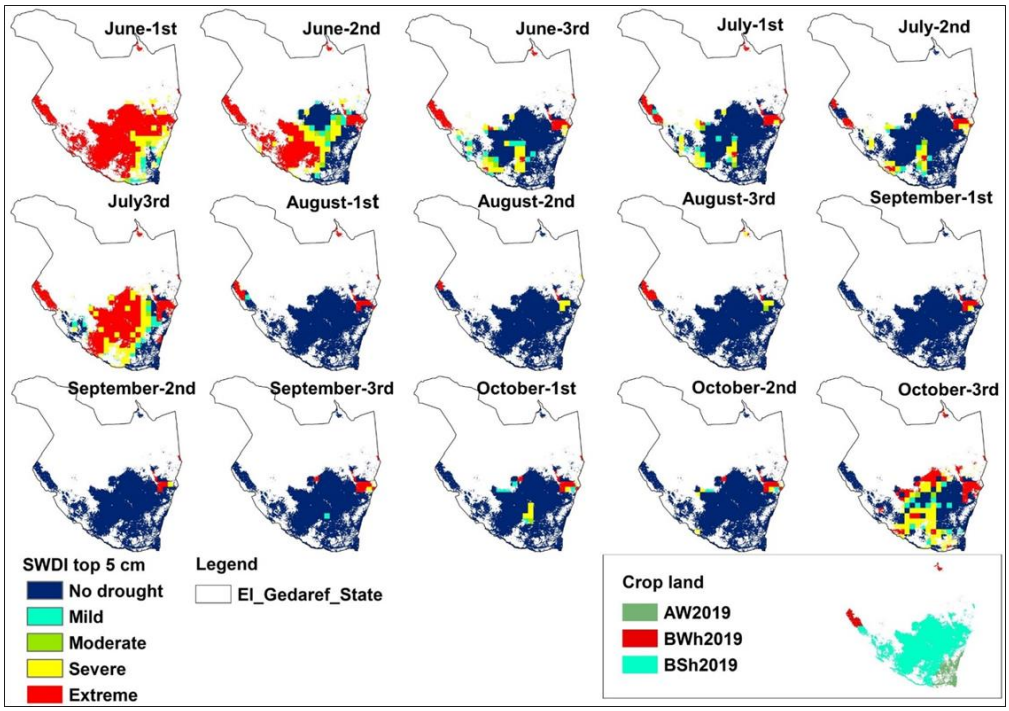

Figure 3-15 Spatial variations in the top 5cm SWDI over climatic zones across the study area such as tropical savanna (AW), warm semi-arid climate (BSh), and warm desert climate (BWh) during the growing season of 2019

CHAPTER 4. Does soil moisture compensate for the evapotranspiration demand of sorghum in El Gedaref State?

4.1. Introduction

By 2030, more billion people are anticipated to inhabit the planet. If dietary patterns are projected to persist, there will be a pressing need to increase agricultural production more quickly to keep up with population growth (Ray et al., 2013). Consequently, this will put more pressure on water, land, and energy resources. Increasing agricultural production will be one of the most significant challenges to face humanity shortly (Godfray et al., 2010, Licker et al., 2010). Among the many aspects of this challenge, available water for crop production has become a central issue (Elliott et al., 2014).

Agronomic activities must undergo optimally while prioritizing the sustainability of natural resources (e.g., water) to produce enough food to meet the unstoppable growth of the world population (Fanzo, 2019). Filling the yield gaps is not always associated with expansion in agricultural land. Instead, identifying the significant factors that are contributing to filling those yield gaps, for example, the application and extension of existing technologies worldwide, advances in crop production, e.g., development of integrated soil-crop systems management, continued genetic improvement in crop varieties (Anderson, 2017, Fan et al., 2012, Fanzo, 2019).

World agricultural productivity has the potential to increase, while low productivity has become an inherent feature of the African continent (Bjornlund et al., 2020). In Sub-Saharan Africa (SSA), 75% of the poor people derive their food from agriculture (Ogundipe et al., 2017). It is well acknowledged that SSA did not enjoy rapid and widespread improved technology that helps increase productivity (Sheahan, Barrett, 2017). As a topic of many studies, SSA has been portrayed as the most affected region in the world by climate change and variability (Kotir, 2011, Kula et al., 2013, Shishaye, 2015, van Wesenbeeck et al., 2016). Agricultural productivity is affected and will continue to be acutely affected due to climate extremes like droughts and floods.

Rainfed agriculture plays a significant role in the food supply in many regions worldwide (Parry et al., 2005, Siderius et al., 2016). This farming system provides about 60% of the total global food demand (Biradar et al., 2009) and will continue to evolve global food production in the future (Birhanu et al., 2019). In the Nile Basin, more than 87% of cultivated lands use rainfed agriculture. Since rainfed agriculture is more sensitive to climate change than irrigated systems (Valverde et al., 2015), rainfed systems in both global and regional scales are characterized by low crop yields (Rockström et al., 2010).

The low production of rainfed agriculture is attributed mainly to its direct link to climate inputs (Vanschoenwinkel, van Passel, 2018). One of the immediate impacts of climate is the little water (Golam Kibria et al., 2016, Singh et al., Vanschoenwinkel, van Passel, 2018, Verner, World Bank Group, 2012). Mechanization helped move from arduous subsistence farming to intensification in rainfed agriculture (Mano et al., 2020). Furthermore, mechanization can make it possible to time the growth more precisely (Aune et al., 2017). Mechanized farming is found to have a positive impact and lead to increasing the efficiency of sorghum cultivation in the African subtropical condition (Masaka et al., 2020).

With effective adaptability strategies and actions, studying drought risk can help implement the articulated 17 United Nations Sustainable Development Goals (SDGs) adopted in 2015. from different aspects (e.g., feeding the world with sustainable agriculture that does not destroy nature, in this context, it deals directly with the goal 2 zero hunger (Streimikis, Baležentis, 2020). From a water perspective, studying drought can help achieve goal 6 by evaluating water resources' efficiency to achieve sustainable water management in the agricultural sector (Timko et al., 2018) and sanitation (Weststrate et al., 2019).

4.2. Literature review

Sorghum ranks as the fifth most-produced cereal crop globally (Elagib et al., 2019a). More than 90% of the total cultivated area of sorghum lies in developing countries, mainly in Africa and Asia. In arid and semi-arid regions, sorghum is predominantly grown under rainfed sys-

tems. The direct connection between crop development and climate induces significant production losses. Triggers recurrent droughts pose a great threat to crop productivity (Bosire et al., 2018, Eshetu et al., 2020, Minoli et al., 2019, Msongaleli et al., 2015, Tack et al., 2017).

Sorghum is the staple crop for most Sudanese people (Abdelhalim et al., 2021), it is the larger crop ranked by area in Sudan, and most of it is rain-fed (Ehab A. M. Frah, 2016). The harvested area of sorghum in Sudan constitutes 17% and 24% of the total global and African harvested areas, respectively (FAO, 2019). El Gedaref state, where agricultural machinery is used, is the most essential and well-adapted region for sorghum cultivation (Lotfie et al., 2018).To highlight the significance of the current situation for Sudan, the status of sorghum production (harvested area, production, and yield) is compared with the global output using FAO (2019) statistics; this statistic features the sorghum production for some countries over the world.

Among the top sorghum-producing countries, Sudan is the first and most prominent country in terms of harvested area of sorghum (Figure 4-1). Despite the large harvested area of sorghum in Sudan, which equals fourfold that of Ethiopia, the latter left Sudan behind in total production. On average, with almost the same harvested area, the top sorghum producer in the world is the United States of America (USA), along with 11 million tons.

Sudan continues to be ranked 6th with 4.5 million metric tons. However, with an annual global production of 62 million metric tons, Sudan only produces an average of 4.5 metric tons of global output, Mexico and USA are significant producers of sorghum, 4.5 and 8.9 5 metric tons of the total global production on average, respectively, while simultaneously being the largest consumers (McGinnis, Painter, 2020). In both countries, sorghum is mainly produced as animal feed supplements (Yun Xiong et al., 2019) and for the production of bioethanol (López-Sandin et al., 2021). The yield level in Mexico surpasses that in Sudan by more than 80%. The high sorghum yield in Mexico was highly improved through breeding and production research (García et al., 2017).

Comparison of the sorghum production in Sudan with that in countries with harsh socio-economic conditions like Ethiopia and Nigeria increased substantially in both countries with

lower performance in Sudan (Sujay Rakshit et al., 2014). With a harvested area of only 32% of that in Sudan, Ethiopia produces around 86% of Sudan's total sorghum production. The Ethiopian government has been pursuing a strategy of improving sorghum productivity through genetic signs of progress for the last four decades. To understand the reasons behind such a poor performance of sorghum production in Sudan, a more detailed analysis and discussion of results are therefore given in the following sections.

To our knowledge, we successfully observed drought-related crop yield losses in response to Water Requirement Satisfaction Index (WRSI), the crop water balance model for maize crops in Tanzania (Tarnavsky et al., 2018), Ethiopia (Senay and Verdin, 2003), Southern Africa, Zimbabwe (Verdin, Klaver, 2002), Kenya, Malawi, Mozambique and Niger (millet) (Jayanthi et al., 2014). Similarly, a comprehensive analysis of WRSI sensitivity to soil moisture inputs from different products for sorghum has not been conducted.

Given the above background, there seems to be a fundamental need for understanding the performance of the rainfed sorghum system under different climate conditions. Analyzing the statistics of rainfed sorghum would help understand the current status of this important agricultural sector. Such an analysis will help to adopt acceptable practices for the future.

Therefore, the objective of this study is threefold: (1) to develop crop water requirements map helpful in assessing the drought state in the El Gedaref state of Sudan as an example for mechanized rainfed agriculture, (2) to examine the sensitivity of WRSI to rainfall and soil moisture inputs and sorghum varieties in Sudan (3) characterizing the Spatio-temporal, and soil state of agricultural productivity of the mechanized rainfed, farming-based under dry and moist years on using SMAP soil moisture data and remotely-sensed vegetation indices for a case study using the adapted WRSI and sorghum statistics measured on the ground, therefore, to provide a piece of complete information to understand the opportunities and challenges for food security and sustainability of this system in Sudan.

The previous research conducted on rainfed sorghum agriculture in the El Gedaref state includes, among others, cultural practices and their effects on sorghum yield (Yousif, Taha, 2013), impacts of economic return on agricultural research (Ahmed, 1995), governmental policies on sorghum production (Abdelgalil, Adeeb, 2015, O'Brien, 1985, Teklu et al., 1992),

sorghum vulnerability and resilience to climate (Elagib et al., 2019a), and factors determining the growing dates of sorghum (Bussmann et al., 2016a). Although this literature delivers valuable information about the main sorghum husbandry in Sudan, an inclusive overview of the role of this farming system is still lacking.

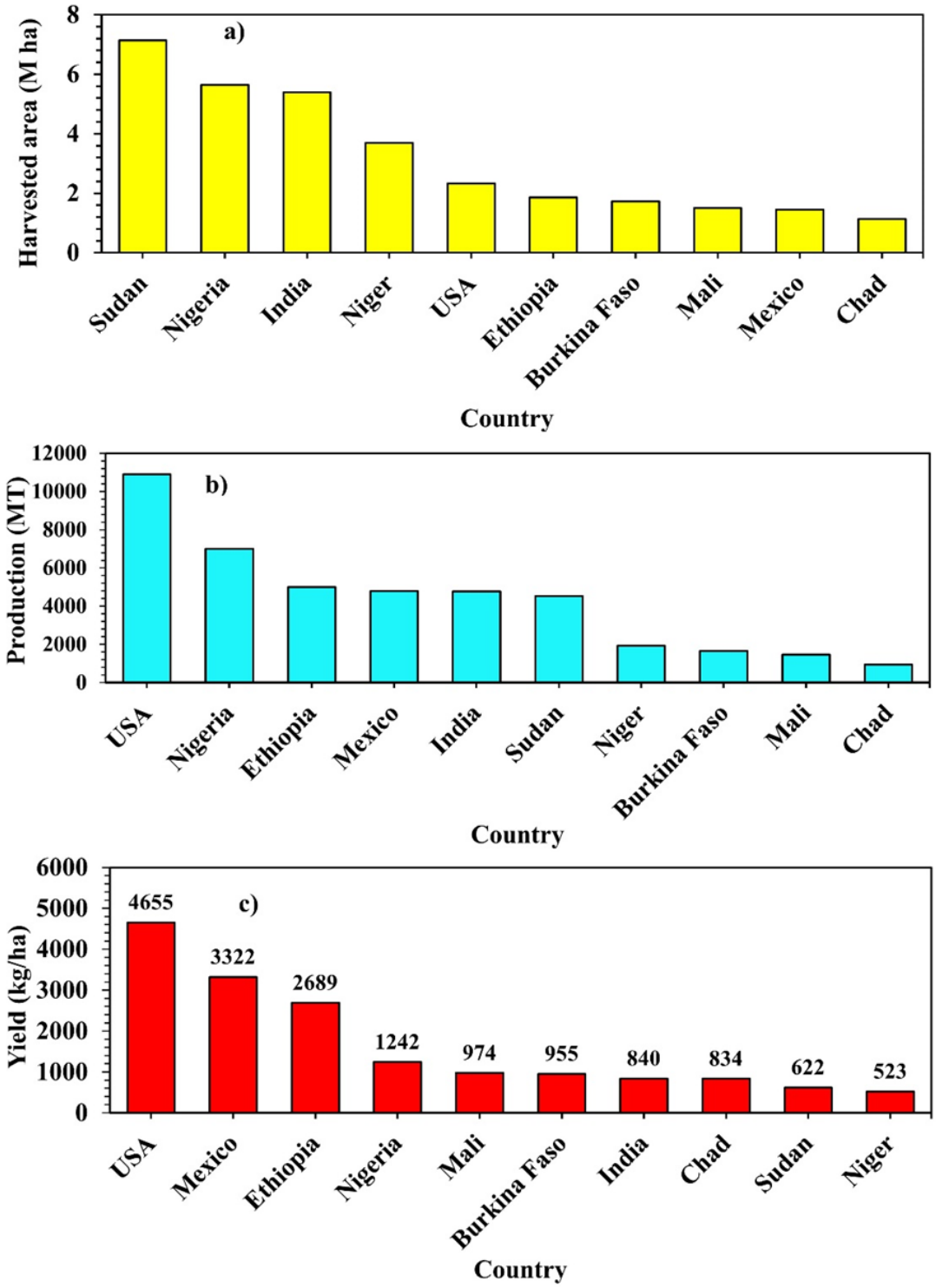

Figure 4-1 Ranking of the top sorghum-producing countries in terms of a)harvested area, (b) production and c) yield. The data represent the multi-year averages (2015–2019) as calculated using FAOSTAT data (http://www.fao.org/Faostat/en/#data/QC)

4.3. Materials and methods

4.3.1. Data

The dataset used in this study consists of a collection of climatic data (from stations and gridded data sources), sorghum statistics, and satellite-based vegetation indices. The data on rainfed sorghum statistics, i.e., planted and harvested areas, production, and yield come from the ministry of agriculture of El Gedaref state. These statistics were available from 1940 to 2020. Sorghum is selected for the current investigation because it is the main staple major food crop cultivated in the region, as mentioned before.

Lastly, the sorghum yield was calculated as the ratio of regional sorghum production to the regional harvested sorghum area in El Gedaref state. El Gedaref state was considered for a thorough analysis of the Spatio-temporal variation of climate and vegetation productivity, using gridded data on climate and soil elements, i.e., precipitation, soil moisture, actual and potential evapotranspiration. The gridded data for El Gedaref state were acquired as shown in Table 4.1 and are described below. As described previously, sorghum is the main crop cultivated in El Gedaref state.

As detailed farm data are not available in Sudan, obtaining data only for the sorghum region poses a significant challenge to reducing uncertainty. This information has been confirmed for El Gedaref province by Mustafa (2006). In other words, “Data from various sources are averaged and recorded for the entire region without detailed details. It is unsystematic and short term” (Mustafa, 2006). by Mustafa (2006) for El Gedaref state; thus: the data obtained from different sources [are] recorded on average for the whole region without in-depth details. The methods of keeping records on area grown, area harvested, costs, production, and yield are not regular, not systematic, and only for a short period”(Mustafa, 2006).

Therefore, in the present study, I relatively attempted to overcome this limitation, as discussed in the next section.The Climate Hazards Group Infrared Precipitation with Station data (CHIRPS) was used in this study. It is a global precipitation dataset that starts at 50°S-50°N and covers all longitudes. The data was launched in 1981 and has continued to near-present. The CHIRPS combines 0.05° resolution satellite imagery with ground station data

(satellite-gauge product) to form a rainfall network time series for trend analyses and drought monitoring. Version 2.0 of CHIRPS was completed on 12 February 2015 and became accessible for public use. (For more and elaborated information on CHIRPS, please refer to (Funk et al., 2015). Since 1999 techniques have been developed by the United States Geological Survey (USGS) and Climate Hazard Center (CHC) scientists supported by funding from USAID, NASA, and National Oceanic and Atmospheric Administration (NOAA) to produce maps, especially in regions with limited spatial coverage. This precipitation product is broadly used for floods and drought studies (Saeidizand et al., 2018). Dekadal precipitation data of CHIRPS were processed online using the GIOVANNI tool.

Dekadal actual evapotranspiration data (AET) were obtained from the website of Famine Early Warning System Networks (FEWS NET), as indicated in Table 4.1. These gridded data were produced using the climate variables output from the Global Data Assimilation Systems (GLDAS).

AET data of this global product were calculated following the standard method of FAO Penman-Montieth for grass reference evapotranspiration, ET_o (Allen et al., 1998). The Moderate Resolution Imaging Spectroradiometer (MODIS) satellite was used in this study as the source of NDVI data. This dataset is maintained by the United States Geological Survey (USGS) Earth Resources Observation and Science (EROS) Center. For the current research, dekadal data (10-day composites) with a spatial resolution of 250 m for the years 2015 through 2019 were downloaded from the website of FEWS Net.

Dekadal Actual Evapotranspiration (AEP) was produced using the Operational Simplified Surface Energy Balance (SSEBop) model from the website of Famine Early Warning System Networks (FEWS NET). The SSEBop setup is based on the Simplified Surface Energy Balance (SSEB) approach (Senay et al., 2007, 2011) with a unique parameterization for operational applications. It combines ET fractions from remotely sensed MODIS thermal imagery acquired at the dekadal time step with reference ET using a thermal index approach. The unique feature of the SSEBop parameterization is that it uses a pre-defined, seasonally and spatially dynamic surface psychrometer parameter to calculate ET fraction as the difference

between observed Land Surface Temperature (LST) (dry-bulb) and a cold/wet boundary condition (wet-bulb) using the principle of satellite psychrometric calculation test (Senay, 2018). The basic construction of SSEB is an adaptation of the hot and cold pixel principle of SEBAL (Bastiaanssen et al., 1998) and Mapping Evapotranspiration with Internalized Calibration (METRIC) (Allen et al., 2007) models. A current evaluation of the global ETa product shows the promising performance of ETa anomaly for drought monitoring purposes. At the same time, water budget studies requiring absolute magnitudes may need to apply a local/region-specific bias correction procedure (Senay et al., 2020).

Table 4-1 WRSI model input data (AET =Actual Evapotranspiration; PET-PM Potential Evapotranspiration (reference) with Penman-Montieth equation; CHIRPS= Climate Hazards Group InfraRed Precipitation with Station data; SM= SMAP Soil Moisture 3 hour temporal resolution aggregated every dekad.

Variable	Data source	Spatial resolution	Temporal resolution	File format	References
AET	FEWS NET	0.01º	Dekadal	GeoTiff	(Sawadogo Alidou et al., 2020)
PET-PM	FEWS NET	0.01º	Dekadal	GeoTiff	(Shraddhanand Shukla et al., 2017)
Precipitation	CHIRPS	0.05 º	Dekadal	GeoTiff	(Tufa Dinku et al., 2018)
SM	SMAP	0.9º	3-hourly	GeoTiff	(Stillman, Zeng, 2018)

4.3.2. Processing of gridded datasets

Processing of the remote sensing imagery datasets, i.e., actual evapotranspiration (AET), rainfall was done in the Geographic Information System (GIS 10.3.1). To relatively overcome the limitation of unavailable data on exact sorghum fields, the current study considered the approach of masking the agricultural pixels alone with a threshold of WRSI between (available soil moisture content and permanent wilting point), as adopted in chapter (3) for the El Gedaref state different isohyets.

4.3.3. Modeling approach

The spatially explicit Water Requirement Satisfaction Index (WRSI) was used in this study as an indicator of sorghum performance during its growing season. WRSI is a simplified crop water stress model widely used in drought and famine early warning systems (Tarnavsky et al., 2018), This model has been used widely for drought studies in African countries. WRSI estimation needs rainfall, evapotranspiration ($ET_{o)}$, soil water holding capacity, cultivar length, and crop coefficient (Kc) which varies by crop cultivar and phonological stage, and described in FAO Penman-Montieth equation was used in the assessment of the station data on temperature were used to calculate the ET_o using the method developed by. The WRSI crop model output was run for the 5-year time period for which there were available production data. The model was run to simulate the crop water requirement of sorghum for the rainy season from 2015 through 2019, the start of the season from June to October.

The dekadal WRSI is Africa's primary 10-day time step of agro meteorological monitoring. Every month of the year consists of three dekads: the 1st through the 10th, the 2nd through the 20th, and a final dekad of 8 and 9 during February in simple and leap years, 10 or 11 days. Dekad is a technical term for the World Meteorological Organization (WMO). The dekad represents a compromise between a monthly time step, which is inadequate to resolve main crop growth stages, and a daily time step, which imposes a significant data-processing burden without a commensurate gain in agro meteorological information.

WRSI for a dekad is based on the water supply and demand a crop experiences during a dekad period step. It is calculated as the ratio of dekadal actual evapotranspiration (AET_d) to the dekadal crop water requirement (WR):

$$\text{WRSI} = \left(\frac{\sum_{d=1}^{d} AET_d}{\sum_{d=1}^{d} PET_d}\right) \times 100 \quad (9)$$

where d is the dekadal period; AET_d represents the actual amount of water withdrawn from the soil water reservoir or actual evapotranspiration of the crop for the dekadal period, and PETd is the Penman-Montieth potential evapotranspiration of the crop for dekadal period. PETd was calculated using crop coefficient (Kc).

The crop's water requirement (PET_d) at a dekadal time step in the growing season is calculated by multiplying dekadal standard reference crop ET_o by the crop coefficient (Kc).

$$\text{PET}_d = \text{ETo} \times \text{Kc} \quad (10)$$

Depending on the plant's available water (PAW) in the “bucket” the value of AETc is determined by the following set of functions (Senay and Verdin, 2003).

4.3.4. The adopted WRSI model

The adapted WRSI developed here compared available soil moisture with PET; this allows the sensitivity of sorghum to sufficiency/insufficiency of water during its different phonological metrics such as the start of the season (SOS), length of the growing period (LGP), and end of the season (EOS). Dekadal values of available soil moisture were obtained from SMAP. Preliminary results found by applying satellite information showed a good agreement between the surface energy balance algorithm for land (SEBAL) estimations of evapotranspiration and the corresponding values simulated by the soil moisture assessment techniques.

Below is the prognostic equation for the available soil moisture:

$$\Delta W = (P - E_I) - (E_T + E_S),\ O \leq W \leq W^* \quad (11)$$

Where:

W: available soil moisture at the wilting vegetation stage

*W**: maximum available soil moisture (the difference between the soil's field capacity and the vegetation's permanent wilting point).

P: dekadal rainfall

E_I: dekadal interception (the water that evaporates from the wet surface of the vegetation and soil during and immediately following precipitation).

E_T: dekadal transpiration (the water transferred from the root zone of the soil to the atmosphere through the root stem-leaf system of the vegetation).

Es: dekadal soil evaporation (the water directly transferred from the soil to the atmosphere by upward hydraulic diffusion through the soil's pores).

In this study, the dekadal precipitation P is always treated as rainfall, and $(P\text{-}E_I) < O$ is the dekadal infiltration of water into the soil. $(E_T+Es+E_I) = E$ is the dekadal evapotranspiration. When W= W*, $(P\text{-}E_I) > O$ is the dekadal surplus and contribution to the annual runoff.

- ✓ dekadal values of WRSI were derived in a repeatable cycle based on the available soil moisture on the surface and at the root zone.

4.4. Sorghum LGP in Sudan

All sorghum varieties in Sudan fall into three categories in terms of LGP (Alasha, 2022):

- ✓ Late-maturing varieties take more than 120 days to reach physiological maturity, like Wad Alfahal (released variety) and Safra (unreleased variety).

- ✓ Minimum to late maturing varieties, which take 90 to 100 days to reach physiological maturity, like Wad Ahmed and Tabat (both are released varieties).
- ✓ Medium to early maturing varieties, which take 70-80 days to physiological maturities, like HD-1, HD-2, Hageen Gezira, Hageen Gedarif, PAC-501, and PAN-601 (all are released hybrids).
- ✓ Early maturing varieties take 60-75 days to reach physiological maturity like AG-8, Butana, and Bashaier (all are released varieties).

The LGP can be divided into four distinct growing stages that depict crop phenology. Initial, vegetative development, reproductive, and maturity (D. W. Meyer, M. Badaruddin, 2001). The analysis was performed on short, medium, and long-season sorghum varieties and hybrids with 70-day (7 dekads), 90-day (9 dekads), and 120-day (12 dekads) growing periods, respectively.

The estimated values of K_c for Sorghum by the FAO ET_o Penman-Monteith method at the four crop growth stages are 0.53, 0.82, 1.24, and 0.85, respectively. The FAO ET_o Penman-Monteith recommended for use with daily time steps (mm day^{-1}) Eq. (13):
WRSI values for different growing dates starting from the 1st dekad of June to the 3rd dekad of September were determined for all the varieties. LGP can be defined when the rate of rainfall exceeds 50% of the total reference evapotranspiration (Tarnavsky et al., 2018).

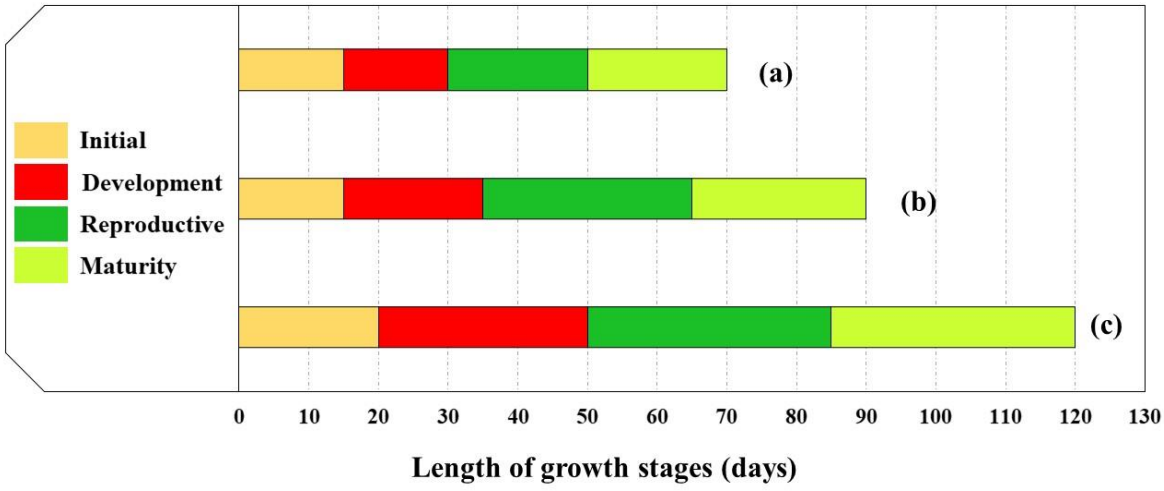

Figure 4-2 Four distinct growing stages for the three sorghum varieties: short a), medium b), and long c)

$$ET_o = \frac{0.408\Delta\,(R_n - G) + \gamma(900/(T+273))u_2(e_{s-}\, e_a)}{\Delta + \gamma(1 + 0.34u_2)} \quad (12)$$

where R_n is the net radiation at the crop surface (MJ m^{-2} day^{-1}), G is the soil heat flux density (MJ m^{-2} day^{-1}), γ is the psychrometer constant in (kPa $°C^{-1}$), T is the air temperature (°C), u_2 is the mean wind speed at 2 m height (m s^{-1}), e_s the vapor pressure of the air at saturation (kPa), e_a the actual vapor pressure (kPa), Δ the slope of the vapor pressure curve (kPa $°C^{-1}$) Allen et al. (1998).

4.5. Crop Data

Sorghum production data were obtained from the Mechanized Rainfed Agriculture Authority, El Gedaref state. Information about sorghum LGP was obtained from the Agricultural Research Corporation (ARC) of Sudan (Alasha, 2022). In this study, LGPs are indicative of general sorghum conditions in Sudan but may vary significantly from region to region, with climate and cropping conditions. The sorghum production data included the cultivated area in hectares and production in metric tons at El Gedaref State (Table 4-2). Sorghum production data were available from 1940 through 2020. Only the five years (2015-2019) data were used; the rainy season represents the primary growing season in Sudan, encompassing the period between June and October. The rainy season accounts for 90-95% of the annual crop production of the country (FEWS NET, 2001).

To implement spatial analysis in GIS, the production data were related to El Gedaref state map files in ArcView (ESRI, 2000). Various database utilities from Microsoft Access (Microsoft, 2013) were used to classify the data by year, season, and crop variety.

Table 4-2 El Gedaref state five years of sorghum data in terms of cultivated area, productive area (a) non-productive area, production, and yield

Season	Cultivated area (M ha)	Productive area (M ha)	Non-productive area (M ha)	Production (MT)	Yield (kg/ha)
2015	6.5	3.1	3.4	0.6	474
2016	6.0	5.1	0.8	1.9	876
2017	5.7	3.0	2.7	0.7	579
2018	5.1	4.2	0.8	1.4	762
2019	5.4	2.9	2.5	0.7	548

4.6. Results and discussion

In this section, the findings from the assessment of rainfall seasonality were presented, as the sensitivity of WRSI to chirps rainfall input data and correlations of WRSI, seasonal rainfall, and median SMAP soil moisture with reported yield for sorghum in El Gedaref State.

4.6.1. Assessment of SOS, LGP, and EOS seasonality

Concerning SOS timing and spatial patterns, LGP and EOS. Figure (4-3) shows the difference between SOS, LGP, and EOS covered by chirps, SMAP, and actual evapotranspiration. In areas between 500 mm and 800 mm, isohyets being the cropland. The rainy season onset in the first decked of June, followed by heavy showers in July and August. In September, rain-fall starts to slacken down before it ends up towards the first dekad of October.

As EOS is derived by adding LGP to SOS, the spatial pattern of EOS reflects the above discussion with simulations using SMAP as input soil moisture data enabling estimation of the EOS practicably, i.e., on average in all years. The CHIRPS and SMAP estimated the slightly earlier SOS and shorter LGP at 5 cm, respectively, compared to the SOS and LGP estimated with the SMAP at the root zone.

The spatial patterns of SOS in SMAP at the root zone and the top 5 cm, and at CHIRPS, are similar, with an earlier season onset in the CHIRPS product on average (dekad 16 corresponding to the first dekad of June, SD =10.2) than in SMAP (dekad 17 corresponding to dekad 2 of June SD=7.3 and 7.5, at the root zone and the top 5 cm respectively).

Figure 4-3 shows the average across the cropland of El Gedaref state SOS, LGP, and EOS values over time as evaluated by MODIS actual evapotranspiration, SMAP soil moisture at the root zone and the top 5 cm, and CHIRPS rainfall products. Generally, SMAP at the root zone shows the lowest mean SOS dekad (dekad 28–29 corresponding to dekads 1–2 of October) and the highest variability over time (SD =3.6). For CHIRPS and SMAP, these are dekad 30 (corresponding to dekad 3 of October) with SD of 2.8 and 2.7, respectively. Concerning LGP, SMAP at the root zone shows the longest LGP of 14 dekads and the lowest SD of 0.6. MODIS actual evapotranspiration and CHIRPS are corresponding LGP of 9 and 10

dekads with SD of 0.7 and 0.9. Concerning EOS, the inconsistency is much fewer in all products input datasets, generating average EOS around dekad 18 (corresponding to dekad 3 in June) and SD of 0.7, 0.8, and 0.9 for SMAP, CHIRPS, and MODIS, respectively.

The above analysis shows the comparable differences between the capabilities of all products in detecting the onset of the growing season, estimating LGP, and then EOS. The variability of SOS, LGP and EOS detection has necessary implications for seasonal WRSI assessment, crop yield monitoring, forecasting and agrometeorological risk analysis based on the WRSI model, and assessment of WRSI sensitivity to climate and soil moisture inputs.

Illustration of the spatial pattern of the average seasonal WRSI (Figure 4-4) calculated using the standard WRSI method for SOS based on precipitation, soil moisture, and the actual evapotranspiration threshold. The length of the growing season (LGP) is determined by the period when precipitation, soil moisture, and actual evapotranspiration are ≥ 0.5 of the potential evapotranspiration from CHIRPS, SMAP , and MODIS , respectively. The average WRSI values over time from the simulations with the data inputs from all three products are above 70%, indicating that, on average, sorghum moisture requirements are satisfactorily met by available water.WRSI during the crop growth period of sorghum.

Demonstration of the effect of different types of input data on seasonal WRSI (Figure 4.5) under the three conditions of the stable length of the growing season, i.e., 70, 90, and 120 days, and the scenarios through which LGP differs as a function of the persistence of rainfall, soil moisture, and actual evapotranspiration over potential evapotranspiration. The results in lower variability over time of WRSI simulations with CHIRPS rainfall input and no years detected of averaged WRSI below 70% when I used CHIRPS rainfall and SMAP soil moisture at the root zone as input to the WRSI model at 70 days LGP. In contrast, for SMAP 5 cm and MODIS, actual evapotranspiration WRSI was below 60 % for 120 days LGP in 2015 and for 70, 90, and 120 days LGP in all years, owing to the preceding SOS and short-term LGP detected by CHIRPS and MODIS. Generally, WRSI estimates based upon CHIRPS rainfall and SMAP root zone-soil moisture input data are higher than those with the MODIS actual evapotranspiration and SMAP soil moisture at the 5 cm products.

MODIS-based WRSI simulations also show the widest variation in standard deviation (SD) and CV, respectively, between 2.9 and 3% for the 90-day growing length simulation and 5.4 and 6% for the 120-day growing length simulation. CHIRPS-based WRSI simulations result in the lowest SD and CV of 3.0 and 3% for the 90-day and WRSI method developing length scenarios and 4.0 and 4% for the 90–120 days growing length scenarios. WRSI results with SMAP at root zone as the soil moisture input dataset are similar to those with CHIRPS, although less variable with SD and CV of 3.4 and 4% for the 70-days and WRSI method and 4.8 and 5.2% for the 90–120 days growing length scenarios.

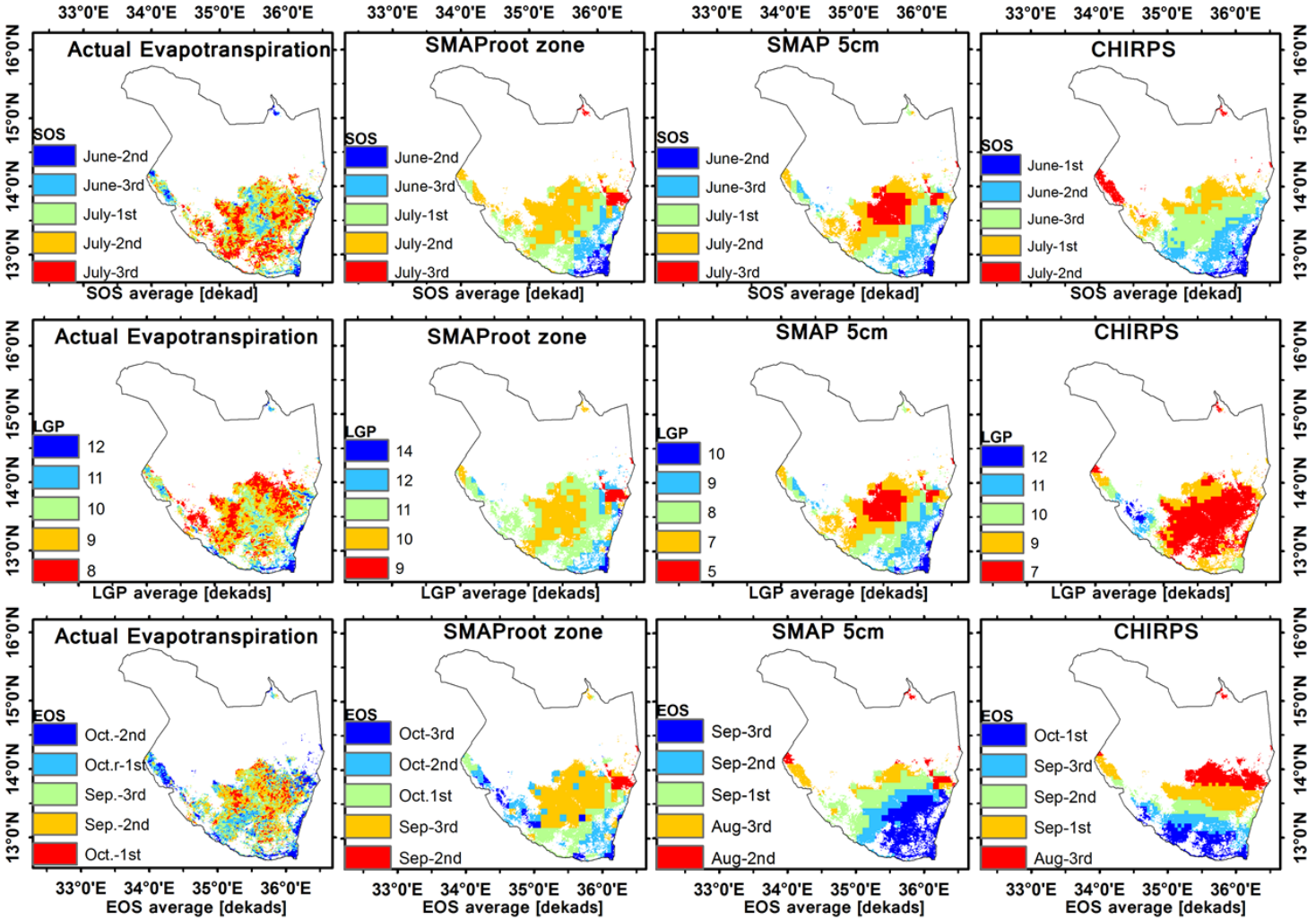

Figure 4-3 Average start of season (SOS) dekad determined using the WRSI values derived from actual evapo-transpiration, SMAP soil moisture at root zone and top 5 cm, CHIRPS rainfall threshold method ≥ 0.5 PET (top), WRSI average length of growing period (LGP) (middle), and WRSI average end of season (EOS) dekad (bottom) determined from the period (2015-2019).

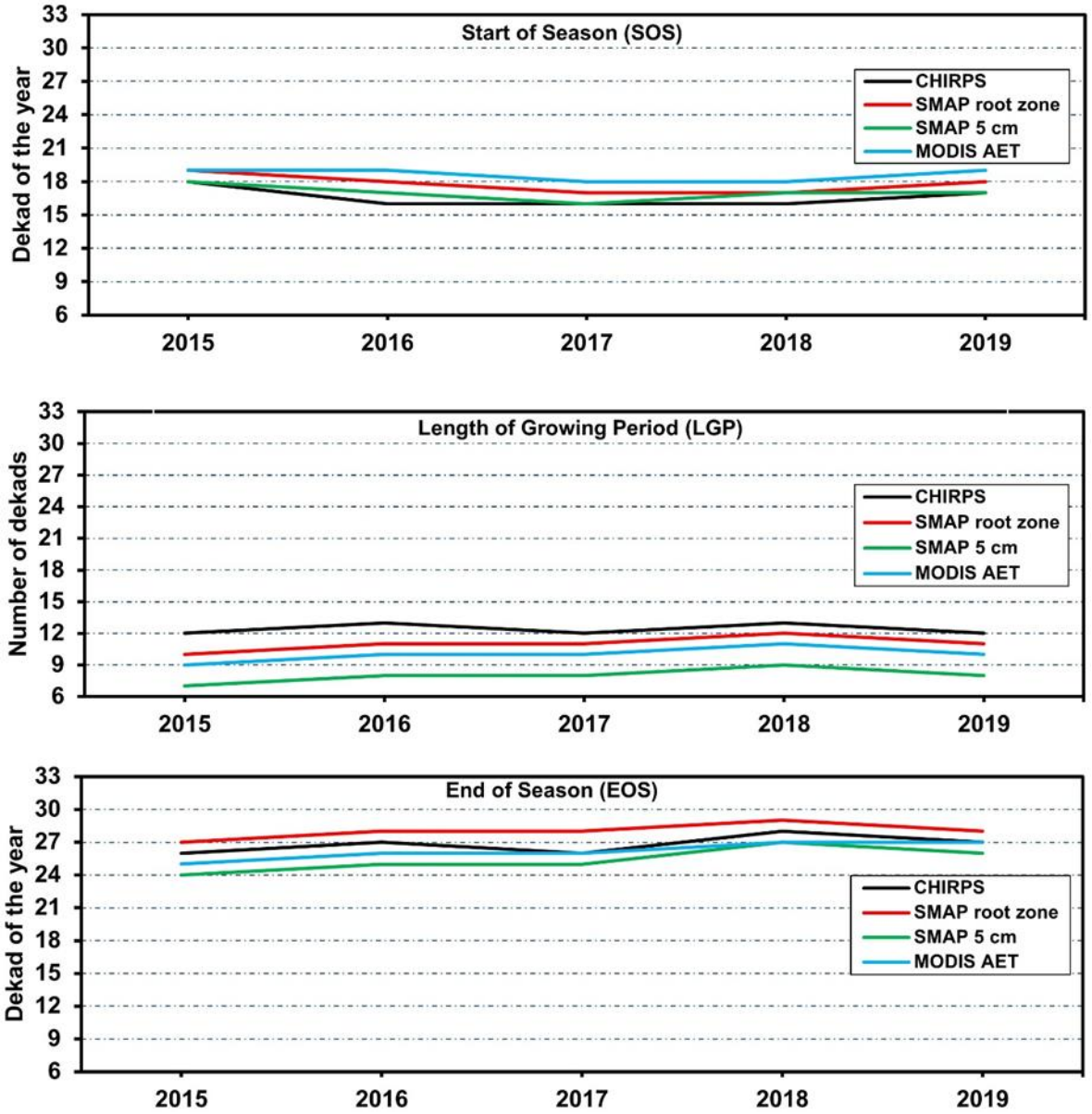

Figure 4-4 Cropland averaged start of the season (SOS) determined using rainfall, soil moisture, and actual evapotranspiration threshold, length of growing period (LGP) defined using the WRSI method of rainfall, soil moisture, actual evapotranspiration ≥ 0.5 PET, and end of season (EOS) determined from CHIRPS rainfall, SMAP soil moisture, MODIS actual evapotranspiration products

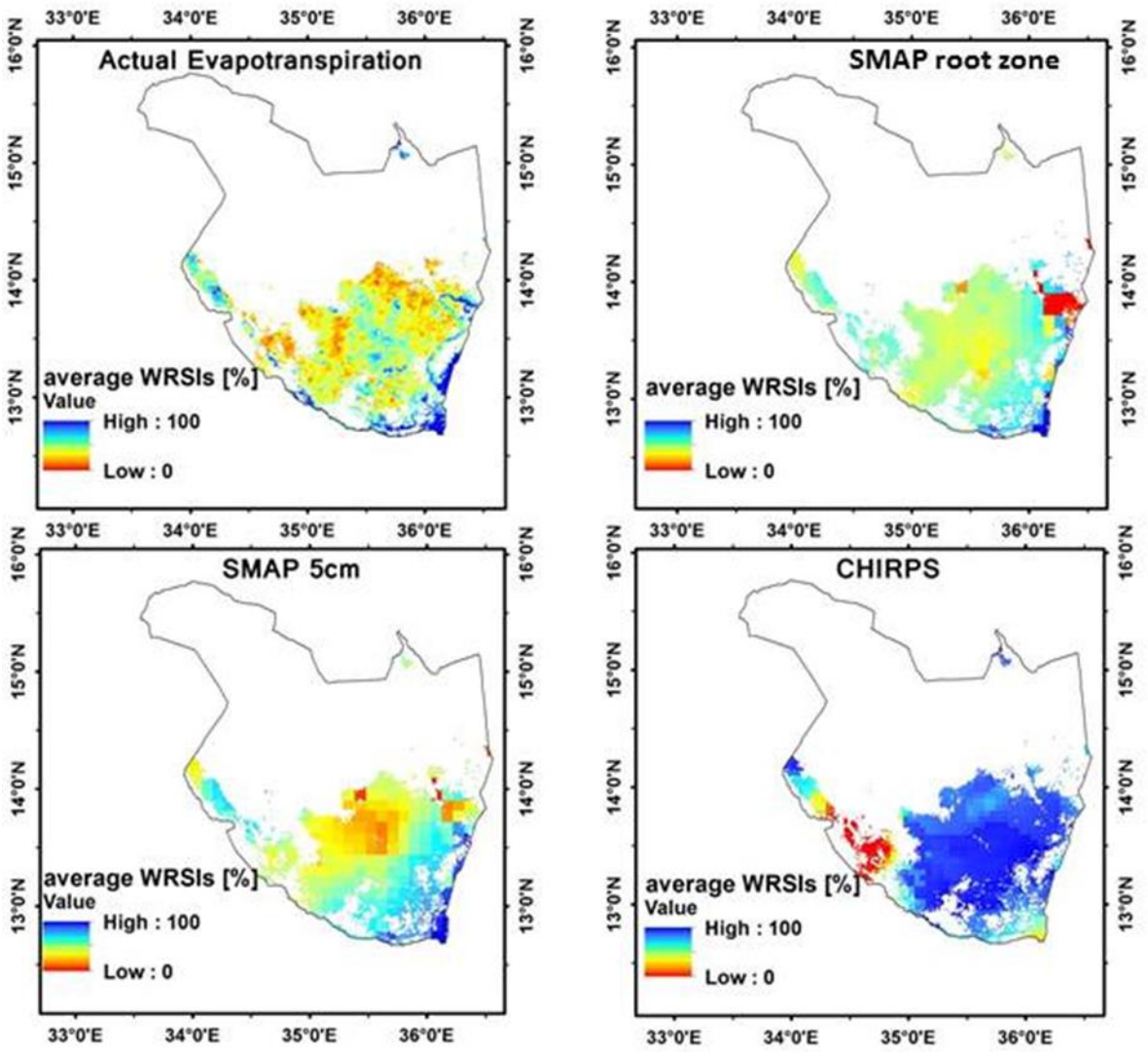

Figure 4-5 Average seasonal Water Requirements Satisfaction Index (WRSI) with the WRSI method for start of season (SOS) detection based on (actual evapotranspiration, soil moisture, and a rainfall threshold) and length of growing period (LGP) defined as the length of growing period (LGP) defined as the length of time that (actual evapotranspiration, soil moisture, and a rainfall) ≥ 0.5 PET from the MODIS, SMAP at the root zone and 5 cm, and CHIRPS products.

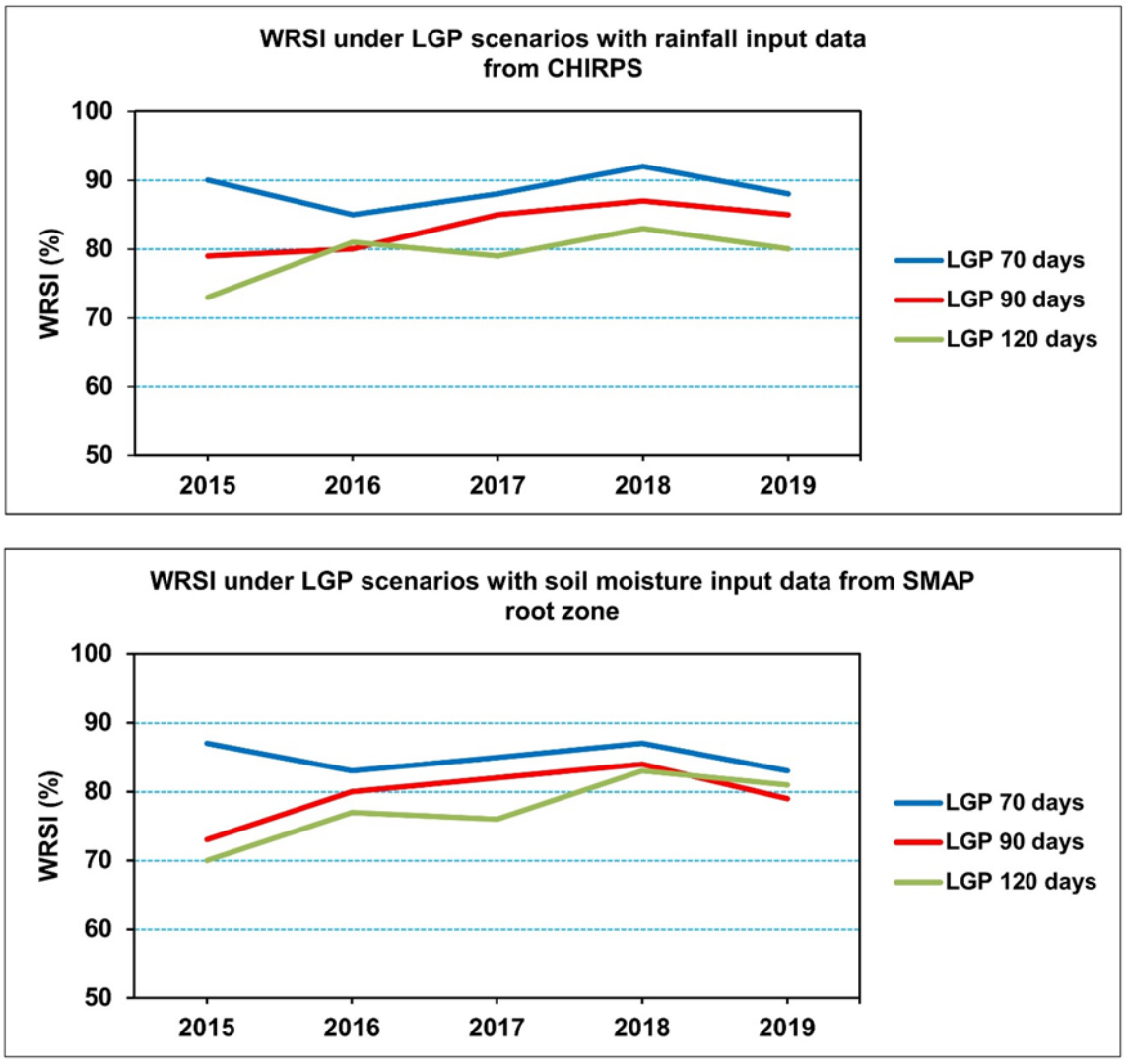

Figure 4-6 Averaged WRSI as defined by a fixed length of the growing period (LGP) and using the WRSI method of rainfall ≥ 0.5 PET from the CHIRPS, SMAP at the root zone and top 5 cm of the soil, and MODIS actual evapotranspiration products.

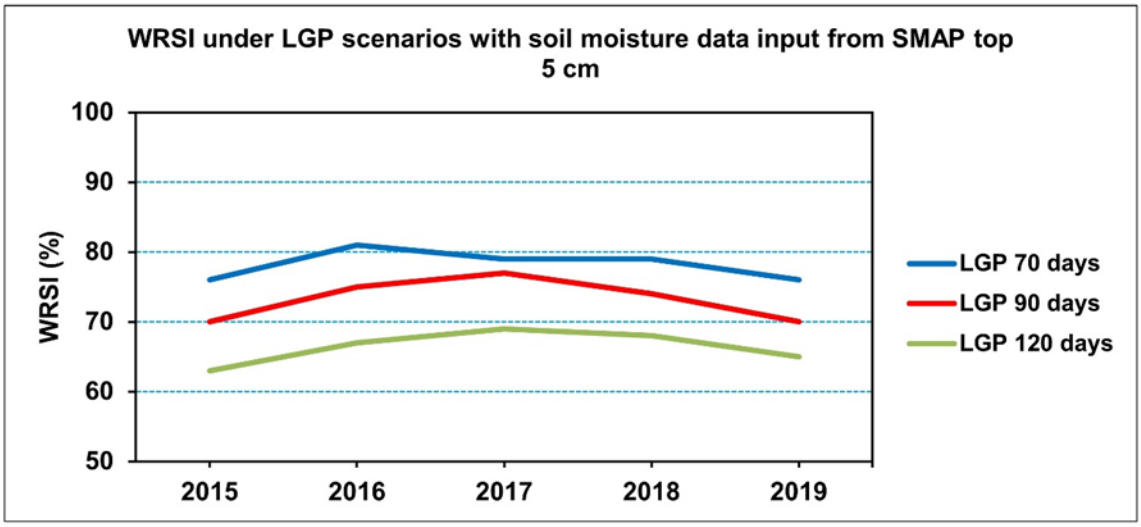

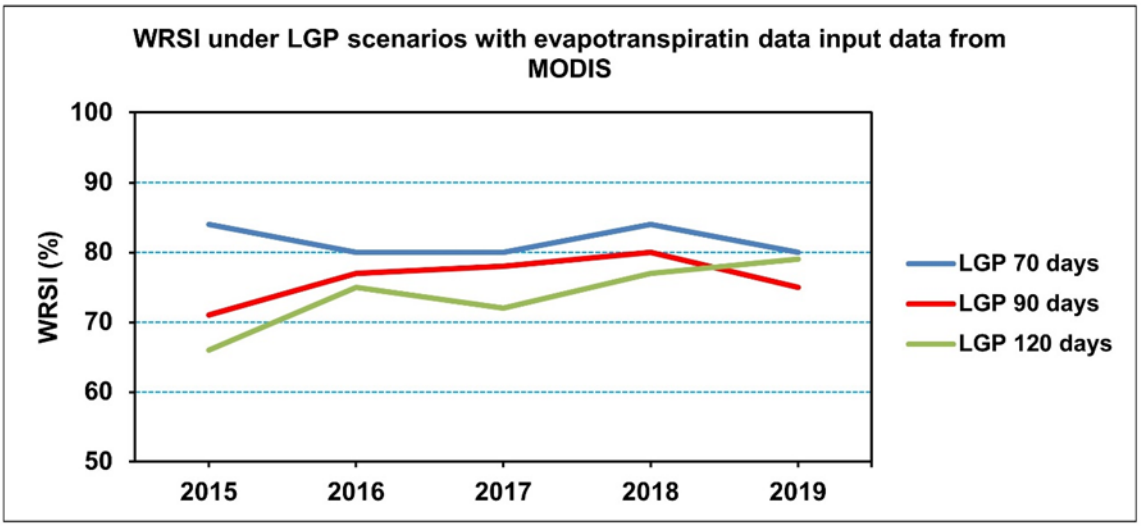

Figure 4-6 (Continued)

CHAPTER 5. Conclusion and Recommendations

5.1. Conclusion

This research aimed to monitor agricultural drought in Sudan, El Gedaref state, as a case study using SMAP soil moisture product. First, in situ soil moisture measurements were carried out at two-pixel size to identify the robustness of SMAP level-4, 3-hourly soil moisture product to meet its quantified requirements. 17 soil moisture measured points during the rainy season of 2018 over the agricultural lands of El Gedaref State, central clay plain (CCP) of Sudan. The findings seem skillful in terms of performance based on three errors. The data of the SMAP product has the potential to show an evident Spatio-temporal variation of soil moisture in both study sites. I can transfer this study to similar climates and environments, such as the Semi-humid wooded to Semi-arid Savannah zone of the African continent, between latitudes 15o and 20o north and 15o to 25o south with average rainfall ranging from 200 to 800 mm. The major soils are of high clay, such as those of the study locations.

Due to the limited sample size and the fact that this is the first observatory of the SMAP soil moisture product in Sudan, the results of this study prerequisite to be considered preliminary and, indeed, need to be confirmed and excavated in future campaigns. The effect can be carefully examined before use in other regions. To some extent, this observatory study has shed light on how soil moisture observations varied in CCP and discussed related causes. The emerging results of this study agreed with the findings of several previous studies, as discussed earlier. This study highlighted some agronomic measures to reduce the effects of low soil moisture on sorghum yield in different growing stages.

Remote sensing products that are dedicated to measuring soil moisture in the top surface of the soil and root zone can be used as suitable alternatives to ground-based methods to predict agricultural drought in Sudan. The top layer of the soil is sufficient for seed germination at the beginning of the growing stages. Root zone soil moisture also constitutes an essential factor in crop development; the deeper it goes, the more benefits it provides to the root system. In chapter three, a new method for monitoring agricultural drought in Sudan is provided by integrating the SM and vegetation index (NDVI). The current research findings confirmed

that SWDI-SMAP SM showed a reliable and expected response of capturing seasonal dynamics concerning the vegetation index (NDVI).

In general, SWDI derived from Level 4 SM datasets from recently launched SMAP were evaluated for agricultural drought monitoring over three different climatic sites in the El Gedaref state, Sudan, tropical savanna, warm semi-arid climate, and warm desert climate. Compared with rain and soil moisture, SWDI-SMAP showed good potential for assessing drought conditions. The SWDI-SMAP performed relatively well in all locations. The promising results portend that SWDI-SMAP will be a promising tool for monitoring agricultural drought with a high temporal resolution across Sudan. Such studies will enable us to link climate information with agricultural information for a more climate-resilient agriculture sector and include this in an established agricultural droughts information service, such as early warnings and preparedness.

In chapter four, the evaluation of the WRSI method extended for assessing agro-meteorological risks such as drought on sorghum production through an adapted gridded version of the model and sensitivity analysis to meteorological inputs from two different sources, i.e., the MODIS actual evapotranspiration, CHIRPS rainfall, and soil moisture input, i.e., SMAP products. We defined the Spatio-temporal variation of the onset of rains and available soil moisture. We analyzed the impact of different input datasets and the approaches for restricting the start-of-season (SOS) and the growing period (LGP) length on WRSI outputs. The analysis showed that the SMAP at the 5 cm soil moisture and CHIRPS datasets credibly designate season onset patterns. Still, CHIRPS performs best in detecting SOS patterns and assessing the LGP, resulting in the highest correlations with WRSI.

Understanding the influence of using diverse input datasets in WRSI supports recognizing regions likely to face identical agro-meteorological risks as relevant for the design and structure of risk management instruments such as weather index-based insurance. As a minimum, our results indicate that correlation between Water Requirements Satisfaction Index (WRSI), rainfall, and median soil moisture and sorghum information data (2015–2019) from Sudan (ARC) across El Gedaref state sorghum growing areas.

WRSI simulations 1–3 use a fixed length of the growing period (LGP) of 70, 100, and 120 days, and simulation 5 uses variable LGP defined from the persistence of rainfall over evapotranspiration.

Using a new methodology can be a remedy for inclusive investigation of remotely sensed soil moisture, not only for agricultural drought purposes but also for other hydrological activities associated with climate change in Sudan. The result of this research is significant and valuable to support the continuous development and improvement of satellite soil moisture retrieval to produce soil moisture products with higher accuracy in semi-arid regions.

Future studies of agricultural drought based on soil moisture remote sensing products need a greater focus on Sudan, as the retrieval of soil moisture needs to be taken cautiously before using it in different climatic regions of the world. Sudan is not an exception, and validation versus in-situ measurements is imperative.

5.2. Recommendations

I make the following recommendations for Sudan:

The use of field campaigns to establish relationships, time stability for soil moisture product validation, and monitoring agricultural drought are some promising applications of remote sensing soil moisture products. Moreover, further studies concerning monitoring agricultural drought using new techniques, e.g., RS and GIS, are needed.

The study recommends setting up new meteorological and weather stations to increase the density of sporadic existing networks by providing data from sterile sites.

References

A. H. Bunting and J. D. Lea. The Soils and Vegetation of the Fung, East Central Sudan **1962**.

A. T. Ayoub. Land degradation, rainfall variability and food production in the Sahelian zone of the Sudan. *Land Degradation & Development* **1999,** *10* (5), 489–500. DOI: 10.1002/(SICI)1099-145X(199909/10)10:5<489:AID-LDR336>3.0.CO;2-U.

Abdalla and Abdel Nour. The Agricultural Potential of Sudan [Online] **2001,** *28*. https://larouchepub.com/eiw/public/2001/eirv28n08-20010223/eirv28n08-20010223_037-the_agricultural_potential_of_su.

Abdelgalil, E. E. B.; Adeeb, A. M. Impact of changing policies on agricultural productivity: a case of the Gezira scheme, Sudan. *IJSAMI* **2015,** *1* (1), 49. DOI: 10.1504/IJSAMI.2015.069045.

Abdelhalim, T. S.; Abdelhalim, N. S.; Kamal, N. M.; Mohamed, E. E.; Hassan, A. B. Exploiting the potential of Sudanese sorghum landraces in biofortification: Physicochemical quality of the grain of sorghum (Sorghum bicolor L. Moench) landraces. *Food Chemistry* [Online] **2021,** *337*, 127604. http://dx.doi.org/10.1016/j.foodchem.2020.127604.

Ahmed, M. Returns from research in economies with policy distortions: hybrid sorghum in Sudan. *Agricultural Economics* **1995,** *12* (2), 183–192. DOI: 10.1016/0169-5150(95)01138-B.

Ahmed, S. M. Impacts of drought, food security policy and climate change on performance of irrigation schemes in Sub-saharan Africa: The case of Sudan. *Agricultural Water Management* **2020,** *232* (2), 106064. DOI: 10.1016/j.agwat.2020.106064.

Ainiwaer, M.; Ding, J.; Kasim, N.; Wang, J.; Wang, J. Regional scale soil moisture content estimation based on multi-source remote sensing parameters. *International Journal of Remote Sensing* **2020,** *41* (9), 3346–3367. DOI: 10.1080/01431161.2019.1701723.

Al-Ain, F.; Attar, J.; Hussein, F.; Heng, L. K. Comparison of nuclear and capacitance-based soil water measuring techniques in salt-affected soils. *Soil Use and Management* **2009,** *25* (4), 362–367. DOI: 10.1111/j.1475-2743.2009.00246.x.

Alasha. *Length of the growing season of different sorghum varieties of Sudan*: Agricultural research Corporation, Wad Medani, Sudan, **2022**. https://arc.gov.sd/ (accessed 24.January.2022).

Alemaw, B. F.; Simalenga, T. Climate Change Impacts and Adaptation in Rainfed Farming Systems: A Modeling Framework for Scaling-Out Climate Smart Agriculture in Sub-Saharan Africa. *AJCC* **2015,** *04* (04), 313–329. DOI: 10.4236/ajcc.2015.44025.

Allen; R; Tasumi; M; Trezza, a. Satellite-Based Energy Balance for Mapping Evapotranspiration with Internalized Calibration, **2007** (METRIC)Model [Online]. https://doi.org/10.1061/(ASCE)0733-9437(2007)133:4(380)

Allen R.G., Pereira L.S., Raes D. & Smith M. **1998**. Crop evapotranspiration: Guidelines for computing crop requirements. Irrigation and Drainage Paper No. 56, FAO, Rome, Italy.

Al-Hedny, S. M.; Muhaimeed, A. S. Drought Monitoring for Northern Part of Iraq Using Temporal NDVI and Rainfall Indices. *Environmental Remote Sensing and GIS in Iraq*; Springer, Cham, **2020**; pp 301–331. DOI: 10.1007/978-3-030-21344-2_13.

ALI, Y. S.A.; CROSATO, A.; MOHAMED, Y. A.; ABDALLA, S. H.; WRIGHT, N. G. Sediment balances in the Blue Nile River Basin. *International Journal of Sediment Research* **2014,** *29* (3), 316–328. DOI: 10.1016/S1001-6279(14)60047-0.

Anderson, R. L. Improving resource-use-efficiency with no-till and crop diversity. *Renew. Agric. Food Syst.* **2017,** *32* (2), 105–108. DOI: 10.1017/S1742170516000090.

Anderson, W.; Taylor, C.; McDermid, S.; Ilboudo-Nébié, E.; Seager, R.; Schlenker, W.; Cottier, F.; Sherbinin, A. de; Mendeloff, D.; Markey, K. Violent conflict exacerbated drought-related food insecurity between 2009 and 2019 in sub-Saharan Africa. *Nat Food* **2021,** *2* (8), 603–615. DOI: 10.1038/s43016-021-00327-4.

Anderson, W. B.; Zaitchik, B. F.; Hain, C. R.; Anderson, M. C.; Yilmaz, M. T.; Mecikalski, J.; Schultz, L. Towards an integrated soil moisture drought monitor for East Africa. *Hydrol. Earth Syst. Sci.* **2012,** *16* (8), 2893–2913. DOI: 10.5194/hess-16-2893-2012.

Anwar, F.; Bhanger, M. I. Analytical characterization of Moringa oleifera seed oil grown in temperate regions of Pakistan. *J. Agric. Food Chem.* **2003,** *51* (22), 6558–6563. DOI: 10.1021/jf0209894.

Arora, N. K.; Mishra, J. COVID-19 and importance of environmental sustainability. *Environmental Sustainability* **2020,** *3* (2), 117–119. DOI: 10.1007/s42398-020-00107-z.

Aune, J. B.; Coulibaly, A.; Giller, K. E. Precision farming for increased land and labour productivity in semi-arid West Africa. A review. *Agron. Sustain. Dev.* **2017,** *37* (3). DOI: 10.1007/s13593-017-0424-z.

Badou, D. F.; Diekkrüger, B.; Montzka, C. Validation of satellite soil moisture in the absence of in situ soil moisture: the case of the Tropical Yankin Basin. *SA J of Geomatics* **2019,** *7* (3), 243. DOI: 10.4314/sajg.v7i3.3.

Baig, M. B.; Shahid, S. A.; Straquadine, G. S. Making rainfed agriculture sustainable through environmental friendly technologies in Pakistan: A review. *International Soil and Water Conservation Research* **2013,** *1* (2), 36–52. DOI: 10.1016/S2095-6339(15)30038-1.

Baily, R. E. H. The Anglo-Egyptian Sudan. *International Affairs* **1935,** *14* (2), 280–282. DOI: 10.2307/2602139.

Bali, N.; Singla, A. Emerging Trends in Machine Learning to Predict Crop Yield and Study Its Influential Factors: A Survey. *Arch Computat Methods Eng* **2021**, 1–18. DOI: 10.1007/s11831-021-09569-8.

Banik, D. Achieving Food Security in a Sustainable Development Era. *Food ethics* **2019,** *4* (2), 117–121. DOI: 10.1007/s41055-019-00057-1.

Batjes, N. H. A world dataset of derived soil properties by FAO?UNESCO soil unit for global modelling. *Soil Use & Management* **1997,** *13* (1), 9–16. DOI: 10.1111/j.1475-2743.1997.tb00550.x.

Baugh, C.; Rosnay, P. de; Lawrence, H.; Jurlina, T.; Drusch, M.; Zsoter, E.; Prudhomme, C. The Impact of SMOS Soil Moisture Data Assimilation within the Operational Global Flood Awareness System (GloFAS). *Remote Sensing* [Online] **2020,** *12* (9), 1490. https://www.mdpi.com/710304.

Beck, H. E.; Pan, M.; Miralles, D. G.; Reichle, R. H.; Dorigo, W. A.; Hahn, S.; Sheffield, J.; Karthikeyan, L.; Balsamo, G.; Parinussa, R. M.; van Dijk, A. I. J. M.; Du, J.; Kimball, J. S.; Vergopolan, N.; Wood, E. F. Evaluation of 18 satellite- and model-based soil moisture products using in situ measurements from 826 sensors [Online] **2020**.

Beck, H. E.; Zimmermann, N. E.; McVicar, T. R.; Vergopolan, N.; Berg, A.; Wood, E. F. Present and future Köppen-Geiger climate classification maps at 1-km resolution. *Scientific data* **2018,** *5*, 180214. DOI: 10.1038/sdata.2018.214.

Behnke, R.; Young, H.; Sulieman, H. M.; Robinson, S.; Idris, A. E. The seasonal imperative: Environmental drivers of livestock mobility in East Darfur, Sudan. *Land Use Policy* [Online] **2020,** *99*, 105014. http://dx.doi.org/10.1016/j.landusepol.2020.105014.

Bernard, R.; Taconet, O.; Vidal-Madjar, D.; Thony, J. L.; Vauclin, M.; Chapoton, A.; Wattrelot, F.; Lebrun, A. Comparison of Three in Situ Surface Soil Moisture Measurements And Application to C-Band Scatterometer Calibration. *IEEE Trans. Geosci. Remote Sensing* [Online] **1984,** *GE-22* (4), 388–394. http://dx.doi.org/10.1109/tgrs.1984.350642.

Biradar, C. M.; Thenkabail, P. S.; Noojipady, P.; Li, Y.; Dheeravath, V.; Turral, H.; Velpuri, M.; Gumma, M. K.; Gangalakunta, O. R. P.; Cai, X. L.; Xiao, X.; Schull, M. A.; Alankara, R. D.; Gunasinghe, S.; Mohideen, S. A global map of rainfed cropland areas (GMRCA) at the end of last millennium using remote sensing. *International Journal of Applied Earth Observation and Geoinformation* **2009,** *11* (2), 114–129. DOI: 10.1016/j.jag.2008.11.002.

Birhanu, B. Z.; Traoré, K.; Gumma, M. K.; Badolo, F.; Tabo, R.; Whitbread, A. M. *A watershed approach to managing rainfed agriculture in the semiarid region of southern Mali: integrated research on water and land use* 21, 2019.

Bjornlund, V.; Bjornlund, H.; van Rooyen, A. F. Why agricultural production in sub-Saharan Africa remains low compared to the rest of the world – a historical perspective. *International Journal of WaterResources Development* **2020,** *36* (sup1), S20-S53. DOI: 10.1080/07900627.2020.1739512.

Bolten, J. D.; Crow, W. T.; Zhan, X.; Jackson, T. J.; Reynolds, C. A. Evaluating the Utility of Remotely Sensed Soil Moisture Retrievals for Operational Agricultural Drought Monitoring. *IEEE J. Sel. Top. Appl. Earth Observations Remote Sensing* **2010,** *3* (1), 57–66. DOI: 10.1109/JSTARS.2009.2037163.

Bosire, E.; Karanja, F.; Ouma, G.; Gitau, W. Assessment of Climate Change Impact on Sorghum Production in Machakos County. *SFP* **2018,** *3*, 25–45. DOI: 10.18052/www.scipress.com/SFP.3.25.

Brocca, L.; Massari, C.; Ciabatta, L.; Moramarco, T.; Penna, D.; Zuecco, G.; Pianezzola, L.; Borga, M.; Matgen, P.; Martínez-Fernández, J. Rainfall estimation from in situ soil moisture observations at several sites in Europe: an evaluation of the SM2RAIN algorithm. *Journal of Hydrology and Hydromechanics* **2015,** *63* (3), 201–209. DOI: 10.1515/johh-2015-0016.

Brokensha, D.; Hill, P. Studies in Rural Capitalism in West Africa. *Man* **1971,** *6* (1), 136. DOI: 10.2307/2798465.

Brown, T. C.; Mahat, V.; Ramirez, J. A. Adaptation to Future Water Shortages in the United States Caused by Population Growth and Climate Change. *Earth's Future* **2019,** *7* (3), 219–234. DOI: 10.1029/2018EF001091.

Brust, C.; Kimball, J. S.; Maneta, M. P.; Jencso, K.; He, M.; Reichle, R. H. Using SMAP Level-4 soil moisture to constrain MOD16 evapotranspiration over the contiguous USA. *Remote Sensing of Environment* [Online] **2021,** *255*, 112277. https://www.sciencedirect.com/science/article/pii/s0034425720306507.

Bussmann, A.; Elagib, N. A.; Fayyad, M.; Ribbe, L. Sowing date determinants for Sahelian rainfed agriculture in the context of agricultural policies and water management. *Land Use Policy* **2016a,** *52*, 316–328. DOI: 10.1016/j.landusepol.2015.12.007.

Bussmann, A.; Elagib, N. A.; Fayyad, M.; Ribbe, L. Sowing date determinants for Sahelian rainfed agriculture in the context of agricultural policies and water management. *Land Use Policy* [Online] **2016b,** *52*, 316–328. http://dx.doi.org/10.1016/j.landusepol.2015.12.007.

Caldwell, T. G.; Bongiovanni, T.; Cosh, M. H.; Jackson, T. J.; Colliander, A.; Abolt, C. J.; Casteel, R.; Larson, T.; Scanlon, B. R.; Young, M. H. The Texas Soil Observation Network:A Comprehensive Soil Moisture Dataset for Remote Sensing and Land Surface Model Validation. *Vadose zone j.* **2019,** *18* (1), 1–20. DOI: 10.2136/vzj2019.04.0034.

Camici, S.; Crow, W. T.; Brocca, L. Recent advances in remote sensing of precipitation and soil moisture products for riverine flood prediction. *Extreme Hydroclimatic Events and Multivariate Hazards in a Changing Environment* **2019**, 247–266. DOI: 10.1016/B978-0-12-814899-0.00010-9.

Carrão, H.; Russo, S.; Sepulcre-Canto, G.; Barbosa, P. An empirical standardized soil moisture index for agricultural drought assessment from remotely sensed data. *International Journal of Applied Earth Observation and Geoinformation* **2016,** *48*, 74–84. DOI: 10.1016/j.jag.2015.06.011.

Chamaille-Jammes, S.; Fritz, H.; Murindagomo, F. Spatial patterns of the NDVI–rainfall relationship at the seasonal and interannual time scales in an African savanna. *International Journal of Remote Sensing* **2006,** *27* (23), 5185–5200. DOI: 10.1080/01431160600702392.

Champagne, C.; Rowlandson, T.; Berg, A.; Burns, T.; L'Heureux, J.; Tetlock, E.; Adams, J. R.; McNairn, H.; Toth, B.; Itenfisu, D. Satellite surface soil moisture from SMOS and Aquarius: Assessment for applications in agricultural landscapes. *International Journal of Applied Earth Observation and Geoinformation* **2016,** *45*, 143–154. DOI: 10.1016/j.jag.2015.09.004.

Chaves, M. M.; Costa, J. M.; Zarrouk, O.; Pinheiro, C.; Lopes, C. M.; Pereira, J. S. Controlling stomatal aperture in semi-arid regions—The dilemma of saving water or being cool? *Plant Science* [Online] **2016,** *251*, 54–64. http://dx.doi.org/10.1016/j.plantsci.2016.06.015.

Churchill, W. S. *The River War*. *An Account of the Reconquest of the Sudan;* Skyhorse, 1889.

Cohen, M. J. Let them Eat Promises: Global Policy Incoherence, Unmet Pledges, and Misplaced Priorities Undercut Progress on SDG 2. *Food ethics* [Online] **2019,** *4* (2), 175–187. https://link.springer.com/article/10.1007/s41055-019-00048-2.

Colliander, A.; Jackson, T. J.; Bindlish, R.; Chan, S.; Das, N.; Kim, S. B.; Cosh, M. H.; Dunbar, R. S.; Dang, L.; Pashaian, L.; Asanuma, J.; Aida, K.; Berg, A.; Rowlandson, T.; Bosch, D.; Caldwell,

T.; Caylor, K.; Goodrich, D.; al Jassar, H.; Lopez-Baeza, E.; Martínez-Fernández, J.; González-Zamora, A.; Livingston, S.; McNairn, H.; Pacheco, A.; Moghaddam, M.; Montzka, C.; Notarnicola, C.; Niedrist, G.; Pellarin, T.; Prueger, J.; Pulliainen, J.; Rautiainen, K.; Ramos, J.; Seyfried, M.; Starks, P.; Su, Z.; Zeng, Y.; van der Velde, R.; Thibeault, M.; Dorigo, W.; Vreugdenhil, M.; Walker, J. P.; Wu, X.; Monerris, A.; O'Neill, P. E.; Entekhabi, D.; Njoku, E. G.; Yueh, S. Validation of SMAP surface soil moisture products with core validation sites. *Remote Sensing of Environment* **2017,** *191*, 215–231. DOI: 10.1016/j.rse.2017.01.021.

Cong, D.; Zhao, S.; Chen, C.; Duan, Z. Characterization of droughts during 2001–2014 based on remote sensing: A case study of Northeast China. *Ecological Informatics* [Online] **2017,** *39*, 56–67. https://www.sciencedirect.com/science/article/pii/s1574954116301005.

Crespo Cuaresma, J.; Fengler, W.; Kharas, H.; Bekhtiar, K.; Brottrager, M.; Hofer, M. Will the Sustainable Development Goals be fulfilled? Assessing present and future global poverty. *Palgrave Commun* **2018,** *4* (1), 226. DOI: 10.1057/s41599-018-0083-y.

D. W. Meyer; M. Badaruddin. Frost Tolerance of Ten Seedling Legume Species at Four Growth Stages. *Crop Science* **2001,** *41* (6), 1838–1842. DOI: 10.2135/cropsci2001.1838.

Dai, A.; Fyfe, J. C.; Xie, S.-P.; Dai, X. Decadal modulation of global surface temperature by internal climate variability. *Nature Clim Change* **2015,** *5* (6), 555–559. DOI: 10.1038/nclimate2605.

Deckers, J.; Spaargaren, O.; Nachtergaele, F. Vertisols: genesis, properties and soilscape management for sustainable development. In *The sustainable management of vertisols*; Syers, J. K., Penning de Vries, F. W. T., Nyamudeza, P., Eds.; CABI: Wallingford, 2001; pp 3–20. DOI: 10.1079/9780851994505.0003.

Ding, M.; Zhang, Y.; Liu, L.; Zhang, W.; Wang, Z.; Bai, W. The relationship between NDVI and precipitation on the Tibetan Plateau. *J. Geogr. Sci.* **2007,** *17* (3), 259–268. DOI: 10.1007/s11442-007-0259-7.

Ehab A. M. Frah. Sudan Production of Sorghum; Forecasting 2016-2030 Using Autoregressive Integrated Moving Average ARIMA Model. *American Journal of Mathematics and Statistics* **2016,** *6* (4). DOI: 10.5923/j.ajms.20160604.06.

El Karouri, Ed., 1st edition; Al Hana Commercial Printing Press: Khartoum, **2010**. *Mechanized Rainfed Agriculture in the Sudan*. *Present Situation and Future Development;*

Elagib, N. A. Development and application of a drought risk index for food crop yield in Eastern Sahel. *Ecological Indicators* **2014,** *43*, 114–125. DOI: 10.1016/j.ecolind.2014.02.033.

Elagib, N. A.; Khalifa, M.; Rahma, A. E.; Babker, Z.; Gamaledin, S. I. Performance of major mechanized rainfed agricultural production in Sudan: Sorghum vulnerability and resilience to climate since 1970. *Agricultural and Forest Meteorology* **2019a,** *276-277*, 107640. DOI: 10.1016/j.agrformet.2019.107640.

Elagib, N. A.; Khalifa, M.; Rahma, A. E.; Babker, Z.; Gamaledin, S. I. Performance of major mechanized rainfed agricultural production in Sudan: Sorghum vulnerability and resilience to climate since 1970. *Agricultural and Forest Meteorology* **2019b,** *276-277*, 107640. DOI: 10.1016/j.agrformet.2019.107640.

Elhadary. Challenges facing land tenure system in relation to pastoral livelihood security in Gedarif State, Eastern Sudan [Online] **2010,** *3(9)*. https://www.researchgate.net/profile/Yasin-Elhadary-3/publication/366248591_Challenges_facing_land_tenure_system_in_relation_to_pastoral_livelihood_security_in_Gedarif_State_Eastern_Sudan/links/63998074484e65005b0a47bd/Challenges-facing-land-tenure-system-in-relation-to-pastoral-livelihood-security-in-Gedarif-State-Eastern-Sudan.pdf.

Elliott, J.; Deryng, D.; Müller, C.; Frieler, K.; Konzmann, M.; Gerten, D.; Glotter, M.; Flörke, M.; Wada, Y.; Best, N.; Eisner, S.; Fekete, B. M.; Folberth, C.; Foster, I.; Gosling, S. N.; Haddeland, I.; Khabarov, N.; Ludwig, F.; Masaki, Y.; Olin, S.; Rosenzweig, C.; Ruane, A. C.; Satoh, Y.; Schmid, E.; Stacke, T.; Tang, Q.; Wisser, D. Constraints and potentials of future irrigation water availability on agricultural production under climate change. *Proceedings of the National Academy of Sciences of the United States of America* **2014,** *111* (9), 3239–3244. DOI: 10.1073/pnas.1222474110.

Erfurt, M.; Glaser, R.; Blauhut, V. Changing impacts and societal responses to drought in southwestern Germany since 1800. *Reg Environ Change* **2019,** *19* (8), 2311–2323. DOI: 10.1007/s10113-019-01522-7.

Erik S. Krueger; Tyson E. Ochsner; Steven M. Quiring. Development and Evaluation of Soil Moisture-Based Indices for Agricultural Drought Monitoring. *Agronomy Journal* **2019,** *111* (3), 1392–1406. DOI: 10.2134/agronj2018.09.0558.

Eshetu, Z.; Gebre, H.; Lisanework, N. Impacts of climate change on sorghum production in North Eastern Ethiopia. *Afr. J. Environ. Sci. Technol.* **2020,** *14* (2), 49–63. DOI: 10.5897/AJEST2019.2803.

Evan J. Coopersmith; Michael H. Cosh; Walt A. Petersen; John Prueger; James J. Niemeier. Soil Moisture Model Calibration and Validation: An ARS Watershed on the South Fork Iowa River. *Journal of Hydrometeorology* [Online] **2015,** *16* (3), 1087–1101. https://journals.ametsoc.org/view/journals/hydr/16/3/jhm-d-14-0145_1.xml.

Fan, M.; Shen, J.; Yuan, L.; Jiang, R.; Chen, X.; Davies, W. J.; Zhang, F. Improving crop productivity and resource use efficiency to ensure food security and environmental quality in China. *Journal of experimental botany* **2012,** *63* (1), 13–24. DOI: 10.1093/jxb/err248.

Fanzo, J. Healthy and Sustainable Diets and Food Systems: the Key to Achieving Sustainable Development Goal 2? *Food ethics* **2019,** *4* (2), 159–174. DOI: 10.1007/s41055-019-00052-6.

FAOSTAT. *FAOSTAT 2005_ FAO statistical databases*: Rome, 2005. https://agris.fao.org/agris.

Farwell. *Prisoners of the Mahdi: the story of the Mahdist revolt from the fall of Khartoum to the reconquest of the Sudan by Kitchener fourteen years later, and of the …*, 1967.

Felix N. Kogan. Satellite-Observed Sensitivity of World Land Ecosystems to El Nin˜o/La Nin˜a [Online] **2000**.

Fisher, H. J. R. S. O'Fahey and J. L. Spaulding: Kingdoms of the Sudan. (Studies in African History, 9.) ix, 235 pp. London: Methuen and Co. Ltd., 1974. £4.90. *Bulletin of the School of Oriental and African Studies* **1976,** *39* (1), 225–227. DOI: 10.1017/s0041977x00052666.

Forgotson, C.; O'Neill, P. E.; Carrera, M. L.; Belair, S.; Das, N. N.; Mladenova, I. E.; Bolten, J. D.; Jacobs, J. M.; Cho, E.; Escobar, V. M. How Satellite Soil Moisture Data Can Help to Monitor the Impacts of Climate Change: SMAP Case Studies. *IEEE J. Sel. Top. Appl. Earth Observations Remote Sensing* [Online] **2020,** *13*, 1590–1596. http://dx.doi.org/10.1109/jstars.2020.2982608.

Funk, C.; Peterson, P.; Landsfeld, M.; Pedreros, D.; Verdin, J.; Shukla, S.; Husak, G.; Rowland, J.; Harrison, L.; Hoell, A.; Michaelsen, J. The climate hazards infrared precipitation with stations--a new environmental record for monitoring extremes. *Scientific data* **2015,** *2*, 150066. DOI: 10.1038/sdata.2015.66.

G. T. Renner. A Famine Zone in Africa: The Sudan [Online] **1926**.

Gaikwad, S. V.; Kale, K. V.; Kulkarni, S. B.; Varpe, A. B.; Pathare, G. N. Agricultural Drought Severity Assessment using Remotely Sensed Data: A Review. *IJARSG* **2015,** *4* (1), 1195–1203. DOI: 10.23953/cloud.ijarsg.128.

García, C. A.; Manzini, F.; Islas, J. M. Sustainability assessment of ethanol production from two crops in Mexico. *Renewable and Sustainable Energy Reviews* [Online] **2017,** *72*, 1199–1207. http://dx.doi.org/10.1016/j.rser.2016.10.035.

Gebrehiwot, T.; van der Veen, A.; Maathuis, B. Governing agricultural drought: Monitoring using the vegetation condition index. *Ethiop. J. Env Stud & Manag* **2016,** *9* (3), 354. DOI: 10.4314/ejesm.v9i3.9.

Ghorbani, M. A.; Shamshirband, S.; Zare Haghi, D.; Azani, A.; Bonakdari, H.; Ebtehaj, I. Application of firefly algorithm-based support vector machines for prediction of field capacity and permanent wilting point. *Soil and Tillage Research* **2017,** *172* (19), 32–38. DOI: 10.1016/j.still.2017.04.009.

Godfray, H. C. J.; Beddington, J. R.; Crute, I. R.; Haddad, L.; Lawrence, D.; Muir, J. F.; Pretty, J.; Robinson, S.; Thomas, S. M.; Toulmin, C. Food security: the challenge of feeding 9 billion people. *Science* **2010,** *327* (5967), 812–818. DOI: 10.1126/science.1185383.

Golam Kibria; Haroon, Y.; Dayanthi Nugegoda. *Climate Change & Water Security;* New India Publishing Agency, New Delhi-88, India, 2016.

Gruber, A.; Lannoy, G. de; Albergel, C.; Al-Yaari, A.; Brocca, L.; Calvet, J.-C.; Colliander, A.; Cosh, M.; Crow, W.; Dorigo, W.; Draper, C.; Hirschi, M.; Kerr, Y.; Konings, A.; Lahoz, W.; McColl, K.; Montzka, C.; Muñoz-Sabater, J.; Peng, J.; Reichle, R.; Richaume, P.; Rüdiger, C.; Scanlon, T.; van der Schalie, R.; Wigneron, J.-P.; Wagner, W. Validation practices for satellite soil moisture retrievals: What are (the) errors? *Remote Sensing of Environment* **2020,** *244* (6), 111806. DOI: 10.1016/j.rse.2020.111806.

Gude, V. G. Desalination and water reuse to address global water scarcity. *Rev Environ Sci Biotechnol* **2017,** *16* (4), 591–609. DOI: 10.1007/s11157-017-9449-7.

Gülser, C.; Candemir, F. Using soil moisture constants and physical properties to predict saturated hydraulic conductivity. *EJSS* **2014,** *3* (1), 77. DOI: 10.18393/ejss.69966.

Hadebe, S. T.; Modi, A. T.; Mabhaudhi, T. Drought Tolerance and Water Use of Cereal Crops: A Focus on Sorghum as a Food Security Crop in Sub-Saharan Africa. *J Agro Crop Sci* **2017,** *203* (3), 177–191. DOI: 10.1111/jac.12191.

Haitham R Elramlawi; Hassan I Mohammed; Ali W Elamin; Omer A Abdallah; A M Taha. *Adaptation of Sorghum (Sorghum bicolor L. Moench) Crop Yield to Climate Change in Eastern Dryland of Sudan*, 2018.

Hao, Z.; Hao, F.; Singh, V. P.; Ouyang, W.; Cheng, H. An integrated package for drought monitoring, prediction and analysis to aid drought modeling and assessment. *Environmental Modelling & Software* **2017a,** *91*, 199–209. DOI: 10.1016/j.envsoft.2017.02.008.

Hao, Z.; Yuan, X.; Xia, Y.; Hao, F.; Singh, V. P. An Overview of Drought Monitoring and Prediction Systems at Regional and Global Scales. *Bulletin of the American Meteorological Society* **2017b,** *98* (9), 1879–1896. DOI: 10.1175/BAMS-D-15-00149.1.

Haubrock, S.-N.; Chabrillat, S.; Lemmnitz, C.; Kaufmann, H. Surface soil moisture quantification models from reflectance data under field conditions. *International Journal of Remote Sensing* **2008,** *29* (1), 3–29. DOI: 10.1080/01431160701294695.

Hazaymeh, K.; K. Hassan, Q. Remote sensing of agricultural drought monitoring: A state of art review. *AIMS Environmental Science* **2016,** *3* (4), 604–630. DOI: 10.3934/environsci.2016.4.604.

Hazra, A.; Maggioni, V.; Houser, P.; Antil, H.; Noonan, M. A Monte Carlo-based multi-objective optimization approach to merge different precipitation estimates for land surface modeling. *Journal of Hydrology* **2019,** *570* (1), 454–462. DOI: 10.1016/j.jhydrol.2018.12.039.

Helen Young; Musa Adam Ismail. Complexity, continuity and change: livelihood resilience in the Darfur region of Sudan. *Disasters* **2019,** *43*, S318-S344. DOI: 10.1111/disa.12337.

Hu, F.; Wei, Z.; Zhang, W.; Dorjee, D.; Meng, L. A spatial downscaling method for SMAP soil moisture through visible and shortwave-infrared remote sensing data. *Journal of Hydrology* [Online]**2020,***590*,125360.https://www.sciencedirect.com/science/article/pii/s0022169420308209.

Hussein M. Sulieman. Expansion of mechanised rain-fed agriculture and land-use/land-cover change in Southern Gadarif, Sudan. *AJAR* **2010,** *5* (13), 1609–1615. DOI: 10.5897/AJAR09.078.

Huth, N. I.; Poulton, P. L. An electromagnetic induction method for monitoring variation in soil moisture in agroforestry systems. *Soil Res.* **2007,** *45* (1), 63. DOI: 10.1071/SR06093.

IAC. *Home _ IFPRI _ International Food Policy Research Institute*, 2004. https://www.ifpri.org/.

Ibrahim, F. Causes of the famine among the rural population of the Sahelian zone of the Sudan. *GeoJournal* [Online] **1988,** *17* (1), 133–141. https://link.springer.com/article/10.1007/bf00209083.

Ivanov, V. Y.; Fatichi, S.; Jenerette, G. D.; Espeleta, J. F.; Troch, P. A.; Huxman, T. E. Hysteresis of soil moisture spatial heterogeneity and the “homogenizing” effect of vegetation. *Water Resour. Res.* **2010,** *46* (9), 609. DOI: 10.1029/2009WR008611.

Jackisch, C.; Germer, K.; Graeff, T.; Andrä, I.; Schulz, K.; Schiedung, M.; Haller-Jans, J.; Schneider, J.; Jaquemotte, J.; Helmer, P.; Lotz, L.; Bauer, A.; Hahn, I.; Šanda, M.; Kumpan, M.; Dorner, J.; Rooij, G. de; Wessel-Bothe, S.; Kottmann, L.; Schittenhelm, S.; Durner, W. Soil moisture and matric potential – an open field comparison of sensor systems. *Earth Syst. Sci. Data* **2020,** *12* (1), 683–697. DOI: 10.5194/essd-12-683-2020.

Jalilvand, E.; Tajrishy, M.; Ghazi Zadeh Hashemi, S. A.; Brocca, L. Quantification of irrigation water using remote sensing of soil moisture in a semi-arid region. *Remote Sensing of Environment* [Online]**2019,***231*,111226.https://www.sciencedirect.com/science/article/pii/s0034425719302457.

Javed, T.; Li, Y.; Rashid, S.; Li, F.; Hu, Q.; Feng, H.; Chen, X.; Ahmad, S.; Liu, F.; Pulatov, B. Performance and relationship of four different agricultural drought indices for drought monitoring in China's mainland using remote sensing data. *The Science of the total environment* [Online] **2021,** *759*, 143530. https://www.sciencedirect.com/science/article/pii/s0048969720370613.

Javed, T.; Yao, N.; Chen, X.; Suon, S.; Li, Y. Drought evolution indicated by meteorological and remote-sensing drought indices under different land cover types in China. *Environ Sci Pollut Res* [Online] **2020,** *27* (4), 4258–4274. https://link.springer.com/article/10.1007/s11356-019-06629-2.

Jayanthi, H.; Husak, G. J.; Funk, C.; Magadzire, T.; Adoum, A.; Verdin, J. P. A probabilistic approach to assess agricultural drought risk to maize in Southern Africa and millet in Western Sahel using satellite estimated rainfall. *International Journal of Disaster Risk Reduction* **2014,** *10*, 490–502. DOI: 10.1016/j.ijdrr.2014.04.002.

Kabanda, T. A. Geographical Variability of Drought in Northern South Africa. *JGG* **2017,** *9* (1), 53. DOI: 10.5539/jgg.v9n1p53.

Karthikeyan, L.; Pan, M.; Wanders, N.; Kumar, D. N.; Wood, E. F. Four decades of microwave satellite soil moisture observations: Part 2. Product validation and inter-satellite comparisons. *Advances in Water Resources* **2017,** *109*, 236–252. DOI: 10.1016/j.advwatres.2017.09.010.

Keen, D. III A Disaster for Whom?: Local Interests and International Donors During Famine Among the Dinka of Sudan. *Disasters* **1991,** *15* (2), 150–165. DOI: 10.1111/j.1467-7717.1991.tb00444.x.

Khalifa, M.; Elagib, N. A.; Ahmed, B. M.; Ribbe, L.; Schneider, K. Exploring socio-hydrological determinants of crop yield in under-performing irrigation schemes: pathways for sustainable intensification. *Hydrological Sciences Journal* **2020,** *65* (2), 153–168. DOI: 10.1080/02626667.2019.1688333.

Kim, S.; Zhang, R.; Pham, H.; Sharma, A. A Review of Satellite-Derived Soil Moisture and Its Usage for Flood Estimation. *Remote Sens Earth Syst Sci* [Online] **2019,** *2* (4), 225–246. https://link.springer.com/article/10.1007/s41976-019-00025-7.

Kinyuru, J. N. Nutrient content and lipid characteristics of desert locust (Schistoscerca gregaria) swarm in Kenya. *Int J Trop Insect Sci* **2021,** *41* (3), 1993–1999. DOI: 10.1007/s42690-020-00308-3.

Kolassa, J.; Reichle, R. H.; Draper, C. S. Merging active and passive microwave observations in soil moisture data assimilation. *Remote Sensing of Environment* [Online] **2017,** *191*, 117–130. http://dx.doi.org/10.1016/j.rse.2017.01.015.

Kotir, J. H. Climate change and variability in Sub-Saharan Africa: a review of current and future trends and impacts on agriculture and food security. *Environ Dev Sustain* **2011,** *13* (3), 587–605. DOI: 10.1007/s10668-010-9278-0.

Kountche, B. A.; Jamil, M.; Yonli, D.; Nikiema, M. P.; Blanco-Ania, D.; Asami, T.; Zwanenburg, B.; Al-Babili, S. Suicidal germination as a control strategy for Striga hermonthica (Benth.) in

smallholder farms of sub-Saharan Africa. *Plants People Planet* **2019,** *1* (2), 107–118. DOI: 10.1002/ppp3.32.

Kula, N.; Haines, A.; Fryatt, R. Reducing vulnerability to climate change in sub-Saharan Africa: the need for better evidence. *PLoS medicine* **2013,** *10* (1), e1001374. DOI: 10.1371/journal.pmed.1001374.

Licker, R.; Johnston, M.; Foley, J. A.; Barford, C.; Kucharik, C. J.; Monfreda, C.; Ramankutty, N. Mind the gap: how do climate and agricultural management explain the 'yield gap' of croplands around the world? *Global Ecology and Biogeography* **2010,** *19* (6), 769–782. DOI: 10.1111/j.1466-8238.2010.00563.x.

Liu, L.; Jensen, M. B. Green infrastructure for sustainable urban water management: Practices of five forerunner cities. *Cities* **2018,** *74* (5), 126–133. DOI: 10.1016/j.cities.2017.11.013.

Liu, X.; Zhu, X.; Pan, Y.; Li, S.; Liu, Y.; Ma, Y. Agricultural drought monitoring: Progress, challenges, and prospects. *J. Geogr. Sci.* **2016,** *26* (6), 750–767. DOI: 10.1007/s11442-016-1297-9.

Livada, I.; v. d. Assimakopoulos. Spatial and temporal analysis of drought in greece using the Standardized Precipitation Index (SPI). *Theor. Appl. Climatol.* [Online] **2007,** *89* (3-4), 143–153. https://link.springer.com/article/10.1007/s00704-005-0227-z.

Locke, C. G.; Ahmadi-Esfahani, F. Z. Famine Analysis: A Study of Entitlements in Sudan, 1984-1985. *Economic Development and Cultural Change* **1993,** *41* (2), 363–376. DOI: 10.1086/452015.

López-Sandin, I.; Zavala-García, F.; Levin, L.; Ruiz, H. A.; Hernández-Luna, C. E.; Gutiérrez-Soto, G. Evaluation of Bioethanol Production from Sweet Sorghum Variety Roger under Different Tillage and Fertilizer Treatments. *Bioenerg. Res.* [Online] **2021,** *14* (4), 1058–1069. https://link.springer.com/article/10.1007/s12155-020-10215-7.

Lotfie, A. Y.; Abdelrahman, A. K.; Faisal, M. E.-H.; Ahmed, M. A.; Hussain, S. A.; Abdelhadi, A. W.; Yasunori, K.; Imad-eldin, A. A.-B. Rainfall variability and its implications for agricultural production in Gedarif State, Eastern Sudan. *Afr. J. Agric. Res.* **2018,** *13* (31), 1577–1590. DOI: 10.5897/AJAR2018.13365.

Louvet, S.; Pellarin, T.; al Bitar, A.; Cappelaere, B.; Galle, S.; Grippa, M.; Gruhier, C.; Kerr, Y.; Lebel, T.; Mialon, A.; Mougin, E.; Quantin, G.; Richaume, P.; Rosnay, P. de. SMOS soil moisture product evaluation over West-Africa from local to regional scale. *Remote Sensing of Environment* **2015,** *156* (3), 383–394. DOI: 10.1016/j.rse.2014.10.005.

Lu, J.; Carbone, G. J.; Gao, P. Mapping the agricultural drought based on the long-term AVHRR NDVI and North American Regional Reanalysis (NARR) in the United States, 1981–2013. *Applied Geography* [Online] **2019,** *104*, 10–20. https://www.sciencedirect.com/science/article/pii/s0143622818300365.

Luckstead, J.; Nayga, R. M.; Snell, H. A. Labor Issues in the Food Supply Chain Amid the COVID-19 Pandemic. *Applied economic perspectives and policy* **2021,** *43* (1), 382–400. DOI: 10.1002/aepp.13090.

MAA. Mechanized Agriculture Authority, El Gedaref state, Sudan. *Rainfall data*, 2017.

Magboul Musa Sulieman; Ibrahim Saeed Ibrahim. Genesis, Classification and Evaluation of Some Soils of the River Nile Terraces, Khartoum North, Sudan; Unpublished, 2013. DOI: 10.13140/RG.2.1.1126.6966.

Mahmoud, A.; Obeid, M. Ecological studies in the vegetation of the Sudan. *Plant Ecol* **1971,** *23* (1-2), 153–176. DOI: 10.1007/BF02326660.

Mälicke, M.; Hassler, S. K.; Blume, T.; Weiler, M.; Zehe, E. Soil moisture: variable in space but redundant in time. *Hydrol. Earth Syst. Sci.* **2020,** *24* (5), 2633–2653. DOI: 10.5194/hess-24-2633-2020.

Malin Falkenmark; Johan Rockström. Building resilience to drought in desertification-prone savannas in Sub-Saharan Africa: The water perspective. *Natural Resources Forum* **2008,** *32* (2), 93–102. DOI: 10.1111/j.1477-8947.2008.00177.x.

Mallakh, R. E. Some Economic Aspects of the Aswan High Dam Project in Egypt. *Land Economics* **1959,** *35* (1), 15. DOI: 10.2307/3144704.

Malo, A. R.; Nicholson, S. E. A study of rainfall and vegetation dynamics in the African Sahel using normalized difference vegetation index. *Journal of Arid Environments* **1990,** *19* (1), 1–24. DOI: 10.1016/S0140-1963(18)30825-5.

Mano, Y.; Takahashi, K.; Otsuka, K. Mechanization in land preparation and agricultural intensification: The case of rice farming in the Cote d'Ivoire. *Agricultural Economics* **2020,** *51* (6), 899–908. DOI: 10.1111/agec.12599.

Martínez-Fernández, J.; González-Zamora, A.; Sánchez, N.; Gumuzzio, A. A soil water based index as a suitable agricultural drought indicator. *Journal of Hydrology* **2015,** *522*, 265–273. DOI: 10.1016/j.jhydrol.2014.12.051.

Martínez-Fernández, J.; González-Zamora, A.; Sánchez, N.; Gumuzzio, A.; Herrero-Jiménez, C. M. Satellite soil moisture for agricultural drought monitoring: Assessment of the SMOS derived Soil Water Deficit Index. *Remote Sensing of Environment* **2016,** *177*, 277–286. DOI: 10.1016/j.rse.2016.02.064.

Masaka, J.; Dera, J.; Muringaniza, K. Dryland Grain Sorghum (Sorghum bicolor) Yield and Yield Component Responses to Tillage and Mulch Practices Under Subtropical African Conditions. *Agric Res* **2020,** *9* (3), 349–357. DOI: 10.1007/s40003-019-00427-5.

Mason-D'Croz, D.; Sulser, T. B.; Wiebe, K.; Rosegrant, M. W.; Lowder, S. K.; Nin-Pratt, A.; Willenbockel, D.; Robinson, S.; Zhu, T.; Cenacchi, N.; Dunston, S.; Robertson, R. D. Agricultural investments and hunger in Africa modeling potential contributions to SDG2 – Zero Hunger. *World Development* [Online] **2019,** *116*, 38–53. http://dx.doi.org/10.1016/j.worlddev.2018.12.006.

McDonald, K. C.; Kimball, J. S.; Kim, Y. The Soil Moisture Active/Passive (SMAP) Freeze/Thaw Product: Providing a Crucial Linkage between Earth's Water and Carbon Cycles. *AGU Fall Meeting Abstracts* **2010,** *2010*, H33F-1219.

McGinnis, M. J.; Painter, J. E. Sorghum. *Nutr Today* **2020,** *55* (1), 38–44. DOI: 10.1097/NT.0000000000000391.

Meliho, M.; Khattabi, A.; Jobbins, G.; Sghir, F. Impact of meteorological drought on agriculture in the Tensift watershed of Morocco. *Journal of Water and Climate Change* [Online] **2019**.

Meng, X.; Wang, H.; Chen, J.; Yang, M.; Pan, Z. High-resolution simulation and validation of soil moisture in the arid region of Northwest China. *Scientific reports* **2019,** *9* (1), 17227. DOI: 10.1038/s41598-019-52923-x.

Mengel, M. A.; Delrieu, I.; Heyerdahl, L.; Gessner, B. D. Cholera Outbreaks in Africa. In *Cholera Outbreaks*; Nair, G. B., Takeda, Y., Eds.; Current Topics in Microbiology and Immunology 379; Springer Berlin Heidelberg: Berlin, Heidelberg, 2014; pp 117–144. DOI: 10.1007/82_2014_369.

Mercer, P. Shilluk Trade and Politics from the mid–seventeenth century to 1861. *J. Afr. Hist.* **1971,** *12* (3), 407–426. DOI: 10.1017/S0021853700010859.

Meza, I.; Siebert, S.; Döll, P.; Kusche, J.; Herbert, C.; Eyshi Rezaei, E.; Nouri, H.; Gerdener, H.; Popat, E.; Frischen, J.; Naumann, G.; Vogt, J. V.; Walz, Y.; Sebesvari, Z.; Hagenlocher, M. Global-scale drought risk assessment for agricultural systems. *Nat. Hazards Earth Syst. Sci.* **2020,** *20* (2), 695–712. DOI: 10.5194/nhess-20-695-2020.

Minoli, S.; Müller, C.; Elliott, J.; Ruane, A. C.; Jägermeyr, J.; Zabel, F.; Dury, M.; Folberth, C.; François, L.; Hank, T.; Jacquemin, I.; Liu, W.; Olin, S.; Pugh, T. A. M. Global Response Patterns of Major Rainfed Crops to Adaptation by Maintaining Current Growing Periods and Irrigation. *Earth's Future* **2019,** *7* (12), 1464–1480. DOI: 10.1029/2018EF001130.

Mirza, M. Climate change and extreme weather events: can developing countries adapt? *Climate Policy* **2003,** *3* (3), 233–248. DOI: 10.1016/S1469-3062(03)00052-4.

Mishra, A.; Vu, T.; Veettil, A. V.; Entekhabi, D. Drought monitoring with soil moisture active passive (SMAP) measurements. *Journal of Hydrology* **2017,** *552*, 620–632. DOI: 10.1016/j.jhydrol.2017.07.033.

Msongaleli, B. M.; Rwehumbiza, F.; Tumbo, S. D.; Kihupi, N. Impacts of Climate Variability and Change on Rainfed Sorghum and Maize: Implications for Food Security Policy in Tanzania. *JAS* **2015,** *7* (5). DOI: 10.5539/jas.v7n5p124.

Mueller, M.; Ritmeijer, K.; Balasegaram, M.; Koummuki, Y.; Santana, M. R.; Davidson, R. Unresponsiveness to AmBisome in some Sudanese patients with kala-azar. *Trans R Soc Trop Med Hyg* **2007,** *101* (1), 19–24. DOI: 10.1016/j.trstmh.2006.02.005.

Mukherjee, S.; Mishra, A.; Trenberth, K. E. Climate Change and Drought: a Perspective on Drought Indices. *Curr Clim Change Rep* **2018,** *4* (2), 145–163. DOI: 10.1007/s40641-018-0098-x.

Myeni, L.; Moeletsi, M. E.; Clulow, A. D. Present status of soil moisture estimation over the African continent. *Journal of Hydrology: Regional Studies* [Online] **2019a,** *21*, 14–24. https://www.sciencedirect.com/science/article/pii/s2214581818301617.

Myeni, L.; Moeletsi, M. E.; Clulow, A. D. Present status of soil moisture estimation over the African continent. *Journal of Hydrology: Regional Studies* [Online] **2019b,** *21*, 14–24. http://dx.doi.org/10.1016/j.ejrh.2018.11.004.

Nanzad, L.; Zhang, J.; Tuvdendorj, B.; Nabil, M.; Zhang, S.; Bai, Y. NDVI anomaly for drought monitoring and its correlation with climate factors over Mongolia from 2000 to 2016. *Journal of*

Arid Environments [Online] **2019,** *164*, 69–77. https://www.sciencedirect.com/science/article/pii/s0140196318302659.

Narayanan, R. M.; Hirsave, P. P. Soil moisture estimation models using SIR-C SAR data: a case study in New Hampshire, USA. *Remote Sensing of Environment* **2001,** *75* (3), 385–396. DOI: 10.1016/S0034-4257(00)00181-4.

Nichols, S. Review and evaluation of remote sensing methods for soil-moisture estimation. *J. Photon. Energy* [Online] **2011**, 28001.

O'Brien, J. Sowing the seeds of famine: the political economy of food deficits in Sudan. *Review of African Political Economy* **1985,** *12* (33), 23–32. DOI: 10.1080/03056248508703630.

Ogundipe, A.; Oduntan, E.; Ogunniyi, A.; Olagunju, K. Agricultural Productivity, Poverty Reduction and Inclusive Growth in Africa: Linkages and Pathways. *AJAEES* **2017,** *18* (1), 1–15. DOI: 10.9734/AJAEES/2017/32427.

Pablos, M.; González-Zamora, Á.; Sánchez, N.; Martínez-Fernández, J. Assessment of Root Zone Soil Moisture Estimations from SMAP, SMOS and MODIS Observations. *Remote Sensing* **2018,** *10* (7), 981. DOI: 10.3390/rs10070981.

Park, S.; Im, J.; Jang, E.; Rhee, J. Drought assessment and monitoring through blending of multi-sensor indices using machine learning approaches for different climate regions. *Agricultural and Forest Meteorology* [Online] **2016,** *216*, 157–169. https://www.sciencedirect.com/science/article/pii/s0168192315007467?casa_token=e4j7zzplpruaaaaa:vgqo0vboqwlszvsv voqj5x2iltxs_totsgrhvfplxf0y3yxbtygxlwpagqwjo_3exl4cr28epc.

Parry, M.; Rosenzweig, C.; Livermore, M. Climate change, global food supply and risk of hunger. *Philosophical transactions of the Royal Society of London. Series B, Biological sciences* **2005,** *360* (1463), 2125–2138. DOI: 10.1098/rstb.2005.1751.

Patricia M. Lawston; Joseph A. Santanello; Sujay V. Kumar. Irrigation Signals Detected From SMAP Soil Moisture Retrievals. *Geophysical Research Letters* **2017,** *44* (23), 11,860-11,867. DOI: 10.1002/2017GL075733.

Per Pinstrup-Anders. *Who Wil l Be Fed in the 21s t Century?;* Johns Hopkins University Press, 2001.

Pezij, M.; Augustijn, D. C.M.; Hendriks, D. M.D.; Weerts, A. H.; Hummel, S.; van der Velde, R.; Hulscher, S. J.M.H. State updating of root zone soil moisture estimates of an unsaturated zone metamodel for operational water resources management. *Journal of Hydrology X* [Online] **2019,** *4*, 100040. http://dx.doi.org/10.1016/j.hydroa.2019.100040.

Pires, L. F.; Pereira, A. B. Gamma-ray attenuation to evaluate soil porosity: an analysis of methods. *TheScientificWorldJournal* **2014,** *2014*, 723041. DOI: 10.1155/2014/723041.

Prajapati, V. K.; Khanna, M.; Singh, M.; Kaur, R.; Sahoo, R. N.; Singh, D. K. Evaluation of time scale of meteorological, hydrological and agricultural drought indices. *Nat Hazards* **2021**, 1–21. DOI: 10.1007/s11069-021-04827-1.

Qiu, B.; Xue, Y.; Fisher, J. B.; Guo, W.; Berry, J. A.; Zhang, Y. Satellite Chlorophyll Fluorescence and Soil Moisture Observations Lead to Advances in the Predictive Understanding of Global Terrestrial Coupled Carbon-Water Cycles. *Global Biogeochem. Cycles* **2018,** *32* (3), 360–375. DOI: 10.1002/2017GB005744.

Ramana, M. V. Nuclear Power: Economic, Safety, Health, and Environmental Issues of Near-Term Technologies. *Annu. Rev. Environ. Resour.* **2009,** *34* (1), 127–152. DOI: 10.1146/annurev.environ.033108.092057.

Rattalino Edreira, J. I.; Andrade, J. F.; Cassman, K. G.; van Ittersum, M. K.; van Loon, M. P.; Grassini, P. Spatial frameworks for robust estimation of yield gaps. *Nat Food* **2021,** *2* (10), 773–779. DOI: 10.1038/s43016-021-00365-y.

Ray, D. K.; Mueller, N. D.; West, P. C.; Foley, J. A. Yield Trends Are Insufficient to Double Global Crop Production by 2050. *PLoS ONE* **2013,** *8* (6), e66428. DOI: 10.1371/journal.pone.0066428.

Reichle, R. H.; Lannoy, G. J. M. de; Liu, Q.; Ardizzone, J. V.; Colliander, A.; Conaty, A.; Crow, W.; Jackson, T. J.; Jones, L. A.; Kimball, J. S.; Koster, R. D.; Mahanama, S. P.; Smith, E. B.; Berg, A.; Bircher, S.; Bosch, D.; Caldwell, T. G.; Cosh, M.; González-Zamora, Á.; Holifield Collins, C. D.; Jensen, K. H.; Livingston, S.; Lopez-Baeza, E.; Martínez-Fernández, J.; McNairn, H.; Moghaddam, M.; Pacheco, A.; Pellarin, T.; Prueger, J.; Rowlandson, T.; Seyfried, M.; Starks, P.; Su, Z.; Thibeault, M.; van der Velde, R.; Walker, J.; Wu, X.; Zeng, Y. Assessment of the SMAP Level-4 Surface and Root-Zone Soil Moisture Product Using In Situ Measurements. *Journal of Hydrometeorology* **2017,** *18* (10), 2621–2645. DOI: 10.1175/JHM-D-17-0063.1.

Rempelos, L.; Almuayrifi, M. S. B.; Baranski, M.; Tetard-Jones, C.; Barkla, B.; Cakmak, I.; Ozturk, L.; Cooper, J.; Volakakis, N.; Hall, G.; Zhao, B.; Rose, T. J.; Wang, J.; Kalee, H. A.; Sufar, E.; Hasanalieya, G.; Bilsborrow, P.; Leifert, C. The effect of agronomic factors on crop health and performance of winter wheat varieties bred for the conventional and the low input farming sector. *Field Crops Research* [Online] **2020,** *254*, 107822. http://dx.doi.org/10.1016/j.fcr.2020.107822.

Renzaho, A. M.N.; Kamara, J. K.; Toole, M. Biofuel production and its impact on food security in low and middle income countries: Implications for the post-2015 sustainable development goals. *Renewable and Sustainable Energy Reviews* [Online] **2017,** *78*, 503–516. http://dx.doi.org/10.1016/j.rser.2017.04.072.

Ritchie, J. C.; Haynes, C. V. Holocene vegetation zonation in the eastern Sahara. *Nature* [Online] **1987,** *330* (6149), 645–647. https://idp.nature.com/authorize/casa?redirect_uri=https://www.nature.com/articles/330645a0&casa_token=7jyqxxinyssaaaaa:t3u8y5tmdu0qiihfw9g4uebpxn5vn5y4rz1aiv_w_pusrskt0rpkevvtwhrl3ikn6bpbnxhcit1km._h.

Robinson, D. A.; Campbell, C. S.; Hopmans, J. W.; Hornbuckle, B. K.; Jones, S. B.; Knight, R.; Ogden, F.; Selker, J.; Wendroth, O. Soil Moisture Measurement for Ecological and Hydrological Watershed-Scale Observatories: A Review. *Vadose zone j.* **2008,** *7* (1), 358–389. DOI: 10.2136/vzj2007.0143.

Rockström, J.; Karlberg, L.; Wani, S. P.; Barron, J.; Hatibu, N.; Oweis, T.; Bruggeman, A.; Farahani, J.; Qiang, Z. *Managing water in rainfed agriculture—The need for a paradigm shift* 97, 2010.

Rodríguez-Fernández, N. J.; Muñoz Sabater, J.; Richaume, P.; Rosnay, P. de; Kerr, Y. H.; Albergel, C.; Drusch, M.; Mecklenburg, S. SMOS near-real-time soil moisture product: processor overview and first validation results. *Hydrol. Earth Syst. Sci.* **2017,** *21* (10), 5201–5216. DOI: 10.5194/hess-21-5201-2017.

Rousvel, S.; Armand, N.; Andre, L.; Tengeleng, S.; Alain, T.; Armel, K. Comparison between Vegetation and Rainfall of Bioclimatic Ecoregions in Central Africa. *Atmosphere* **2013,** *4* (4), 411–427. DOI: 10.3390/atmos4040411.

Saeidizand, R.; Sabetghadam, S.; Tarnavsky, E.; Pierleoni, A. Evaluation of CHIRPS rainfall estimates over Iran. *Q J R Meteorol Soc* **2018,** *144* (S1), 282–291. DOI: 10.1002/qj.3342.

Sandeep, P.; Obi Reddy, G. P.; Jegankumar, R.; Arun Kumar, K. C. Monitoring of agricultural drought in semi-arid ecosystem of Peninsular India through indices derived from time-series CHIRPS and MODIS datasets. *Ecological Indicators* [Online] **2021,** *121*, 107033. https://www.sciencedirect.com/science/article/pii/s1470160x20309729.

Saradjian, M. R.; Hosseini, M. Soil moisture estimation by using multipolarization SAR image. *Advances in Space Research* **2011,** *48* (2), 278–286. DOI: 10.1016/j.asr.2011.03.029.

Sawadogo Alidou; Kemal Sulhi Gundogdu; Farid Traore; Louis Kouadio; Tim Hessels. Estimating in-season actual evapotranspiration over a large-scale irrigation scheme in resource-limited conditions. *Comptes rendus de l'Académie bulgare des sciences: sciences mathématiques et naturelles* [Online] **2020,** *73* (10), 1473–1480. https://www.researchgate.net/profile/alidou-sawadogo/publication/345015382_estimating_in-season_actual_evapotranspiration_over_a_large-scale_irrigation_scheme_in_resource-limited_conditions.

Senay, G. B. Satellite Psychrometric Formulation of the Operational Simplified Surface Energy Balance (SSEBop) Model for Quantifying and Mapping Evapotranspiration. *Applied Engineering in Agriculture* **2018,** *34* (3), 555–566. DOI: 10.13031/aea.12614.

Senay and Verdin. Evaluating the Performance of a Crop Water Balance Model in Estimating Regional Crop Production [Online] **2003**.

Shah, R.; Bharadiya, N.; Manekar, V. Drought Index Computation Using Standardized Precipitation Index (SPI) Method For Surat District, Gujarat. *Aquatic Procedia* [Online] **2015,** *4*, 1243–1249. https://www.sciencedirect.com/science/article/pii/s2214241x15001637.

Sheahan, M.; Barrett, C. B. Ten striking facts about agricultural input use in Sub-Saharan Africa. *Food policy* **2017,** *67*, 12–25. DOI: 10.1016/j.foodpol.2016.09.010.

Shellito, P. J.; Small, E. E.; Colliander, A.; Bindlish, R.; Cosh, M. H.; Berg, A. A.; Bosch, D. D.; Caldwell, T. G.; Goodrich, D. C.; McNairn, H.; Prueger, J. H.; Starks, P. J.; van der Velde, R.; Walker, J. P. SMAP soil moisture drying more rapid than observed in situ following rainfall events. *Geophysical Research Letters* **2016,** *43* (15), 8068–8075. DOI: 10.1002/2016GL069946.

Shishaye, H. The Negative Impacts of Climate Change in Sub-Saharan Africa and their Mitigation Measures. *BJAST* **2015,** *11* (5), 1–9. DOI: 10.9734/BJAST/2015/17665.

Showalter, D. N.; Villari, C.; Herms, D. A.; Bonello, P. Drought stress increased survival and development of emerald ash borer larvae on coevolved Manchurian ash and implicates phloem-based traits in resistance. *Agr Forest Entomol* **2018,** *20* (2), 170–179. DOI: 10.1111/afe.12240.

Shraddhanand Shukla; Daniel McEvoy; Mike Hobbins; Greg Husak; Justin Huntington; Chris Funk; Denis Macharia; James Verdin. Examining the Value of Global Seasonal Reference Evapotranspiration Forecasts to Support FEWS NET's Food Insecurity Outlooks. *Journal of Applied Meteorology and Climatology* [Online] **2017,** *56* (11), 2941–2949. https://journals.ametsoc.org/view/journals/apme/56/11/jamc-d-17-0104.1.xml.

Siderius, C.; van Walsum, P.E.V.; Roest, C.W.J.; Smit, A.A.M.F.R.; Hellegers, P.J.G.J.; Kabat, P.; van Ierland, E. C. The role of rainfed agriculture in securing food production in the Nile Basin. *Environmental Science & Policy* **2016,** *61*, 14–23. DOI: 10.1016/j.envsci.2016.03.007.

Singh, V. P.; Mishra, A. K.; Chowdhary, H.; Khedun, C. P. Climate Change and Its Impact on Water Resources [Online].

Sinha, R.; Irulappan, V.; Mohan-Raju, B.; Suganthi, A.; Senthil-Kumar, M. Impact of drought stress on simultaneously occurring pathogen infection in field-grown chickpea. *Scientific reports* **2019,** *9* (1), 5577. DOI: 10.1038/s41598-019-41463-z.

Fire and Sword in the Sudan; Slatin, Ed.; London, New York, E. Arnold, 1896.

Slatin; Carl, R. *Fire and Sword in the Sudan*. *A personal Narrative of fightingand serving the Dervishes;* Edward Arnold: London and New york, 1896.

Spaulding, J. Slavery, Land Tenure and Social Class in the Northern Turkish Sudan. *The International Journal of African Historical Studies* **1982,** *15* (1), 1. DOI: 10.2307/218446.

Statista. *The statistics portal for market data, empwering people with data*, 2020. https://www.statista.com/.

Stillman, S.; Zeng, X. Evaluation of SMAP Soil Moisture Relative to Five Other Satellite Products Using the Climate Reference Network Measurements Over USA. *IEEE Trans. Geosci. Remote Sensing* [Online] **2018,** *56* (11), 6296–6305. http://dx.doi.org/10.1109/tgrs.2018.2835316.

Streimikis, J.; Baležentis, T. Agricultural sustainability assessment framework integrating sustainable development goals and interlinked priorities of environmental, climate and agriculture policies. *Sustainable Development* **2020,** *28* (6), 1702–1712. DOI: 10.1002/sd.2118.

Sujay Rakshit; K. Hariprasanna; Sunil Gomashe; K. N. Ganapathy; I. K. Das; O. V. Ramana; A. Dhandapani; J. V. Patil. Changes in Area, Yield Gains, and Yield Stability of Sorghum in Major Sorghum-Producing Countries, 1970 to 2009. *Crop Science* **2014,** *54* (4), 1571–1584. DOI: 10.2135/cropsci2012.12.0697.

Sulieman, H. M.; Buchroithner, M. F. Degradation and abandonment of mechanized rain-fed agricultural land in the Southern Gadarif region, Sudan: the local farmers' perception. *Land Degrad. Dev.* **2009,** *20* (2), 199–209. DOI: 10.1002/ldr.894.

Surendran, U.; Anagha, B.; Raja, P.; Kumar, V.; Rajan, K.; Jayakumar, M. Analysis of Drought from Humid, Semi-Arid and Arid Regions of India Using DrinC Model with Different Drought Indices. *Water Resour Manage* [Online] **2019,** *33* (4), 1521–1540. https://link.springer.com/article/10.1007/s11269-019-2188-5.

Tack, J.; Lingenfelser, J.; Jagadish, S. V. K. Disaggregating sorghum yield reductions under warming scenarios exposes narrow genetic diversity in US breeding programs. *Proceedings of the National*

Academy of Sciences of the United States of America **2017,** *114* (35), 9296–9301. DOI: 10.1073/pnas.1706383114.

Tao, F.; Yokozawa, M.; Zhang, Z.; Xu, Y.; Hayashi, Y. Remote sensing of crop production in China by production efficiency models: models comparisons, estimates and uncertainties. *Ecological Modelling* [Online] **2005,** *183* (4), 385–396. https://www.sciencedirect.com/science/article/pii/s0304380004004983.

Tarnavsky, E.; Chavez, E.; Boogaard, H. Agro-meteorological risks to maize production in Tanzania: Sensitivity of an adapted Water Requirements Satisfaction Index (WRSI) model to rainfall. *International Journal of Applied Earth Observation and Geoinformation* **2018,** *73*, 77–87. DOI: 10.1016/j.jag.2018.04.008.

Teklu, T.; Braun, J. von; Zaki, E. Drought and Famine Relationships in Sudan: Policy Implications. *Food Nutr Bull* **1992,** *14* (2), 1–3. DOI: 10.1177/156482659201400204.

Ternes, B. Saving for a dry day: investigating well ownership and watering practices during droughts. *Environmental Sociology* **2019,** *5* (1), 93–107. DOI: 10.1080/23251042.2018.1463489.

Timko, J.; Le Billon, P.; Zerriffi, H.; Honey-Rosés, J.; La Roche, I. de; Gaston, C.; Sunderland, T. C. H.; Kozak, R. A. A policy nexus approach to forests and the SDGs: tradeoffs and synergies. *Current Opinion in Environmental Sustainability* **2018,** *34*, 7–12. DOI: 10.1016/j.cosust.2018.06.004.

Tufa Dinku; Chris Funk; Pete Peterson; Ross Maidment; Tsegaye Tadesse; Hussein Gadain; Pietro Ceccato. Validation of the CHIRPS satellite rainfall estimates over eastern Africa. *Quarterly Journal of the Royal Meteorological Society* **2018,** *144*, 292–312. DOI: 10.1002/qj.3244.

Tufaner, F.; Özbeyaz, A. Estimation and easy calculation of the Palmer Drought Severity Index from the meteorological data by using the advanced machine learning algorithms. *Environ Monit Assess* [Online] **2020,** *192* (9), 576. https://link.springer.com/article/10.1007/s10661-020-08539-0.

Valverde, P.; Carvalho, M. de; Serralheiro, R.; Maia, R.; Ramos, V.; Oliveira, B. *Climate change impacts on rainfed agriculture in the Guadiana river basin (Portugal)* 150, 2015.

van Loon, A. F.; Gleeson, T.; Clark, J.; van Dijk, A. I. J. M.; Stahl, K.; Hannaford, J.; Di Baldassarre, G.; Teuling, A. J.; Tallaksen, L. M.; Uijlenhoet, R.; Hannah, D. M.; Sheffield, J.; Svoboda, M.; Verbeiren, B.; Wagener, T.; Rangecroft, S.; Wanders, N.; van Lanen, H. A. J. Drought in a human-modified world: reframing drought definitions, understanding and analysis approaches [Online] **2016**.

van Wesenbeeck, C. F.A.; Sonneveld, B. G.J.S.; Voortman, R. L. Localization and characterization of populations vulnerable to climate change: Two case studies in Sub-Saharan Africa. *Applied Geography* **2016,** *66*, 81–91. DOI: 10.1016/j.apgeog.2015.11.001.

Vanschoenwinkel, J.; van Passel, S. Climate response of rainfed versus irrigated farms: the bias of farm heterogeneity in irrigation. *Climatic Change* **2018,** *147* (1-2), 225–234. DOI: 10.1007/s10584-018-2141-2.

Velpuri, N. M.; Senay, G. B.; Morisette, J. T. Evaluating New SMAP Soil Moisture for Drought Monitoring in the Rangelands of the US High Plains. *Rangelands* [Online] **2016,** *38* (4), 183–190. http://dx.doi.org/10.1016/j.rala.2016.06.002.

Verdin, J.; Klaver, R. Grid-cell-based crop water accounting for the famine early warning system. *Hydrol. Process.* **2002,** *16* (8), 1617–1630. DOI: 10.1002/hyp.1025.

Adaptation to a changing climate in the Arab countries. *A case for adaptation governance and leadership in building climate resilience;* Verner, D., World Bank Group, Eds.; MENA development report; World Bank: Washington DC, 2012.

VOS t. N. C., J. H.; VIRGO, K. J. Soil structure in vertisols of Blue Nile clay plains, Sudan. *Journal of Soil Science* **1969,** *20* (1), 189–206. DOI: 10.1111/j.1365-2389.1969.tb01567.x.

Wang, L.; Qu, J. J. Satellite remote sensing applications for surface soil moisture monitoring: A review. *Front. Earth Sci. China* **2009,** *3* (2), 237–247. DOI: 10.1007/s11707-009-0023-7.

Wesely and Hicks. A review of the current status of knowledge on dry deposition. *Atmospheric Environment* [Online] **2000**.

Weststrate, J.; Dijkstra, G.; Eshuis, J.; Gianoli, A.; Rusca, M. The Sustainable Development Goal on Water and Sanitation: Learning from the Millennium Development Goals. *Soc Indic Res* **2019,** *143* (2), 795–810. DOI: 10.1007/s11205-018-1965-5.

Whittington, D.; Waterbury, J.; Jeuland, M. The Grand Renaissance Dam and prospects for cooperation on the Eastern Nile. *Water Policy* **2014,** *16* (4), 595–608. DOI: 10.2166/wp.2014.011b.

Wood, I. M.; Muchow, R. C.; Ratcliff, D. Effect of sowing date on the growth and yield of kenaf (Hibiscus cannabinus) grown under irrigation in tropical Australia II. Stem production. *Field Crops Research* [Online] **1983,** *7*, 91–102. https://www.sciencedirect.com/science/article/pii/037842908390014x.

World Development Report *2006;* The World Bank, 2005.

Worrall, G. A. Work on improvement of saline-alkali land on the University Farm, Khartoum, 1956–59. *J. Agric. Sci.* **1961,** *57* (3), 367–371. DOI: 10.1017/s0021859600049340.

Wu, B.; Ma, Z.; Yan, N. Agricultural drought mitigating indices derived from the changes in drought characteristics. *Remote Sensing of Environment* [Online] **2020,** *244*, 111813. https://www.sciencedirect.com/science/article/pii/s0034425720301838.

Wu, Q.; Liu, H.; Wang, L.; Deng, C. Evaluation of AMSR2 soil moisture products over the contiguous United States using in situ data from the International Soil Moisture Network. *International Journal of Applied Earth Observation and Geoinformation* **2016,** *45*, 187–199. DOI: 10.1016/j.jag.2015.10.011.

Xie, F.; Fan, H. Deriving drought indices from MODIS vegetation indices (NDVI/EVI) and Land Surface Temperature (LST): Is data reconstruction necessary? *International Journal of Applied Earth Observation and Geoinformation* [Online] **2021,** *101*, 102352. https://www.sciencedirect.com/science/article/pii/s0303243421000593.

Xu, C.; Zeng, W.-Z.; Wu, J.-W.; Huang, J.-S. Effects of Different Irrigation Strategies on Soil Water, Salt, and Nitrate Nitrogen Transport. *Ecological Chemistry and Engineering S* **2015,** *22* (4), 589–609. DOI: 10.1515/eces-2015-0035.

Yagci, A. L.; Liping Di; Meixia Deng. The influence of land cover-related changes on the NDVI-based satellite agricultural drought indices. In *2014 IEEE Geoscience and Remote Sensing Symposium*; IEEE, 2014. DOI: 10.1109/igarss.2014.6946868.

Yousif, L. A.; Taha, M. B. Effect of seedbed preparation, sowing method and nitrogen fertilizer level on sorghum grain yield in rainfed areas, Gedarif, Sudan. *International Journal of Agronomy and Plant Production* [Online] **2013,** *4* ((S)), 3864–3870. http://eprints.icrisat.ac.in/12853/.

Yun Xiong; Pangzhen Zhang; Robyn Dorothy Warner; Zhongxiang Fang. Sorghum Grain: From Genotype, Nutrition, and Phenolic Profile to Its Health Benefits and Food Applications. *Comprehensive Reviews in Food Science and Food Safety* **2019,** *18* (6), 2025–2046. DOI: 10.1111/1541-4337.12506.

Zargar, A.; Sadiq, R.; Khan, F. I. Uncertainty-Driven Characterization of Climate Change Effects on Drought Frequency Using Enhanced SPI. *Water Resour Manage* **2014,** *28* (1), 15–40. DOI: 10.1007/s11269-013-0467-0.